University of Alberta

INDEPENDENT RAYLEIGH, RICEAN, AND NAKAGAMI SUM DISTRIBUTION AND DENSITY APPROXIMATIONS FOR WIRELESS APPLICATIONS

by

Jeremiah Hu ©

A thesis submitted to the Faculty of Graduate Studies and Research in partial fulfillment of the requirements for the degree of **Master of Science.**

Department of Electrical and Computer Engineering

Edmonton, Alberta

Spring 2005

0-494-08082-5

Abstract

The statistical sum distributions of independent Rayleigh, Ricean, and Nakagami random variables occur extensively in the modeling and performance analysis of wireless communication systems. Closed-form expressions do not exist for most of these sum distributions and consequently, they are often approximated or calculated numerically. In this thesis, accurate closed-form approximations for the Rayleigh, Ricean, and Nakagami sum distributions and densities are derived. These approximations are demonstrated to be valid for a wide range of probability values, statistical parameters, and number of summands. The proposed approximations facilitate efficient performance analysis for a broad range of applications. One particular application considered in this thesis is equal gain combining diversity systems. Accurate closed-form expressions for the average error and outage probabilities of these systems are derived.

Acknowledgements

I would like to thank my supervisor Dr. Norman C. Beaulieu for his feedback, guidance, and financial support. In addition, I would like to thank all members of the *i*CORE Wireless Communications Laboratory for their technical advice and friendship. Special thanks to my good friend and classmate, Faruq Rajwani, for helping me throughout my undergraduate and graduate work. Finally, I am extremely grateful to my parents and brother for their continuous love and moral support throughout my university career.

This thesis was financially supported through the Natural Sciences and Engineering Research Council of Canada (NSERC), the Alberta Informatics Circle of Research Excellence (*i*CORE), and the Alberta Ingenuity Fund.

Contents

List of Tables

List of Figures

Acronyms

Acronym	Definition
AWGN	additive white Gaussian noise
BEP	bit error probability
CDF	cumulative distribution function
CFSK	coherent frequency-shift keying
CHF	characteristic function
CPSK	coherent phase-shift keying
DPSK	differential phase-shift keying
EGC	equal gain combining
ISI	intersymbol interference
iid	independent and identically distributed
LOS	line-of-sight
MPSK	M-ary phase-shift keying
MRC	maximal ratio combining
NCFSK	noncoherent frequency-shift keying
PDF	probability density function
RV	random variable
SAA	small argument approximation
SC	selective combining
SEP	symbol error probability
SNR	signal-to-noise ratio

List of Symbols

Symbol	Definition
a_0, a_1, a_2	optimum coefficients for Rayleigh sum CDF and PDF approximations
b	SAA scaling constant
c_1, c_2	optimum coefficients for Nakagami sum CDF and PDF approximations
d_1, d_2	optimum coefficients for Ricean sum CDF and PDF approximations
$\mathrm{E}[\cdot]$	expectation operation
E_{avg}	average symbol energy
E_i	amplitude of the i-th arriving wave
E_z	vertical component of the electric field
$\mathrm{erfc}(\cdot)$	complementary error function
${}_2\mathrm{F}_1(\cdot,\cdot;\cdot;\cdot)$	Gauss hypergeometric function
$F_{Error}(t)$	SAA error term
$F_X(x)$	CDF of RV X
$f_X(x)$	PDF of RV X
f_c	carrier frequency
g_i	complex fading gain of the i-th diversity branch
H	sum of L iid squared RVs
$I_0(\cdot)$	zeroth-order modified Bessel function of the first kind
$I_{L-1}(\cdot)$	$(L-1)$th-order modified Bessel function of the first kind
K	Rice factor
K_i	Rice factor of the i-th RV or i-th diversity branch

L	number of summands or diversity branches
$m(t)$	binary signal
m	Nakagami fading parameter
m_i	Nakagami fading parameter of the i-th RV or i-th diversity branch
N	number of horizontally traveling plane waves
$N_0/2$	power spectral density of the AWGN
$n_i(t)$	AWGN of the i-th diversity branch
n	AWGN
$P_S(\varepsilon \mid R_O)$	SEP conditioned on specific signal envelope at output of linear combiner
$P_S(\varepsilon \mid \gamma)$	SEP conditioned on specific SNR
$P_S(\varepsilon \mid \gamma_O)$	SEP conditioned on specific SNR at output of linear combiner
P_e	average error probability
P_{out}	outage probability
p	probability that instantaneous SNR is below a critical threshold
$Q(\cdot)$	Q-function
$Q_L(\cdot,\cdot)$	generalized Marcum Q-function
R	received signal envelope
R_{EGC}	signal envelope at output of EGC
R_{MRC}	signal envelope at output of MRC
R_{Norm}	normalized signal envelope
R_O	signal envelope at output of linear combiner
R_i	faded signal envelope of the i-th RV or i-th diversity branch
R_{th}	signal threshold envelope for determining outage
$R_{th_{Norm}}$	normalized signal threshold envelope for determining outage
$s_m(t)$	transmitted signal
s^2	noncentrality parameter
s_i^2	noncentrality parameter of the i-th RV or i-th diversity branch
T	symbol duration
t	normalized argument

ν	Ricean sum scaling constant
w_i	combining weight of the i-th diversity branch
X	in-phase component of E_z
X_i	normalized i-th RV
Y	quadrature component of E_z
Z	sum of L iid RVs
$z(t)$	resultant signal at output of linear combiner
$z_{EGC}(t)$	resultant signal at output of EGC
$z_{MRC}(t)$	resultant signal at output of MRC
$z_i(t)$	received signal on the i-th diversity branch
$\Gamma(\cdot)$	gamma function
$\gamma(\cdot,\cdot)$	incomplete gamma function
γ	SNR per symbol
γ_{EGC}	output SNR of EGC
γ_{MRC}	output SNR of MRC
γ_O	SNR at output of linear combiner
γ_{SC}	output SNR of SC
γ_i	instantaneous SNR of the i-th diversity branch
γ_{th}	SNR threshold for determining outage
θ_i	phase of the i-th arriving wave
σ^2	variance of the Gaussian scatter component
σ^2_{EGC}	weighted sum of branch noise powers at output of EGC
σ^2_{MRC}	weighted sum of branch noise powers at output of MRC
σ^2_N	weighted sum of branch noise powers at output of linear combiner
σ^2_X	variance of the in-phase component of E_z
σ^2_Y	variance of the quadrature component of E_z
σ^2_i	variance of the Gaussian scatter component of the i-th RV or i-th diversity branch
ϕ_i	received phase on the i-th diversity branch

Ω	average signal power
Ω_i	average signal power of the *i*-th RV or *i*-th diversity branch

Chapter 1

Introduction

1.1 Overview

The explosive growth of the wireless communications industry can be attributed to many factors. The ongoing replacement of traditional wired telephone service in favor of cellular networks, the popularity of wireless services such as broadband Internet, and the dramatic improvement in hardware implementation technology are just a few reasons. As the wireless industry grows, there are demands for higher data rates, improved quality of service, and lower cost communications. These demands have created the need to design new wireless communication systems.

A fundamental consideration when designing a communication system is the physical channel through which the information is conveyed. This channel is a medium such as a wire, a coaxial cable, a waveguide, an optical fiber, or a radio link. In a way, the channel acts partly like a filter in that it attenuates and distorts the waveform. In addition, the signal is also contaminated along the path by undesirable signals, often termed as noise. Sources of noise include interference from other signals transmitted on nearby channels, human-made noise, radiation from various sources, and thermal noise caused by the motion of electrons in conductors of electronic devices. The signal-to-noise ratio (SNR) is defined as the ratio of signal power to noise power.

Among all the obstacles encountered in wireless system design, the time-varying nature of the propagation channel is probably the most difficult [1]. This time-varying nature and the associated multipath fading inhibit reliable wireless communications and create significant challenges for wireless system design. It is thus important to analyze the effects of multipath fading in wireless communications. This often requires the development of statistical models to accurately depict the channel conditions. Research must also be done on solutions to combat the problems that are caused by multipath fading.

It has been shown that multipath fading causes a degradation in system performance. As a result, several solutions have been proposed and implemented [2]. Techniques including equalization, channel coding, spread spectrum, and diversity have been deployed in modern wireless systems. The degree to which these methods are effective is dependent on the wireless environment and complexity of the system architecture. Diversity is a relatively simple and effective method to reduce the damaging effects of fading.

The following sections provide more details on multipath fading and diversity.

1.2 The Wireless Channel

The wireless channel may vary from a simple line-of-sight (LOS) path between the transmitter and receiver to one that is severely obstructed by mountains, buildings, and other obstacles. Often, a LOS radio link cannot be achieved because the antenna of the mobile unit is below various obstacles. Consequently, radio propagation takes place mainly by way of reflection, diffraction, and scattering from the obstacles. This results in multiple radio waves that arrive simultaneously at the receiver, all with different amplitudes and phases. The constructive and destructive combining of these waves at the receiver leads to the multipath phenomenon known as fading and its existence makes reliable communications challenging [3]. In order to study the effects of multipath fading and improve wireless systems, accurate modeling of the propagation characteristics of the channel is a necessary requirement.

As a result of the randomness or time-varying nature of the wireless channel, modeling is typically done in a statistical manner. That is, by using theoretical insight or empirical measurements, one creates statistical models to describe the effects of the channel on the transmitted signal. In addition to accurately depicting the channel's characteristics, these models provide the benefit of being flexible. Many different fading environments may be represented by simply changing the statistical parameters. Generally, models are grouped into two main categories based on the transmitter and receiver spatial separation being considered. These two categories are large-scale or long-term fading and small-scale or short-term fading [2].

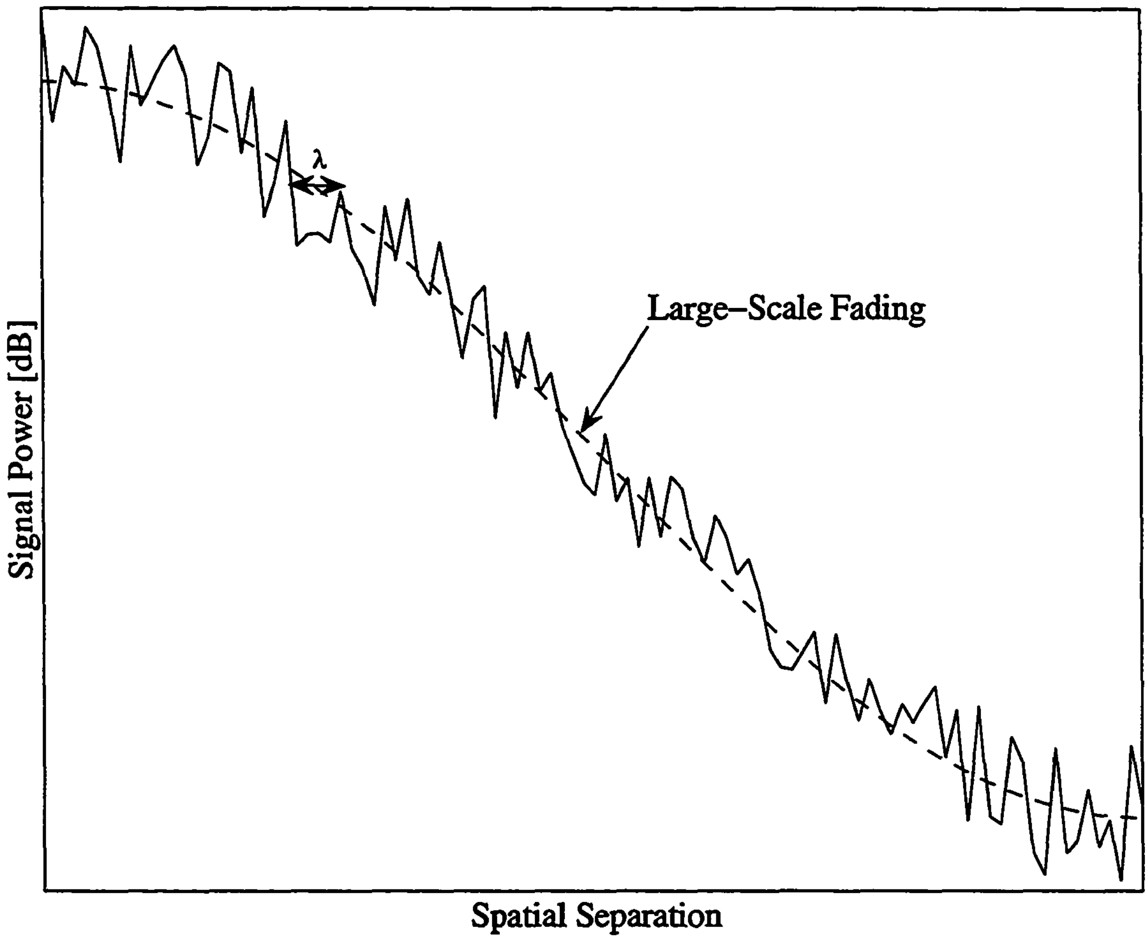

Fig. 1.1. Small-scale fading superimposed on large-scale fading.

Large-scale fading describes the average signal power decay or the path loss due to motion over large areas. This attenuation is caused by the terrestrial and free space losses

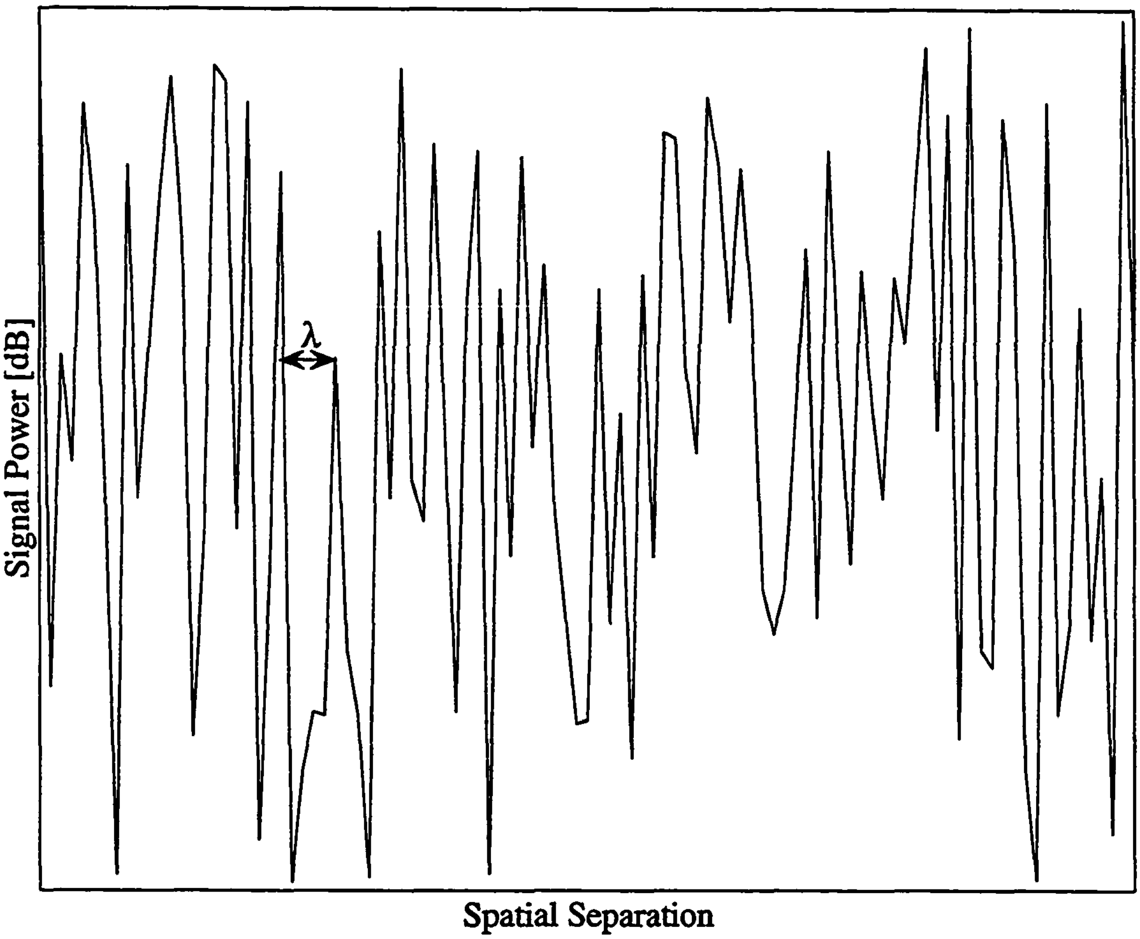

Fig. 1.2. Small-scale fading.

between the transmitter and receiver. The Okumura-Hata and COST 231-Walfish-Ikegami models are commonly used empirical models that have been obtained by curve fitting experimental data [4]. A popular theoretical model for large-scale fading is the lognormal propagation model [5]. This model describes the random shadowing effects due to the presence of terrain features such as buildings, foliage, and hills.

Small-scale fading describes the rapid fluctuations of the received signal strength over very short travel distances, as small as one-half wavelength. Depending on the nature of the propagation environment, different models are used to describe the statistical behavior of the multipath fading envelope. The main statistical models for small-scale fading are the Rayleigh, Ricean, and Nakagami distributions. To limit the scope of this thesis, only the effects of small-scale fading are considered in the analysis.

1.2.1 Small-Scale Fading

As mentioned previously, propagation through the wireless channel takes place by way of reflection, diffraction, and scattering from the objects in the transmission path. This causes multiple signal waves from different directions and with varying time delays to arrive simultaneously at the receiver. Small-scale fading refers to the fluctuations in the instantaneous received signal amplitude and phase that results over a very short distance, typically between a fraction of a wavelength and several wavelengths. Even over these tiny distances, dramatic changes in the power of the signal may occur as the received waves add constructively and destructively. For example, the received signal power may vary by as much as three or four orders of magnitude (30 or 40 dB) when the receiver is moved by only a fraction of a wavelength [6]. To further classify small-scale fading, the time dispersion and frequency dispersion mechanisms of the fading channel must be considered in relation to the nature of the transmitted signal.

The amount of delay spread is used to describe the degree of time dispersion caused by the channel. Time dispersion causes distortion in the signal and manifests itself in the spreading in time of the modulation symbols. This results in successive data symbols being smeared into one another, commonly known as intersymbol interference (ISI). In some cases, a huge degradation in the performance of the communication system may occur when the ISI becomes so severe that the symbols are no longer distinguishable [7]. The reciprocal of the delay spread is called the coherence bandwidth of the channel. This bandwidth is the range of frequencies where the channel passes all spectral components with equal gain and linear phase. The Doppler spread is used to describe the frequency dispersive nature of the channel that results whenever relative motion between the transmitter and the receiver exists. Doppler spreads will increase or decrease the apparent received frequency depending on if the receiver is moving closer or further from the transmitter [6]. The reciprocal of the Doppler spread is called the coherence time. This time is the duration over which two signals will be affected similarly by the channel. The cumulative effect of multipath fading, ISI, and Doppler spread severely degrades the performance of wireless communication systems. Based on the relative relations between the parameters of the fading channel (delay spread and Doppler spread) and the parameters of the transmitted signal (signal bandwidth and symbol period), small-scale fading can be classified into four categories [6]. The following is a brief summary of the four types of small-scale fading.

Frequency Selective Fading: When a wireless channel exhibits a constant gain and linear phase response for a bandwidth that is smaller than the transmitted bandwidth, the received signal will experience frequency selective fading. This scenario arises when the signal bandwidth is large in comparison to the coherence bandwidth.

Flat Fading: Conversely, when a wireless channel exhibits a constant gain and linear phase response for a bandwidth than is larger than the transmitted bandwidth, then the received signal will experience flat fading. Flat fading occurs when the signal bandwidth is small in comparison to the coherence bandwidth.

Fast Fading: A signal is considered to experience fast fading if the channel response changes rapidly within the baseband symbol duration. This occurs when the coherence time of the channel is smaller than the symbol period of the transmitted signal.

Slow Fading: On the other hand, if the symbol duration channel impulse response is static over one or more symbols, then the received signal will experience slow fading. Slow fading occurs when the symbol duration is small in comparison to the coherence time.

In this thesis, we focus on slowly-varying flat fading channels. This is done for two reasons. First, fast fading typically occurs only when very low data rates are used. Thus, most current terrestrial mobile-radio channels can be characterized as slow fading [2]. Secondly, frequency selective fading is much more difficult to model than flat fading. This is because each multipath signal must be modeled individually and the channel must be considered to be a linear filter. Channel measurements or simplified models such as the two-ray Rayleigh fading model are generally used to characterize frequency selective fading [6].

1.2.2 Flat Fading Channel Models

Many fading models have been used to describe the multipath propagation effects in wireless communication channels. The most common distributions used to describe the fading amplitude of a signal in flat fading channels are the Rayleigh, Ricean, and Nakagami distributions. The application of these distributions for modeling the wireless channel can be better understood by first considering Clarke's model [8].

Clarke's Model: In this model it is assumed that a stationary transmitter sends a signal to a moving mobile and the electromagnetic field of the received signal is a result of scattering. At the mobile antenna, the incident field consists of N horizontally traveling plane waves of random phase and equal average amplitude. The phase is assumed to be uniformly distributed between 0 and 2π. Furthermore, it is assumed that the arriving amplitudes and phases are all statistically uncorrelated. The vertical component of the electric field, denoted by E_z, can be written as

$$E_z = \sum_{i=1}^{N} E_i e^{j\theta_i} = X + jY \tag{1.1}$$

where E_i and θ_i respectively represent the amplitude and phase of the i-th arriving wave. Now if N is sufficiently large, E_z is approximately a Gaussian random variable (RV) as a result of the Central Limit Theorem. Thus, the in-phase and quadrature components, denoted by X and Y respectively, are also Gaussian RVs with means and variances given by

$$\mathrm{E}[X] = \mathrm{E}[Y] = 0, \tag{1.2a}$$

$$\sigma_X^2 = \sigma_Y^2 = \sigma^2 \tag{1.2b}$$

where E[$\cdot$] denotes the expectation operation and σ^2 is a constant.

Rayleigh Fading: When the channel impulse response is modeled as a zero-mean complex-valued Gaussian random process as in Clarke's model, the received envelope $R = \sqrt{X^2+Y^2}$ at any time instant is Rayleigh distributed [9]. Thus, the magnitude of the received complex envelope has a Rayleigh probability density function (PDF)

$$f_R(r) = \frac{r}{\sigma^2} e^{-\frac{r^2}{2\sigma^2}}, \quad r \geq 0 \tag{1.3}$$

where $(2-\pi/2)\sigma^2$ is the variance of the density. This fading model is commonly used in environments where no LOS path exists between the transmitter and receiver.

Ricean Fading: In certain environments, where there exists a specular or LOS component in addition to random scatterers, the channel impulse response will have a nonzero-mean value and the envelope of the received signal will follow a Ricean density [9]

$$f_R(r) = \frac{r}{\sigma^2} \exp\left(-\frac{r^2+s^2}{2\sigma^2}\right) I_0\left(\frac{rs}{\sigma^2}\right), \quad r \geq 0 \tag{1.4}$$

where $I_0(\cdot)$ is the zeroth-order modified Bessel function of the first kind, σ^2 is the variance of the Gaussian scatter component, and s^2 is the noncentrality parameter. To describe the degree of fading, it is often convenient to define the Rice factor as the ratio of specular power to scattered power, that is, $K = s^2/2\sigma^2$. When $K = 0$, the channel has no specular component and (1.4) reduces to the Rayleigh PDF. On the other hand, when $K = \infty$, the channel does not exhibit any fading. If $\Omega = \mathrm{E}[r^2] = s^2 + 2\sigma^2$ is used to denote the average power of the received signal, then the PDF of R can be written as

$$f_R(r) = \frac{2r(K+1)}{\Omega} \exp\left(-K - \frac{(K+1)r^2}{\Omega}\right) I_0\left(2r\sqrt{\frac{K(K+1)}{\Omega}}\right), \quad r \geq 0. \tag{1.5}$$

Figure 1.3 shows the Ricean density for several values of K.

Nakagami Fading: The Nakagami distribution (m-distribution) [10] is a generalized distribution which can accurately model different fading environments. Moreover, the versatility

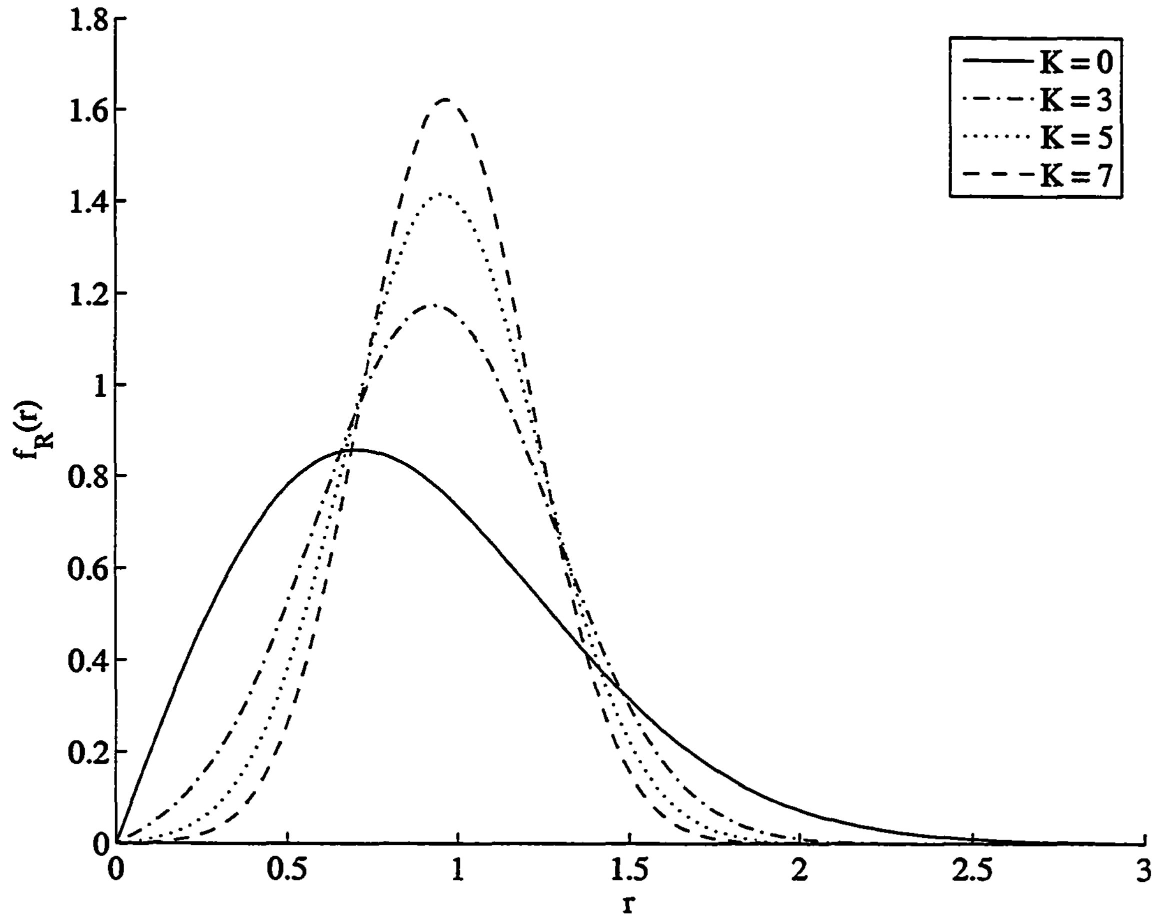

Fig. 1.3. The Ricean PDF for several values of K and $\Omega = 1$.

of the Nakagami distribution allows it to fit some urban wireless channel data better than the commonly used Rayleigh, Ricean, or lognormal distributions [11], [12]. The magnitude of the received envelope in Nakagami fading is described by the density

$$f_R(r) = \frac{2m^m r^{2m-1}}{\Gamma(m)\Omega^m} \exp\left(-\frac{m}{\Omega}r^2\right), \quad r \geq 0 \tag{1.6}$$

where $m \geq 0.5$, $\Omega = \mathrm{E}[R^2]$ controls the spread of the distribution, and $\Gamma(\cdot)$ is the gamma function. In the context of the Nakagami fading model, the constant m is the fading severity parameter and Ω is the average power of the received signal. The Rayleigh ($m = 1$) and one-sided Gaussian ($m = 0.5$) distributions are special cases of the Nakagami distribution, as is the nonfading case ($m = \infty$). In addition, the Rice distribution can sometimes be approximated with a Nakagami distribution by using the following relationship between the Rice factor K and the Nakagami shape factor m [10]

$$K = \frac{\sqrt{m^2 - m}}{m - \sqrt{m^2 - m}}, \quad m > 1 \tag{1.7}$$

$$m = \frac{(K+1)^2}{2K+1}. \tag{1.8}$$

Caution must be exercised in using this approximation as the tails of the Ricean distribution decrease at a different rate than the tails of the Nakagami distribution when $m \neq 1$. Figure 1.4 shows the Nakagami density for several values of m.

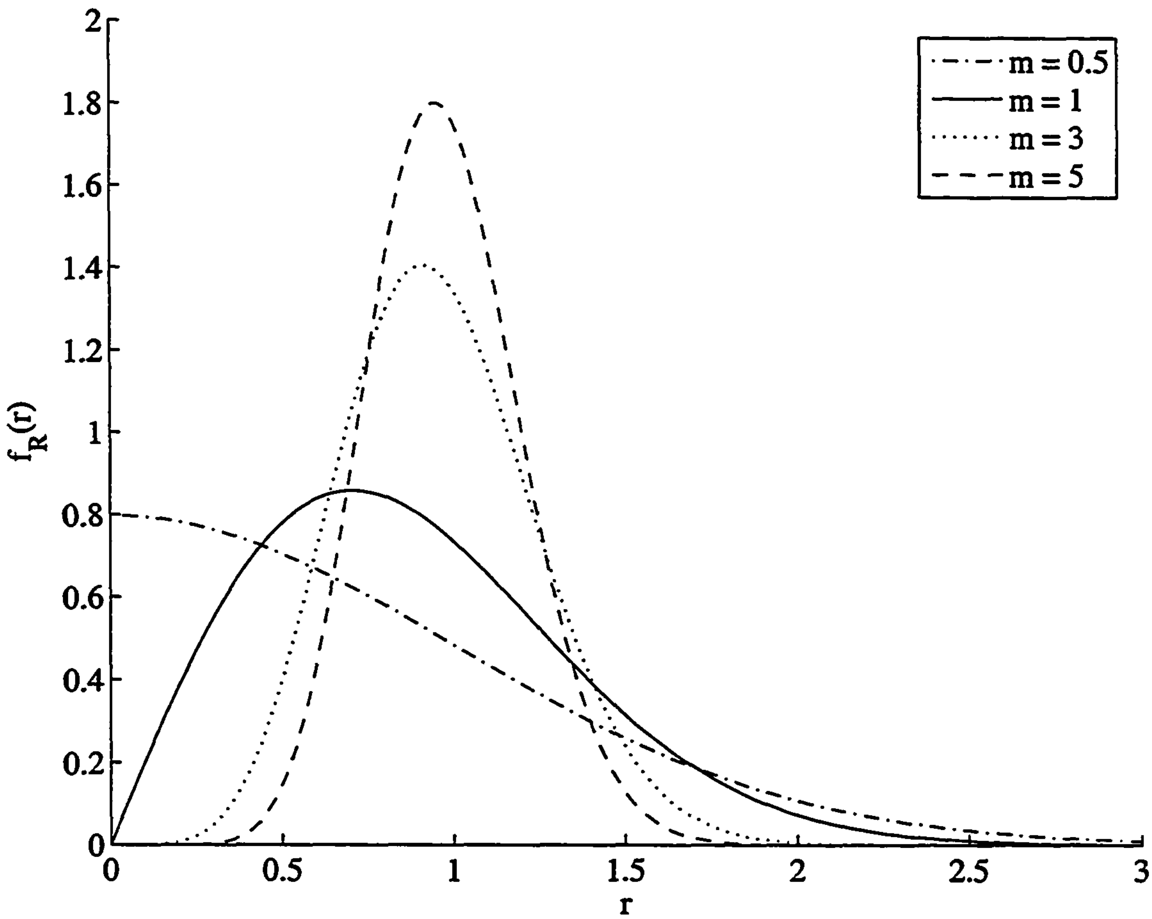

Fig. 1.4. The Nakagami PDF for several values of m and $\Omega = 1$.

1.3 Diversity

Diversity is an effective technique to mitigate the deleterious effects of multipath fading [3], [13]. To understand the basic concept underlying diversity, consider a system where L independently faded replicas of the transmitted signal arrive at the receiver. If p denotes the probability that the instantaneous SNR of each of the copies is below a critical threshold, then p^L is the probability that the instantaneous SNR is below the same critical threshold for all L copies. In general, p^L will be much less than p, resulting in a substantial improvement in the reliability of the communication system.

To obtain multiple copies of the transmitted signal, methods such as frequency diversity, time diversity, and spatial or antenna diversity have been proposed [14]. The common theme behind these methods is to produce multiple versions of the transmitted signal at the receiver, each of which have experienced uncorrelated fading. In frequency diversity, the same signal is sent over multiple channels that are sufficiently spaced. Time diversity is obtained by transmitting the same signal at multiple time periods that are suitably separated. Spatial or antenna diversity uses multiple antennas and relies on the fact that the received signals are essentially uncorrelated if the antennas are separated by one-half wavelength or more apart.

1.3.1 Diversity Combining

Provided that the receiver is able to obtain uncorrelated faded replicas of the original information bearing signal, there are several methods of combining these signals. Here, we will focus on linear diversity combining techniques. In these methods, the signals on each of the L diversity branches are first weighted and then summed together as shown in Figure 1.5. If the combining occurs at radio frequency, then it is called predetection combining. On the other hand, postdetection combining occurs when the combining is done at baseband. In many cases, predetection and postdetection methods will yield the same performance [4]. In this thesis, the predetection combining diversity receiver is considered.

If the signal $s_m(t)$ is transmitted, then the signal on the i-th branch at any time t can be

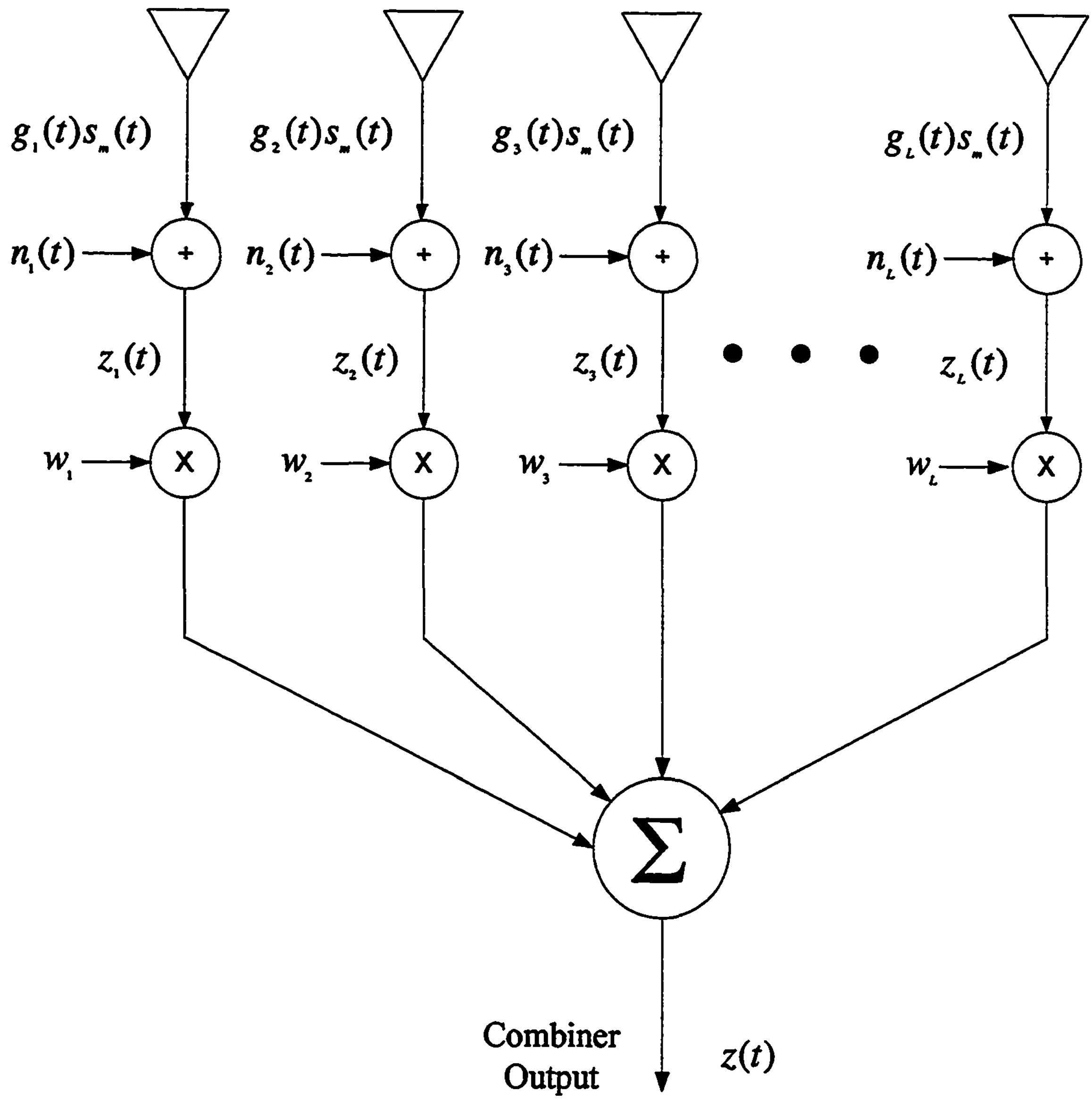

Fig. 1.5. The L-branch linear diversity combiner.

expressed as

$$z_i(t) = g_i(t)s_m(t) + n_i(t), \quad i = 1, \cdots, L \tag{1.9}$$

where

$$g_i(t) = R_i(t)e^{-j\phi_i(t)}, \quad i = 1, \cdots, L \tag{1.10}$$

are the complex fading gains and $n_i(t)$ is additive white Gaussian noise (AWGN) with power spectral density $N_0/2$. AWGN models the thermal noise that is present at the front-end of the receiver and is assumed to be independent of the fading amplitudes. The resultant signal at the output of the linear combiner can be expressed as

$$z(t) = \sum_{i=1}^{L} w_i z_i(t) \tag{1.11}$$

where w_i is the combining weight used on the i-th branch. These weights are determined by the type of combining used and are directly related to the complexity and performance of the system. The most widely considered linear combining techniques are as follows.

Selective Combining (SC): SC operates on the principle that the diversity branch which yields the highest SNR is always selected. That is, the weighting factors are all zero except for the branch with the largest SNR. Thus, the diversity combiner simply yields the output SNR

$$\gamma_{SC} = \max_{i \in 1 \cdots L} \{\gamma_i\} \tag{1.12}$$

where γ_i is the instantaneous SNR of the i-th diversity branch. Since SC requires continuous and instantaneous measurement of all diversity branches, the signal fading rate must be sufficiently slow to allow the selection circuitry adequate time to select the correct branch.

Maximal Ratio Combining (MRC): In MRC, the diversity branches are first weighted by the complex conjugate of their respective fading gains and then combined. Thus, the combiner first generates the weights

$$w_i = g_i^* = R_i e^{j\phi_i}, \quad i = 1, \cdots, L \tag{1.13}$$

and then produces the sum

$$z_{MRC}(t) = \sum_{i=1}^{L} R_i e^{j\phi_i} z_i(t). \tag{1.14}$$

The envelope of the composite signal component after weighting and combining is

$$R_{MRC} = \sum_{i=1}^{L} R_i^2. \tag{1.15}$$

The weighted sum of the branch noise powers is

$$\sigma_{MRC}^2 = \frac{N_0}{2} \sum_{i=1}^{L} R_i^2 \tag{1.16}$$

where $N_0/2$ is the noise power on each of the diversity branches. Thus, the output SNR of the diversity combiner is

$$\gamma_{MRC} = \frac{R_{MRC}^2}{2\sigma_{MRC}^2} = \sum_{i=1}^{L} \frac{R_i^2}{N_0} = \sum_{i=1}^{L} \gamma_i. \tag{1.17}$$

For an AWGN channel, MRC is the optimum combining technique in the sense that it provides a maximum-likelihood receiver. However in some cases, MRC may not be practical due to the complexity in obtaining the channel gains on each diversity branch.

Equal Gain Combining (EGC): In EGC, the diversity branches are co-phased as in MRC, however, the branch weights are not weighted by the fading gains prior to combining. Thus, the combiner first generates the weights

$$w_i = e^{j\phi_i}, \quad i = 1, \cdots, L \tag{1.18}$$

and then produces the sum

$$z_{EGC}(t) = \sum_{i=1}^{L} e^{j\phi_i} z_i(t). \tag{1.19}$$

The envelope of the composite signal component after co-phasing and combining is

$$R_{EGC} = \sum_{i=1}^{L} R_i \tag{1.20}$$

and the weighted sum of the branch noise powers is

$$\sigma_{EGC}^2 = L\frac{N_0}{2}. \tag{1.21}$$

This results in an output SNR of

$$\gamma_{EGC} = \frac{R_{EGC}^2}{2\sigma_{EGC}^2} = \frac{\left(\sum_{i=1}^{L} R_i\right)^2}{LN_0}. \tag{1.22}$$

Despite offering suboptimum performance, EGC is often used in practice because it is less complex than MRC. This is because EGC does not require knowledge of the fading amplitudes, whereas, in MRC, the fading amplitudes in each signal branch must be known. Thus, EGC is commonly used when noncoherent modulation or modulation techniques involving equal energy symbols are employed [4]. These types of modulation typically do not require complete knowledge of the fading gains for demodulation.

As seen in (1.20) and (1.22), if Rayleigh, Ricean, or Nakagami fading is assumed, then the envelope and SNR at the combiner output of an EGC system will involve a sum of Rayleigh, Ricean, or Nakagami RVs, respectively. Under these assumptions, the cumulative distribution function (CDF) or PDF for R_{EGC} and γ_{EGC} do not exist in closed-forms for most cases. For the specific case when $L = 2$ and Rayleigh fading is assumed, closed-form solutions for the CDF and PDF of R_{EGC} and γ_{EGC} are given in [15] and [4], respectively.

1.4 Literature Review

This review provides a summary of the key references used in this thesis.

In his classic diversity paper [3], Brennan describes the difficulty of computing the distribution of a sum of independent Rayleigh RVs. Nevertheless, by numerically integrating the convolutional formula for the distribution of a sum of independent Rayleigh RVs, he publishes accurate values for these distribution functions. These values were used as the standard reference for more than 30 years until an efficient Fourier series solution was proposed. This approximate method proposed by Beaulieu [16] involves using an infinite series to compute the CDF of a sum of independent Rayleigh RVs. The lack of closed-form solutions for the distribution and density of a sum of Rayleigh RVs has also resulted in the development of various numerical routines and approximations. A relatively simple and widely used small argument approximation (SAA) for the sum PDF of Rayleigh RVs was proposed by Stein [14]. This approximation was derived based on the observation that at small SNRs, there is an essentially constant ratio between EGC and MRC statistics.

The literature on EGC performance is meager in comparison to what is available for other popular diversity methods. In fact, after Brennan's quantitative analysis of EGC [3], the first comprehensive paper giving precise analysis of EGC with digital modulation did not appear until the early 1990s. The infinite series technique is employed in [17], [18], and [19] to analyze the performance of EGC in Ricean and Nakagami fading. Other studies on EGC diversity systems in fading channels are found in [20], [21], and [22]. Despite providing accurate analysis, these results are somewhat complex since they require the computation of an infinite series or numerical integration. In [1] and [5], the performance of EGC diversity systems in Rayleigh fading is approximated by utilizing the SAA to simplify the analysis.

1.5 Thesis Outline and Contributions

This thesis is organized as follows. In this chapter, an overview of the time-varying propagation channel and some typical methods of modeling the wireless channel were given. The multipath fading environment is explained and the distinction between large-scale and small-scale fading is made. Next, the four types of small-scale fading are defined. In this thesis, only small-scale fading on slowly-varying flat channels will be considered. The most common statistical models for flat fading are subsequently described. An introduction to diversity and linear combining techniques concluded this chapter. The necessity of finding approximations for the sum distributions and densities of Rayleigh, Ricean, and Nakagami RVs was demonstrated in the context of EGC diversity systems.

Chapter 2 begins by introducing the problem of finding the distribution and density of a sum of independent Rayleigh RVs and the various approaches that have been proposed to handle this problem. A widely used SAA for the sum density is considered and shown to be accurate if only values in the lower tail of the density are considered. If values near the mean or in the upper tail of the density are required, then this approximation lacks sufficient accuracy. In order to achieve accuracy over a wide range of arguments, the SAA is modified and an accurate closed-form approximation to the Rayleigh sum distribution is proposed. In addition, an accurate closed-form approximation to the Rayleigh sum PDF is derived.

Approximations for the distribution and density of a sum of independent Ricean RVs is the focus of Chapter 3. Using insight provided by considering the SAA to the PDF of a Rayleigh sum, accurate closed-form approximations to the Ricean sum CDF and PDF are derived. These approximations are based on modifying the sum distribution of squared Ricean RVs.

Chapter 4 uses a similar argument as Chapter 3 to derive approximations for the distribution and density of a sum of independent Nakagami RVs. Accurate closed-form approximations to the Nakagami sum CDF and PDF are derived by modifying the sum distribution of squared Nakagami RVs.

The performance analysis of EGC diversity systems is the focus of Chapter 5. In particular, the approximations developed in Chapter 4 are applied to determine simple approximate solutions for the performances of these systems in Nakagami fading. Closed-form expressions for the average error and outage probabilities are derived and compared with the solutions found using numerical integration or simulation.

Chapter 6 concludes the thesis with a summary of contributions.

Chapter 2

Accurate Closed-Form Approximations to Rayleigh Sum Distributions and Densities

2.1 Sum of Rayleigh RVs

A longstanding problem in statistics is to determine the PDF, or equivalently, the CDF, of a sum of L independent Rayleigh RVs. In fact, this problem can be traced back to Lord Rayleigh himself, but has never been solved in terms of tabulated functions for $L \geq 3$ [1]. Finding the sum distribution of independent Rayleigh RVs will be useful for several practical wireless communication applications. For example, such sums occur in the measurement of SNR for handoff and in the evaluation of EGC diversity systems when determining the error or outage probabilities [3]. For the case when $L = 2$, Altman and Sichak have found the PDF in closed-form [15]. However, for an arbitrary sum, there is no closed-form solution. As a result, numerical evaluations and approximations have been developed.

Several approaches have been proposed to compute the distribution and density of a sum of Rayleigh RVs. A well known approach [16] involves using an infinite series representation to obtain the CDF precisely. Prior to the publication of this method, curves and tables of the distribution of a sum of Rayleigh RVs for eight or fewer summands were published, for example, in [3] and [23]. These results rely on numerical integration of the convolutional formula for the distribution of a sum of independent Rayleigh RVs. A recent well known text proposes and explains the use of Rayleigh graph paper for calculating receiver noise figures [24]. In this method, the Rayleigh sum CDF is determined graphically.

A relatively simple and widely used SAA for the sum PDF was derived in [14]. Let $r_1, r_2, \ldots, r_L$ be the amplitudes of L statistically independent RVs, which follow the Rayleigh density

$$f_{R_i}(r_i) = \frac{r_i}{\sigma_i^2} e^{-\frac{r_i^2}{2\sigma_i^2}}, \quad r_i \geq 0 \tag{2.1}$$

where $(2-\pi/2)\sigma_i^2$ is the variance of the density. Without loss of generality, consider the normalized (scaled) RV $X_i = R_i/\sigma_i$. Then

$$f_{X_i}(x_i) = x_i e^{-\frac{x_i^2}{2}}, \quad x_i \geq 0. \tag{2.2}$$

Let

$$Z = \sum_{i=1}^{L} X_i = X_1 + X_2 + \cdots + X_L \tag{2.3}$$

be a sum of L independent and identically distributed (iid) Rayleigh RVs. The SAA to the PDF of a Rayleigh sum is

$$f_{SAA}(t) = \frac{t^{2L-1} e^{-\frac{t^2}{2b}}}{2^{L-1} b^L (L-1)!}, \tag{2.4a}$$

$$b = \frac{\sigma^2}{L}[(2L-1)!!]^{1/L} \tag{2.4b}$$

where $(2L-1)!! = (2L-1)(2L-3)\cdots 3\cdot 1$ and $t = x/\sqrt{L}$ is the normalized argument. This SAA originates from [14]; to the best of the author's knowledge, the accuracy of the SAA in (2.4) has not been reported in the open literature. Despite this, the SAA has gained acceptance for describing and examining the statistics of sums of multiple iid Rayleigh fading sources [1], [5], [10]. Interestingly, the PDF approximation (2.4) has the form of the Nakagami density. This is consistent with, and indeed related to, the fact that the statistics of EGC are well approximated by the statistics of MRC with an appropriately scaled argument, for small values of the argument [14]. The exact PDF and the SAA for $L = 3, 8$, and 16 are shown in Figures 2.1-2.3. The solid lines show the exact PDF and the dashed lines represent the SAA. One observes that this approximation is accurate if one considers only values in the lower tail of the density. If values near the mean or in the upper tail of the density are required, then this approximation lacks sufficient accuracy.

In this chapter, an accurate closed-form approximation to the Rayleigh sum distribution is presented. In addition, an accurate closed-form approximation to the Rayleigh sum PDF is derived. These approximations are based on modifying the SAA so that it is accurate for a wide range of arguments.

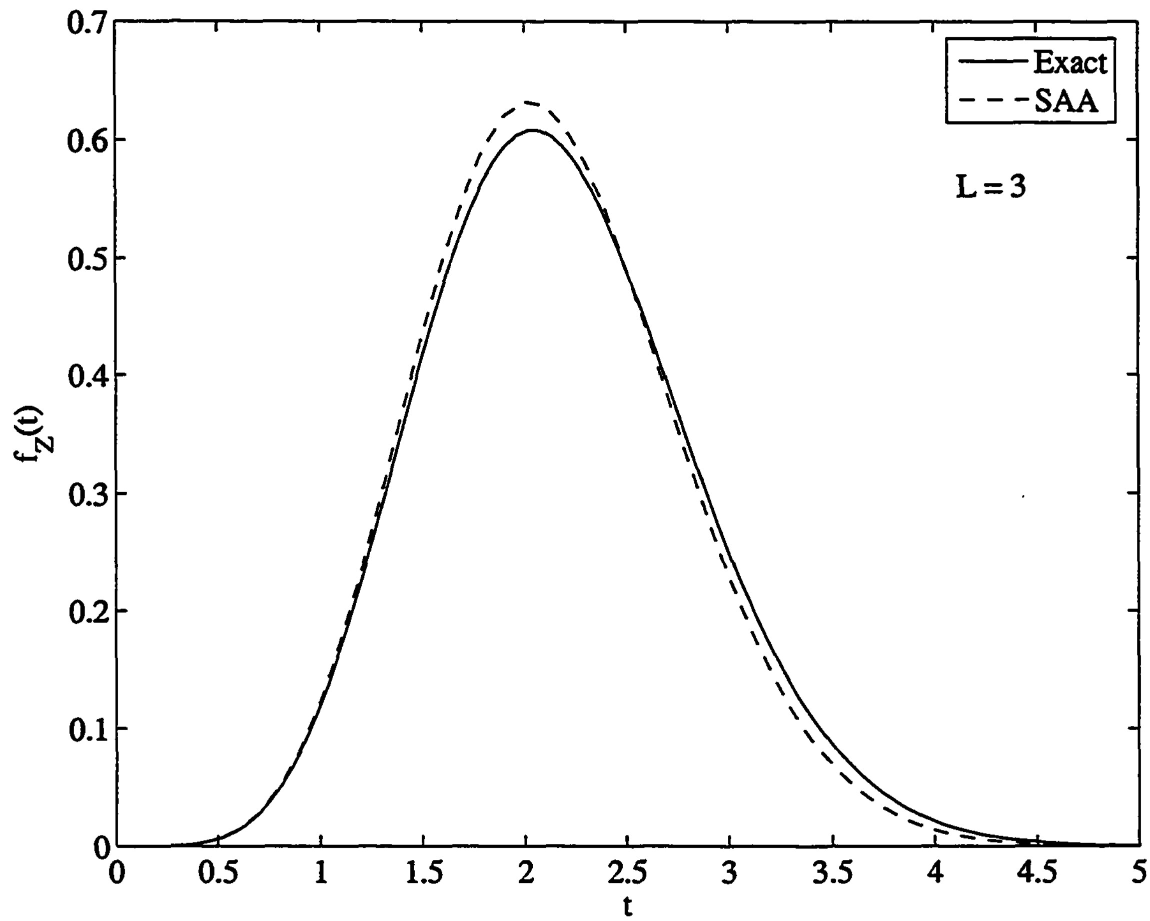

Fig. 2.1. The PDF of a sum of L Rayleigh RVs and the SAA for $L = 3$.

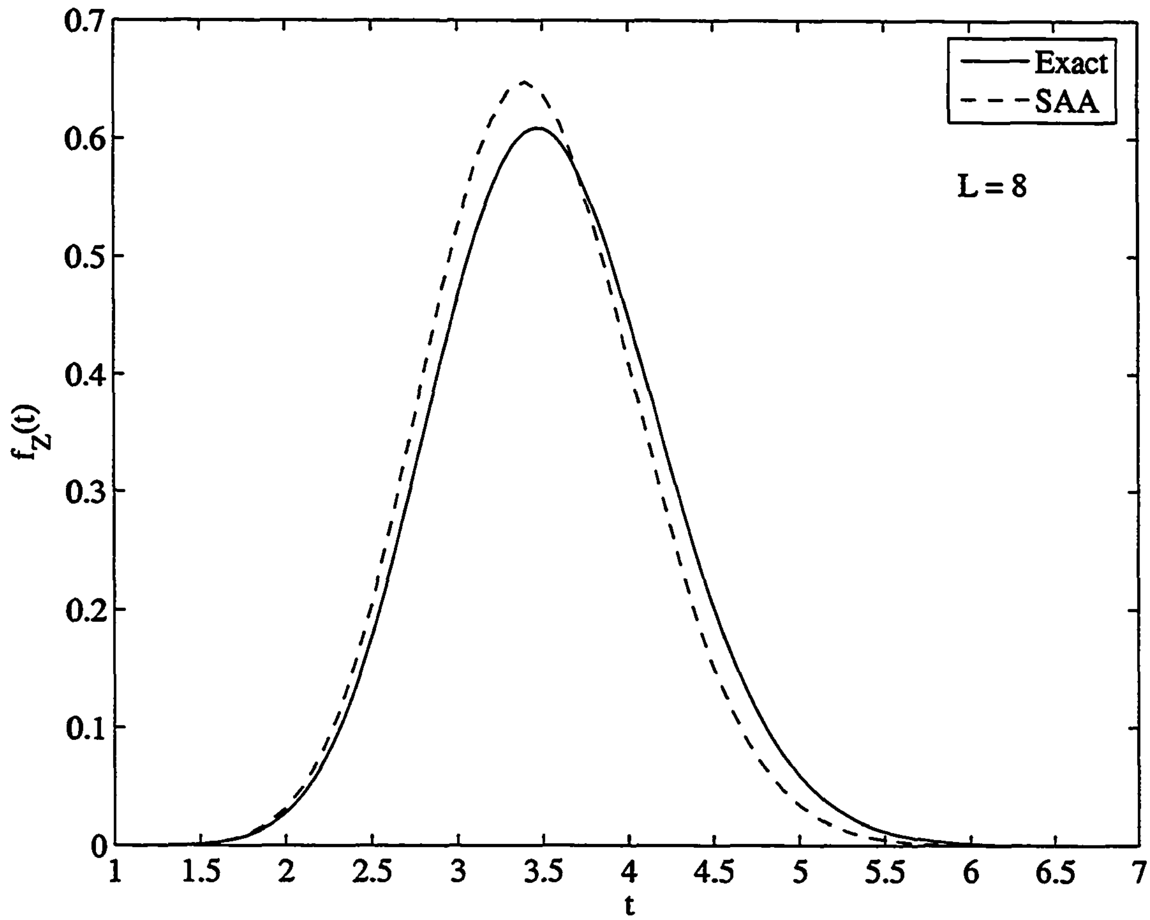

Fig. 2.2. The PDF of a sum of L Rayleigh RVs and the SAA for $L = 8$.

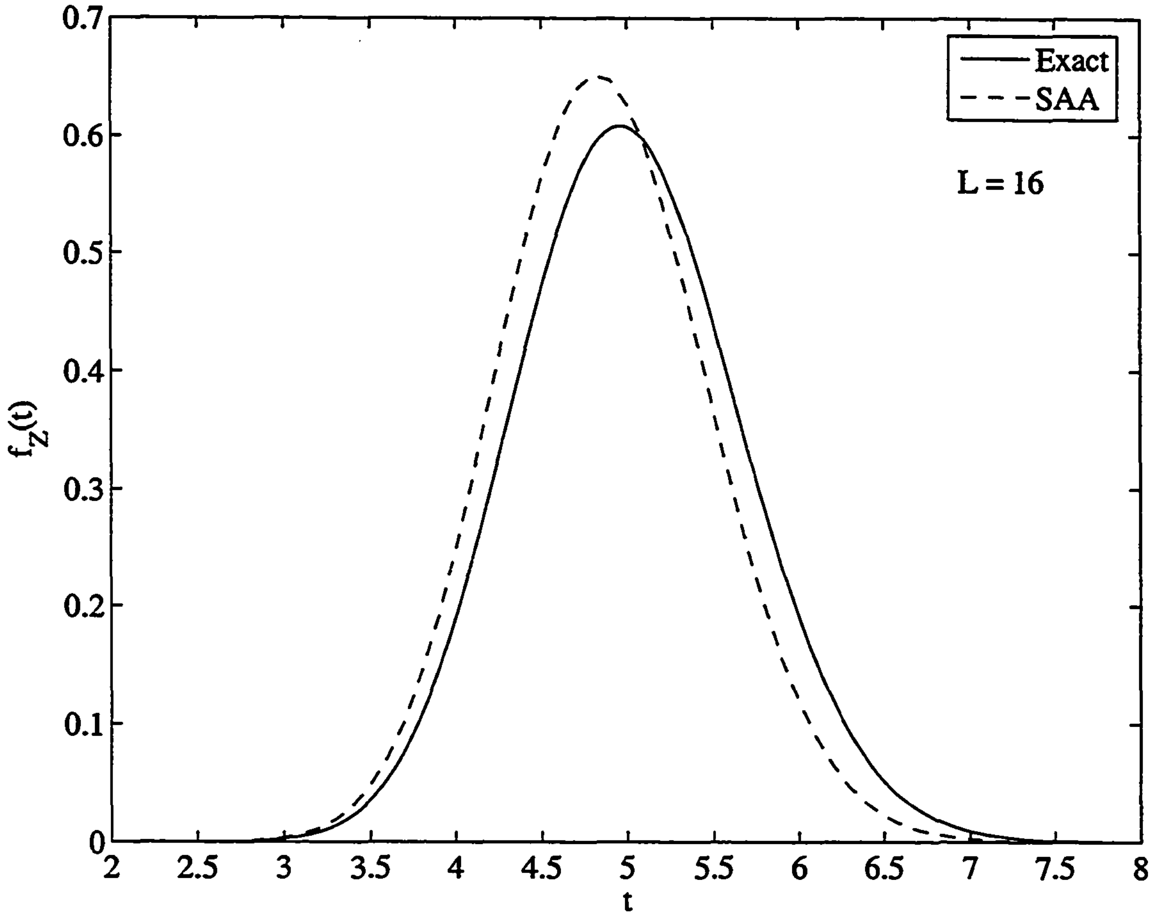

Fig. 2.3. The PDF of a sum of L Rayleigh RVs and the SAA for $L = 16$.

2.2 Rayleigh Sum CDF Approximation

Integration of (2.4) yields a SAA to the CDF of a Rayleigh sum given by

$$F_{SAA}(t) = 1 - e^{-\frac{t^2}{2b}} \sum_{k=0}^{L-1} \frac{\left(\frac{t^2}{2b}\right)^k}{k!} \tag{2.5}$$

which has the form of a simple finite sum. The symbols in Figure 2.4 show the SAA CDF of Z and the solid lines show the exact CDF for values of $L = 3, 5, 8, 12$, and 16 plotted on normal probability paper. One observes from Figure 2.4 that the approximation is excellent for small values of t. However, for medium and large values of t, the approximation is not as good. For example, when the complementary CDF is 2.0×10^{-5}, the SAA complementary CDF is 2.3×10^{-6} and 1.5×10^{-6} for $L = 8$ and $L = 16$, respectively. These SAA values correspond to an overestimate of the exact complementary CDF by more than 8 times for $L = 8$ and more than 13 times for $L = 16$. The SAA is best for the $L = 3$ case and becomes less accurate as L increases. This is expected since the approximation is exact for all values of the argument when $L = 1$.

Improved closed-form approximations to the CDF and PDF of Rayleigh sums will be useful for many applications, including error rate and outage calculations for wireless systems. In order to improve the SAA, the error between the exact CDF and the SAA CDF was first examined. Figure 2.5 shows the error of the small argument CDF approximation for $L = 3, 8, 12$, and 16. It was found empirically that for all values of L considered, the difference is well approximated by a function which has the general form

$$F_{Error}(t) \cong t\, \frac{a_0 (t - a_2)^{2L-1} e^{-\frac{a_1 (t-a_2)^2}{2b}}}{2^{L-1} (\frac{b}{a_1})^L (L-1)!} \tag{2.6}$$

where a_0, a_1, and a_2 are constants to be determined and b is again given by (2.4b). Although ad-hoc, the mathematical form of $F_{Error}(t)$ in (2.6) is intuitive. It approximates the derivative of $F_{SAA}(t)$ multiplied by t; the constant a_2 permits shifting the mode of the approximation to align with the mode of the true PDF; constants a_0 and a_1 allow scaling the amplitude and the spread, respectively, of the correction function to best match the true error.

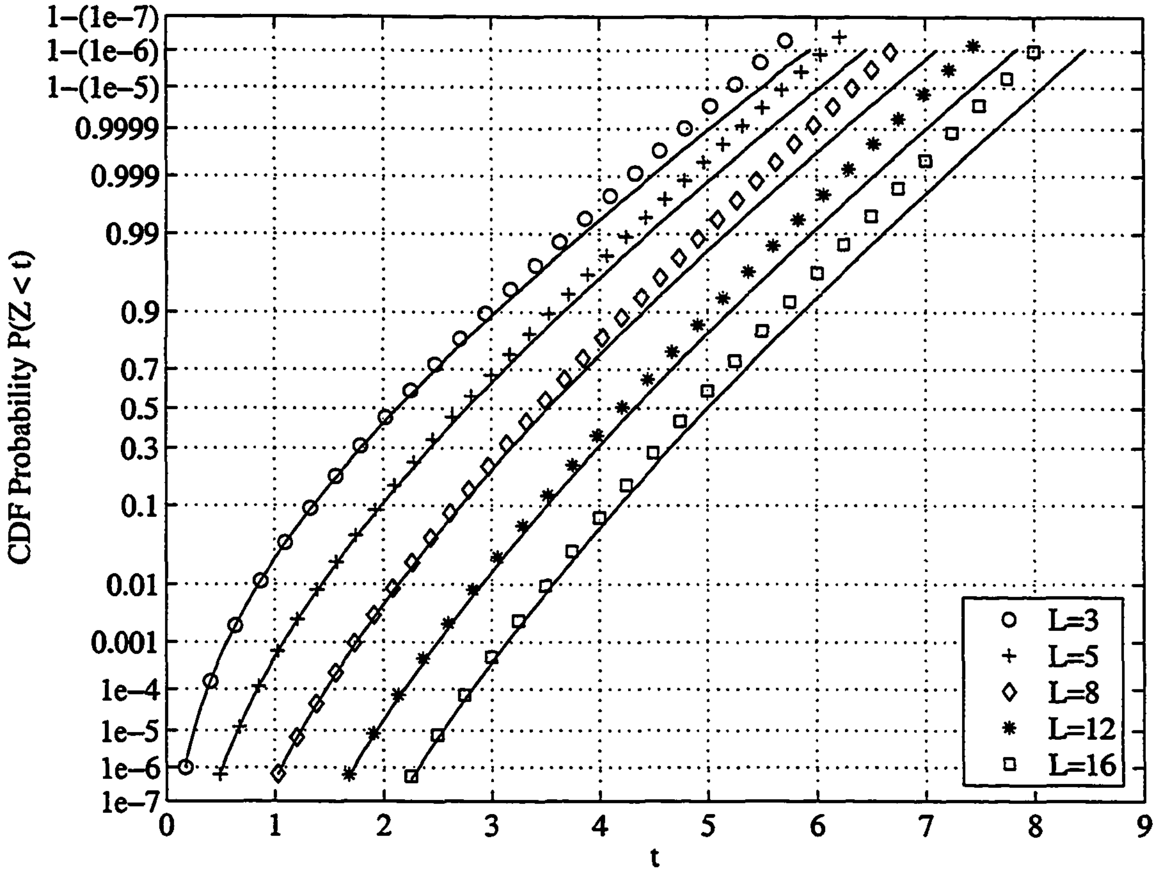

Fig. 2.4. The CDF of a sum of L Rayleigh RVs and the SAA for $L = 3, 5, 8, 12$, and 16.

Thus, the proposed modified approximation for the CDF of Z is given as

$$\begin{aligned} F_L(t) &= F_{SAA}(t) - F_{Error}(t) \\ &= 1 - e^{-\frac{t^2}{2b}} \sum_{k=0}^{L-1} \frac{\left(\frac{t^2}{2b}\right)^k}{k!} - t\,\frac{a_0(t-a_2)^{2L-1} e^{-\frac{a_1(t-a_2)^2}{2b}}}{2^{L-1}(\frac{b}{a_1})^L (L-1)!}. \end{aligned} \tag{2.7}$$

A nonlinear least squares method based on the interior-reflective Newton method described in [25] is used to optimize the constants a_0, a_1, and a_2 in (2.6). These constants are given in Table 2.1. Figure 2.6 compares the new closed-form CDF approximation represented by the symbols with the exact CDF represented by the solid lines. Observe that the approximation is excellent for a very wide range of probabilities and for all values of L considered.

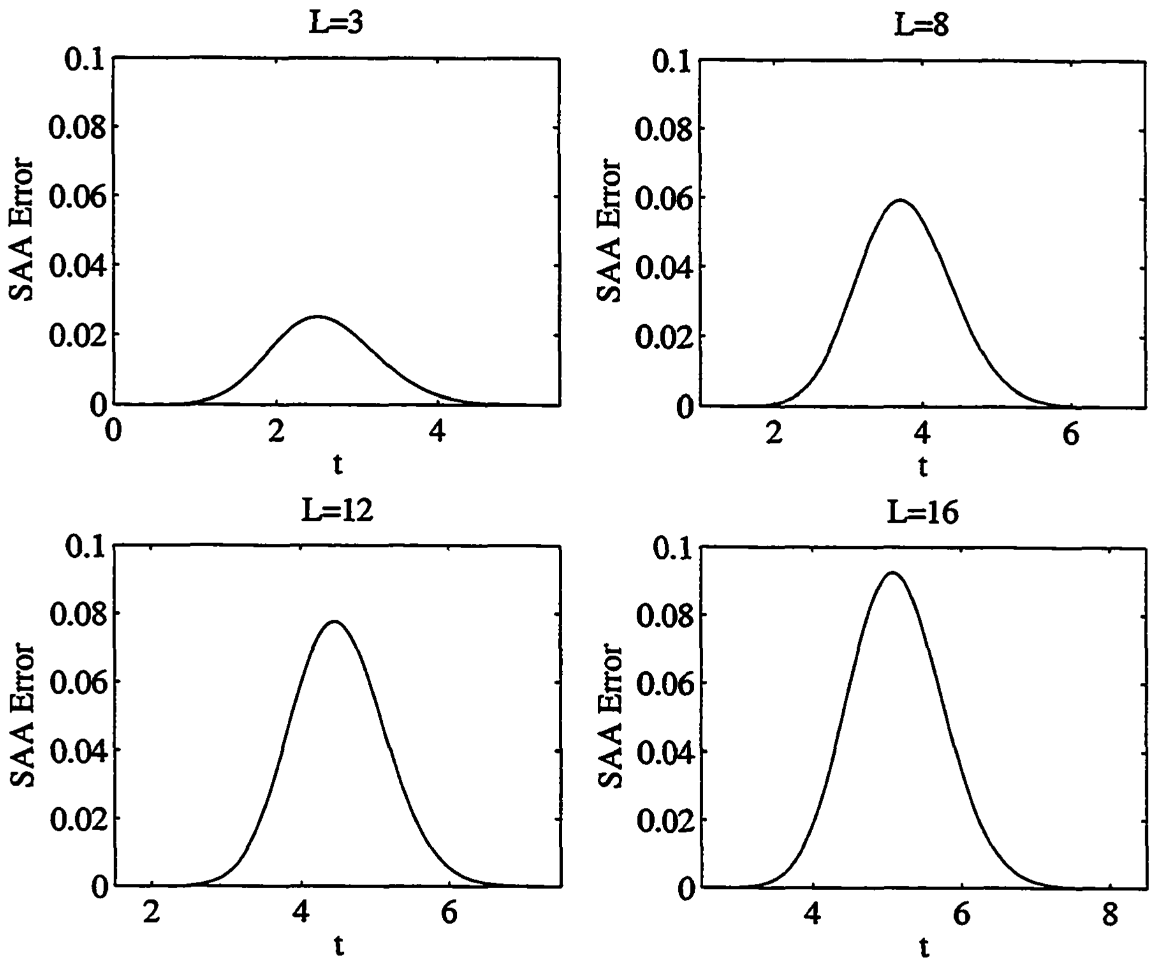

Fig. 2.5. The small argument CDF approximation error for $L = 3$, 8, 12, and 16.

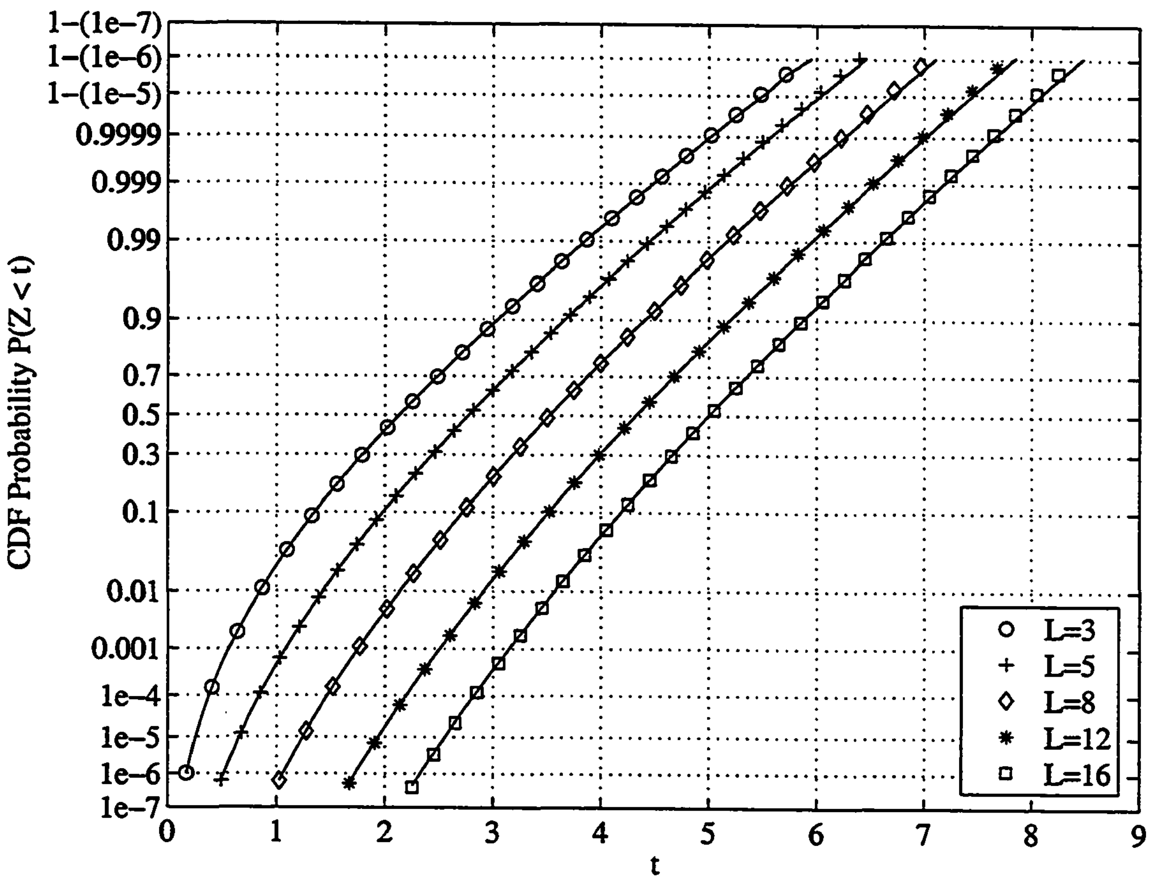

Fig. 2.6. The CDF of a sum of L Rayleigh RVs and the modified closed-form approximation for $L = 3, 5, 8, 12,$ and 16.

2.3 Rayleigh Sum PDF Approximation

A new approximation to the PDF of Z can be formally derived from the CDF approximation by using the following relationship

$$f_L(t) \triangleq \frac{\mathrm{d}F_L(t)}{\mathrm{d}t} \tag{2.8}$$

where $f_L(t)$ is the PDF approximation.

In general, differentiating an accurate approximation to the CDF will not necessarily lead to an accurate approximation of the PDF. For example, consider a Fourier approximation to a square wave, the derivative for the Fourier approximation is finite at a positive transition point while the actual derivative at the transition point is infinite. In this case, however, taking the derivative of the CDF approximation in (2.7) yields an accurate PDF approximation while using the same coefficients given in Table 2.1, as seen in Figures 2.7-2.9. The solid lines show the exact PDF and the circles represent the modified closed-form approximation. The proposed approximation to the PDF of a Rayleigh sum is then

$$f_L(t) = \frac{t^{2L-1}e^{-\frac{t^2}{2b}}}{2^{L-1}b^L(L-1)!} - \frac{(t-a_2)^{2L-2}e^{-\frac{a_1(t-a_2)^2}{2b}}}{2^{L-1}b(\frac{b}{a_1})^L(L-1)!}a_0[b(2Lt-a_2)-a_1t(t-a_2)^2]. \tag{2.9}$$

2.4 Summary

An accurate closed-form approximation to the Rayleigh sum distribution based on modifying the SAA to the PDF of a Rayleigh sum was introduced in this chapter. It was observed that the new approximation is accurate over a wide range of probabilities and number of summands. Furthermore, by differentiating the CDF approximation, it is possible to obtain a closed-form PDF approximation that is also accurate over the same large range.

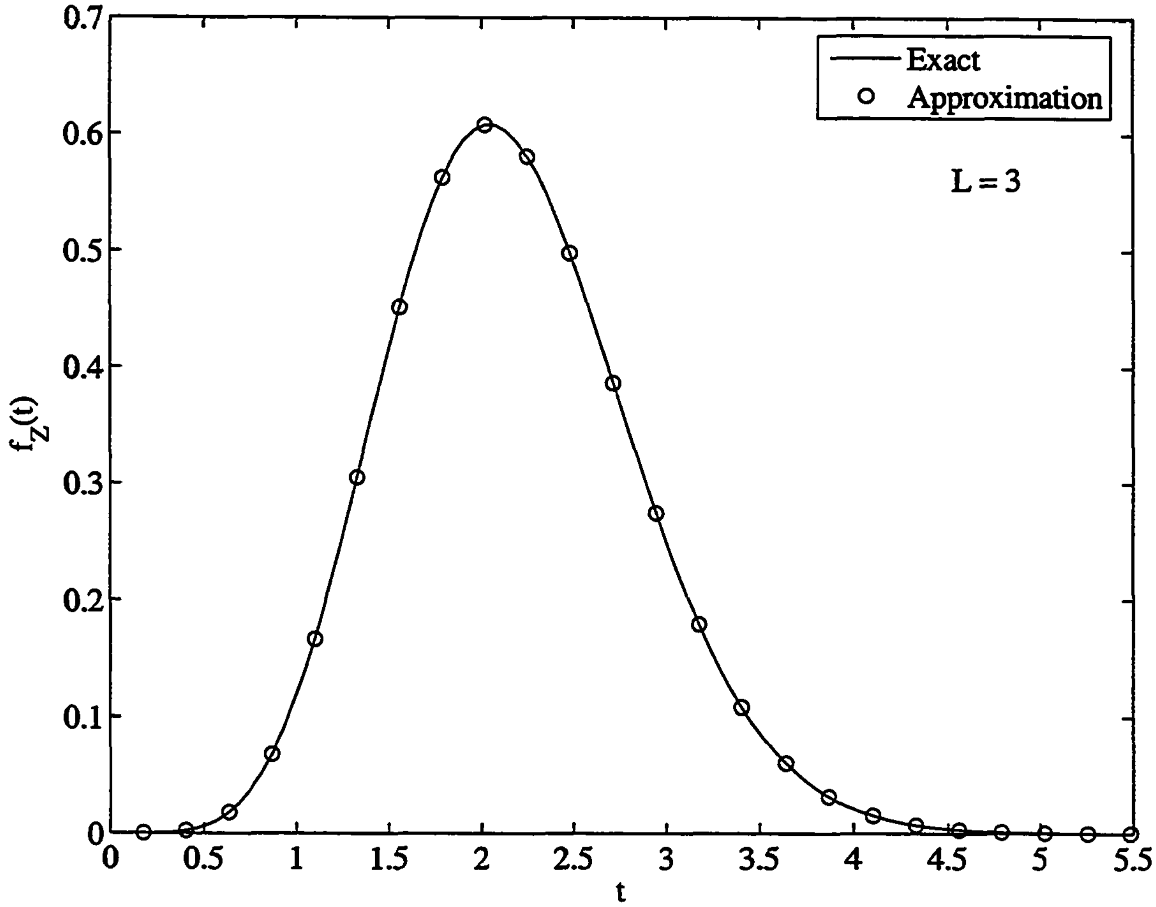

Fig. 2.7. The PDF of a sum of L Rayleigh RVs and the modified closed-form approximation for $L = 3$.

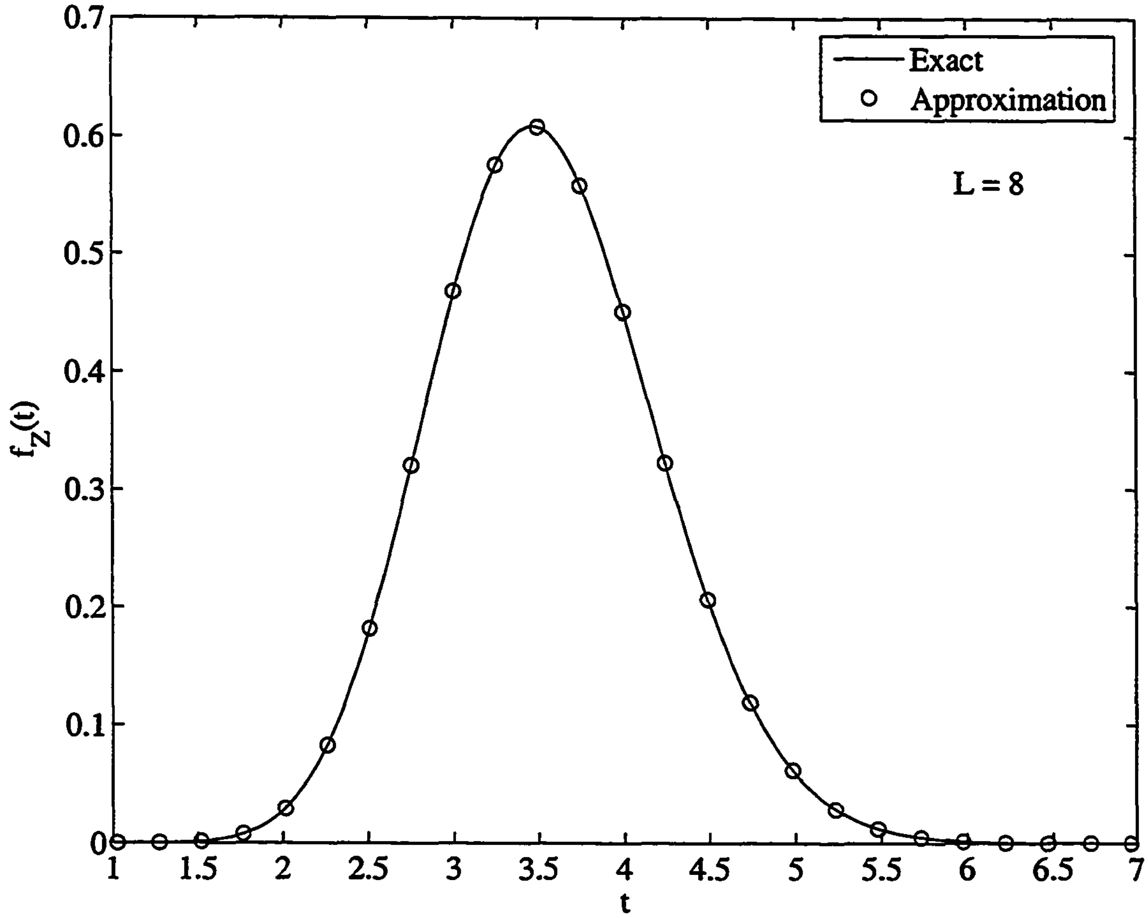

Fig. 2.8. The PDF of a sum of L Rayleigh RVs and the modified closed-form approximation for $L = 8$.

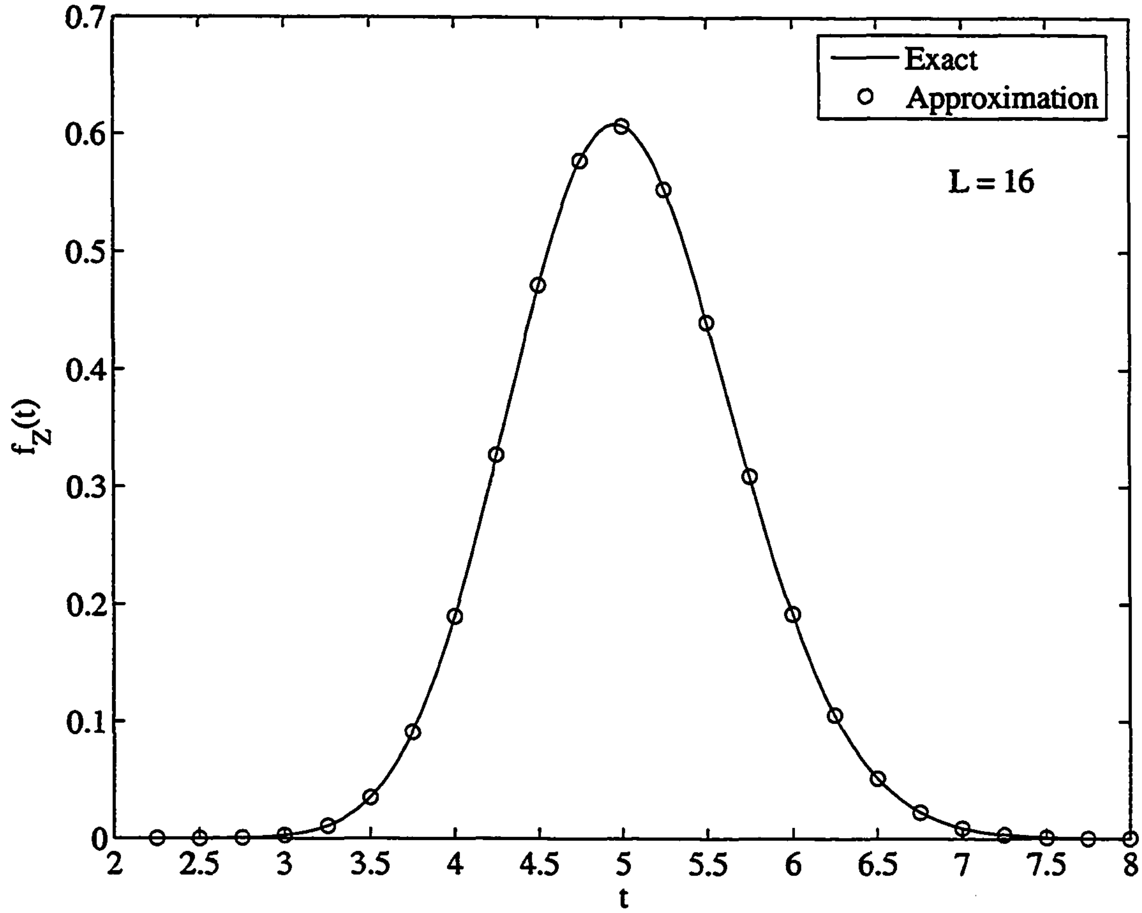

Fig. 2.9. The PDF of a sum of L Rayleigh RVs and the modified closed-form approximation for $L = 16$.

TABLE 2.1

Coefficients for the Rayleigh sum CDF and PDF approximations.

$$F_L(t) = 1 - e^{-\frac{t^2}{2b}} \sum_{k=0}^{L-1} \frac{\left(\frac{t^2}{2b}\right)^k}{k!} - t\,\frac{a_0(t-a_2)^{2L-1} e^{-\frac{a_1(t-a_2)^2}{2b}}}{2^{L-1}(\frac{b}{a_1})^L(L-1)!}$$

$$f_L(t) = \frac{t^{2L-1} e^{-\frac{t^2}{2b}}}{2^{L-1} b^L (L-1)!} - \frac{(t-a_2)^{2L-2} e^{-\frac{a_1(t-a_2)^2}{2b}}}{2^{L-1} b (\frac{b}{a_1})^L (L-1)!} a_0[b(2Lt - a_2) - a_1 t(t-a_2)^2]$$

$$b = \frac{\sigma^2}{L}[(2L-1)!!]^{1/L}, \quad \sigma = 1$$

L	a_0	a_1	a_2
3	0.0164	0.3060	0.9928
4	0.0198	0.2413	0.9760
5	0.0221	0.1972	0.9654
6	0.0236	0.1645	0.9583
7	0.0248	0.1386	0.9531
8	0.0257	0.1172	0.9491
9	0.0264	0.0989	0.9460
10	0.0270	0.0829	0.9434
11	0.0275	0.0686	0.9412
12	0.0279	0.0557	0.9393
13	0.0283	0.0440	0.9377
14	0.0286	0.0330	0.9363
15	0.0288	0.0229	0.9350
16	0.0291	0.0133	0.9338

Chapter 3

Accurate Closed-Form Approximations to Ricean Sum Distributions and Densities

3.1 Sum of Ricean RVs

The analytical evaluation of the performance of a wireless communication system requires that the signal statistics at the receiver be known. Hence, for some systems, there is a need for the accurate computation of the CDF and the PDF of a sum of L statistically independent Ricean RVs. For example, in wireless channels where there exists a LOS between the transmitter and receiver, such sums occur in the evaluation of EGC diversity systems when determining the error probability, level crossing rate, and average fade duration [17], [18].

Despite its wide applicability, few published results on the sum distribution exist. This lack may be attributed to the difficulty in numerically calculating the distribution since there is no closed-form expression for the characteristic function (CHF) of a Ricean RV.

Several approaches have been proposed to compute the distribution of a sum of Ricean RVs. A precise infinite series representation of the CDF is presented in [17]. In [20], the Ricean CHF is written as a finite-range integral and then approximated with a truncated series. However, due to the computational complexity in determining the sum distribution, approximations are often used. One common approach is to use a Nakagami distribution to approximate the Ricean distribution [10], [26], [27]. This substitution is done because the CHF of the Nakagami distribution is known in a tractable closed-form whereas the CHF of the Ricean is not. The Nakagami distribution substitution often leads to convenient closed-form analytical expressions; however, it is shown in [17] and [27] that this simplifying approximation can be inaccurate.

Let $r_1, r_2, \ldots, r_L$ be the amplitudes of L statistically independent RVs, each of which follows the Ricean density

$$f_{R_i}(r_i) = \frac{r_i}{\sigma_i^2} \exp\left(-\frac{r_i^2 + s_i^2}{2\sigma_i^2}\right) I_0\left(\frac{r_i s_i}{\sigma_i^2}\right), \quad r_i \geq 0 \tag{3.1}$$

where σ_i^2 is the variance of the Gaussian scatter component and s_i^2 is the noncentrality parameter of each RV. To describe the degree of fading, the Rice factor is defined as the ratio of specular power to scattered power, that is, $K_i = s_i^2/2\sigma_i^2$. If the channel has no specular component, $K = 0$ and (3.1) reduces to the Rayleigh PDF. On the other hand, when $K = \infty$, the channel does not exhibit any fading. It was reported in [28] that a typical value of K for a microcellular environment is about 7 dB. If $\Omega_i = E[r_i^2] = s_i^2 + 2\sigma_i^2$ is used to denote the average power of each individual Ricean RV, then the PDF of R_i can be written as

$$f_{R_i}(r_i) = \frac{2r_i(K_i+1)}{\Omega_i} \exp\left(-K_i - \frac{(K_i+1)r_i^2}{\Omega_i}\right) I_0\left(2r_i\sqrt{\frac{K_i(K_i+1)}{\Omega_i}}\right). \tag{3.2}$$

Lastly, let

$$Z = \sum_{i=1}^{L} R_i = R_1 + R_2 + \cdots + R_L \tag{3.3}$$

be a sum of L iid Ricean RVs. Note that Z may be used to describe the envelope of the signal component at the combiner output of an EGC system in Ricean fading.

Much insight into formulating an accurate approximation to the distribution of Z in (3.3) can be gained by considering the SAA to the PDF of a Rayleigh sum derived in [14]. As outlined in Section 2.1, an approximation to the density of Rayleigh sums based on the density of sums of squared Rayleigh RVs has been proposed. This approximation is motivated by the observation that at small SNRs, there is an essentially constant ratio between EGC and MRC statistics. Consequently, for small values of the argument, the statistics of EGC are expected to be well approximated by the statistics of MRC with appropriately scaled arguments [14]. Results presented here indicate that this may also be true for large SNRs.

In this chapter, an accurate closed-form approximation to the Ricean sum distribution is presented. In addition, an accurate closed-form approximation to the Ricean sum PDF is derived. These approximations are based on modifying the sum distribution of squared Ricean RVs.

3.2 Ricean Sum CDF Approximation

First consider the RV

$$H = \sum_{i=1}^{L} R_i^2 = R_1^2 + R_2^2 + \cdots + R_L^2 \tag{3.4}$$

where the R_i's are iid Ricean RVs with PDFs given by (3.1). The RV, H, has a noncentral chi-square distribution with $2L$ degrees of freedom. Thus the PDF of H is [7]

$$f_H(r) = \frac{1}{2\sigma^2}\left(\frac{r}{s^2}\right)^{\frac{L-1}{2}} \exp\left(-\frac{r+s^2}{2\sigma^2}\right) I_{L-1}\left(\frac{\sqrt{r}s}{\sigma^2}\right), \quad r \geq 0 \tag{3.5}$$

where $s^2 = \sum_{i=1}^{L} s_i^2$ and $I_{L-1}(\cdot)$ is the $(L-1)$th-order modified Bessel function of the first kind. Integration of (3.5) yields the CDF of H given by

$$F_H(r) = 1 - Q_L\left(\frac{s}{\sigma}, \frac{\sqrt{r}}{\sigma}\right) \tag{3.6}$$

where $Q_L(\cdot,\cdot)$ is the generalized Marcum Q-function. Just as the RV Z describes the envelope of the signal component at the combiner output of an EGC system in Ricean fading, here, the RV H represents the envelope of the signal component at the combiner output of a MRC system in Ricean fading.

Now using the same observation in [14], that is, that the EGC statistics follow appropriately scaled MRC statistics, it may be possible to align the distributions by using appropriate scaling factors. Thus, the proposed approximation for the CDF of Z is given as

$$F_L(t) = 1 - Q_L\left(\frac{v}{d_1}, \frac{t}{d_2}\right), \tag{3.7a}$$

$$v = \sqrt{\frac{LK\Omega}{K+1}} \tag{3.7b}$$

where d_1 and d_2 are constants and $t = r/\sqrt{L}$ is the normalized argument.

A nonlinear least squares method based on the interior-reflective Newton method described in [25] is used to optimize the constants d_1 and d_2 in (3.7). These constants are given in Table 3.1 for practical values of K, L, and for normalized power, $\Omega = 1$. When $K = 0$, that is, Rayleigh fading, the approximation in (3.7) reduces to a form that is similar to the SAA proposed in [14] but with different scaling factors. Figures 3.1-3.4 compare the new closed-form CDF approximation represented by the symbols with the exact CDF represented by the solid lines. Observe that the approximation is very accurate for a very wide range of probabilities and for all values of Rice factors and L considered. It was found empirically that high accuracy is obtained for all values of $K > 0.5$. Other approximations, may be needed for accurate estimation when $K < 0.5$ and, in particular for $K = 0$. In these cases, the approximations developed in Chapter 2 can be used.

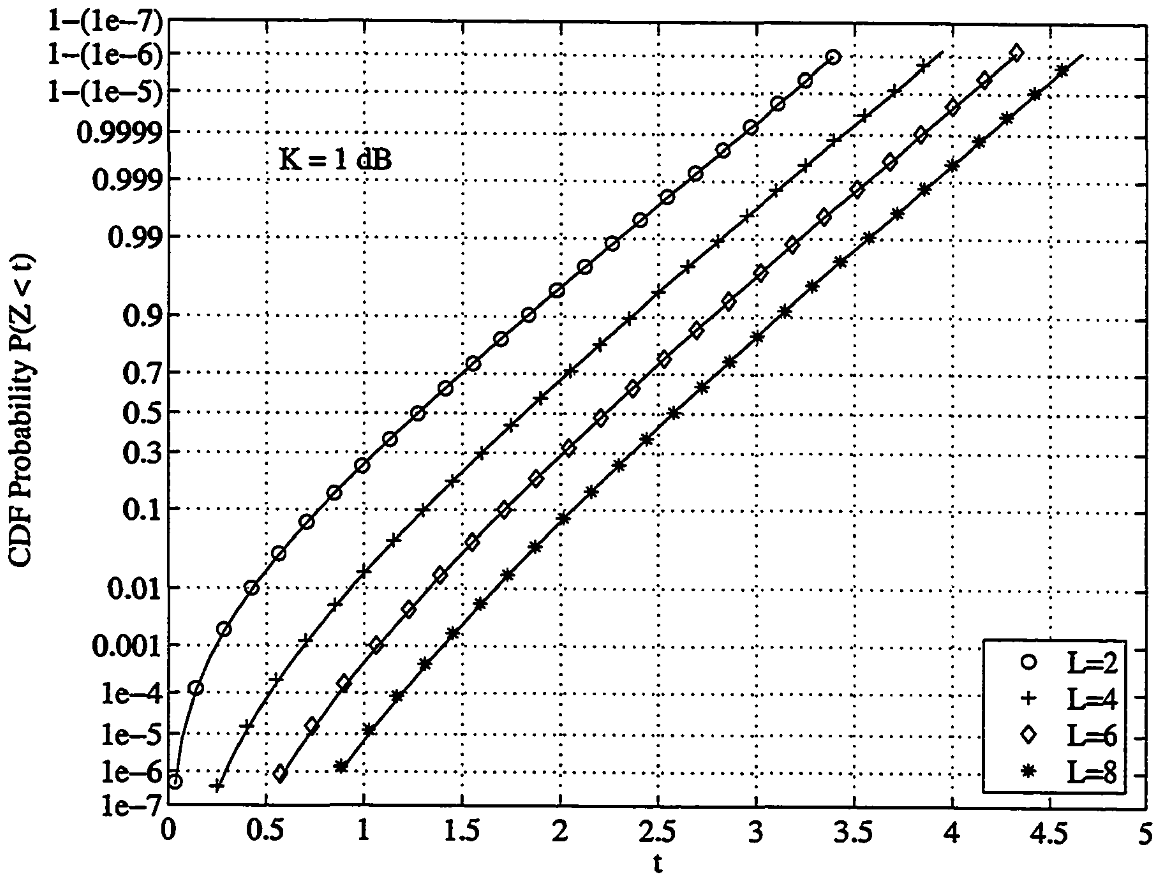

Fig. 3.1. The CDF of a sum of L Ricean RVs and the closed-form approximation for L = 2, 4, 6, and 8 with Rice factor $K = 1$ dB.

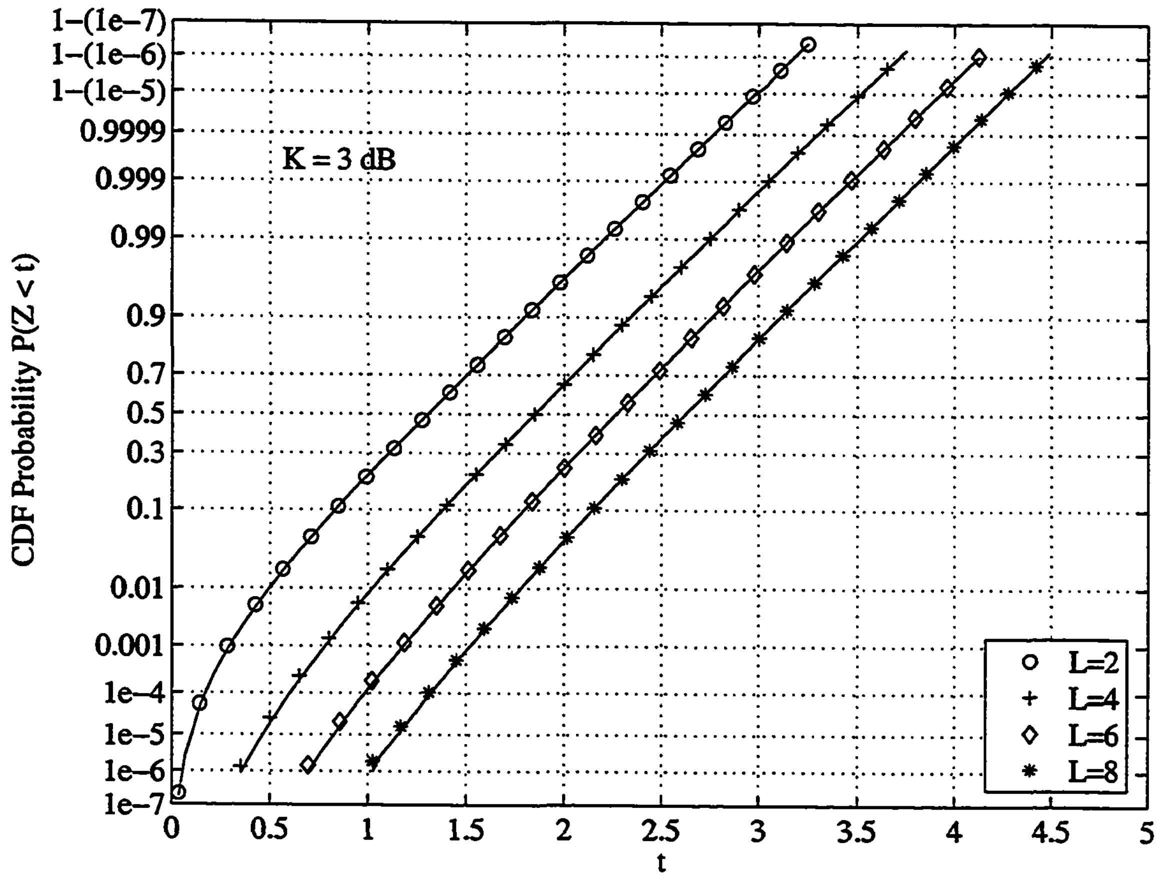

Fig. 3.2. The CDF of a sum of L Ricean RVs and the closed-form approximation for L = 2, 4, 6, and 8 with Rice factor K = 3 dB.

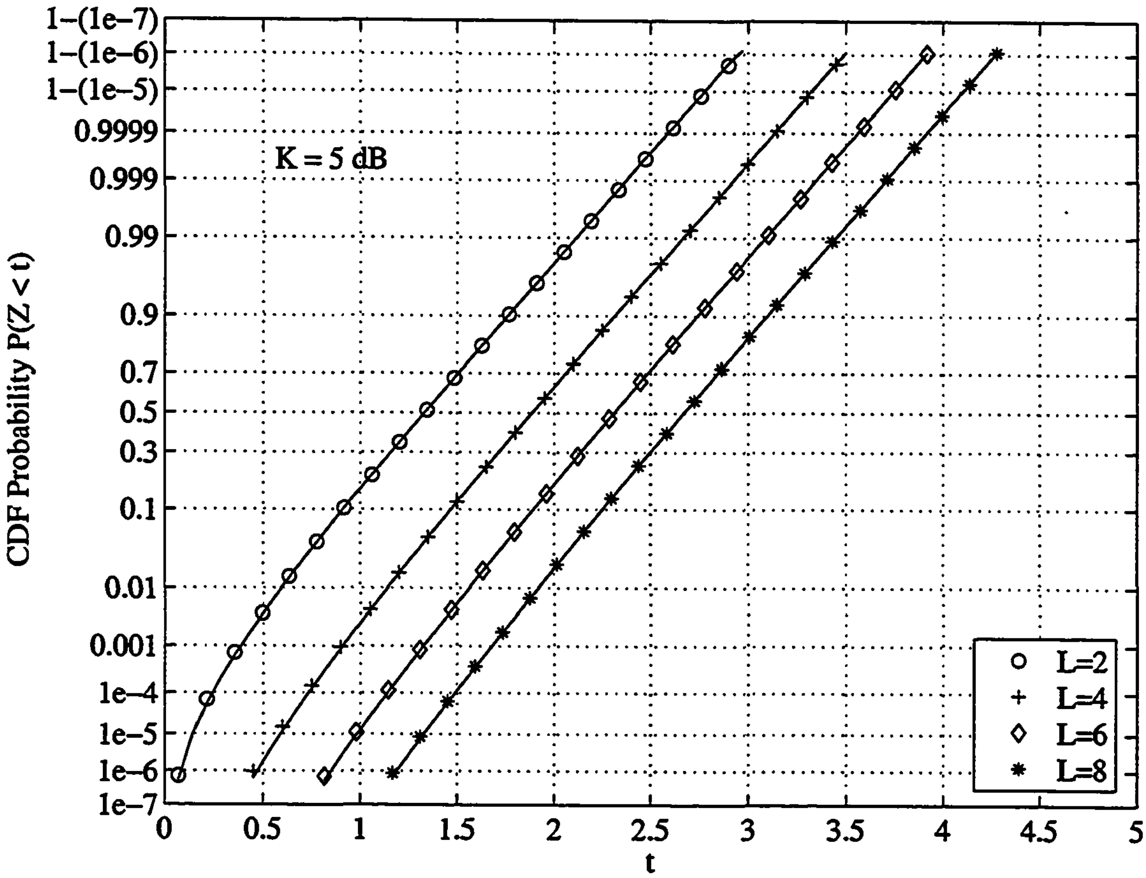

Fig. 3.3. The CDF of a sum of L Ricean RVs and the closed-form approximation for $L =$ 2, 4, 6, and 8 with Rice factor $K = 5$ dB.

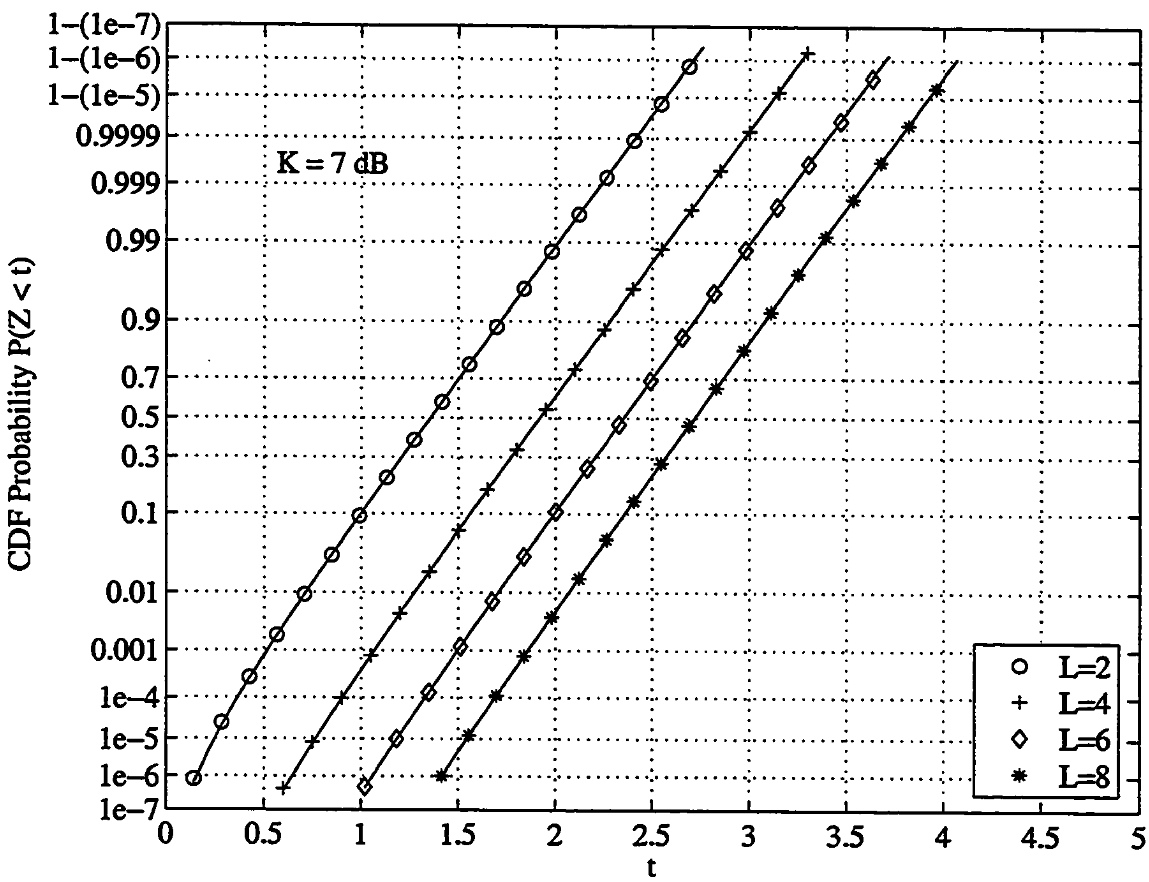

Fig. 3.4. The CDF of a sum of L Ricean RVs and the closed-form approximation for L = 2, 4, 6, and 8 with Rice factor K = 7 dB.

3.3 Ricean Sum PDF Approximation

A new PDF approximation for Z can be formally derived from the CDF approximation as

$$f_L(t) \triangleq \frac{\mathrm{d}F_L(t)}{\mathrm{d}t}. \tag{3.8}$$

Taking the derivative of the CDF approximation given in (3.7) yields an accurate approximation to the PDF that uses the same coefficients given in Table 3.1, as seen in Figures 3.5-3.7. The solid lines show the exact PDF and the circles represent the closed-form approximation. The proposed approximation to the PDF of a Ricean sum is then

$$f_L(t) = \frac{t^L}{d_2^2}\left(\frac{d_1}{d_2 v}\right)^{L-1} \exp\left(-\frac{t^2}{2d_2^2} - \frac{v^2}{2d_1^2}\right) I_{L-1}\left(\frac{tv}{d_1 d_2}\right). \tag{3.9}$$

3.4 Summary

An accurate closed-form approximation to the Ricean sum distribution was introduced in this chapter. This approximation is based on modifying the sum distribution of squared Ricean RVs. It was observed that the new approximation is accurate over a large range of argument values. Furthermore, by simply differentiating the CDF approximation, it is possible to obtain a closed-form PDF approximation that is also accurate over the same large range.

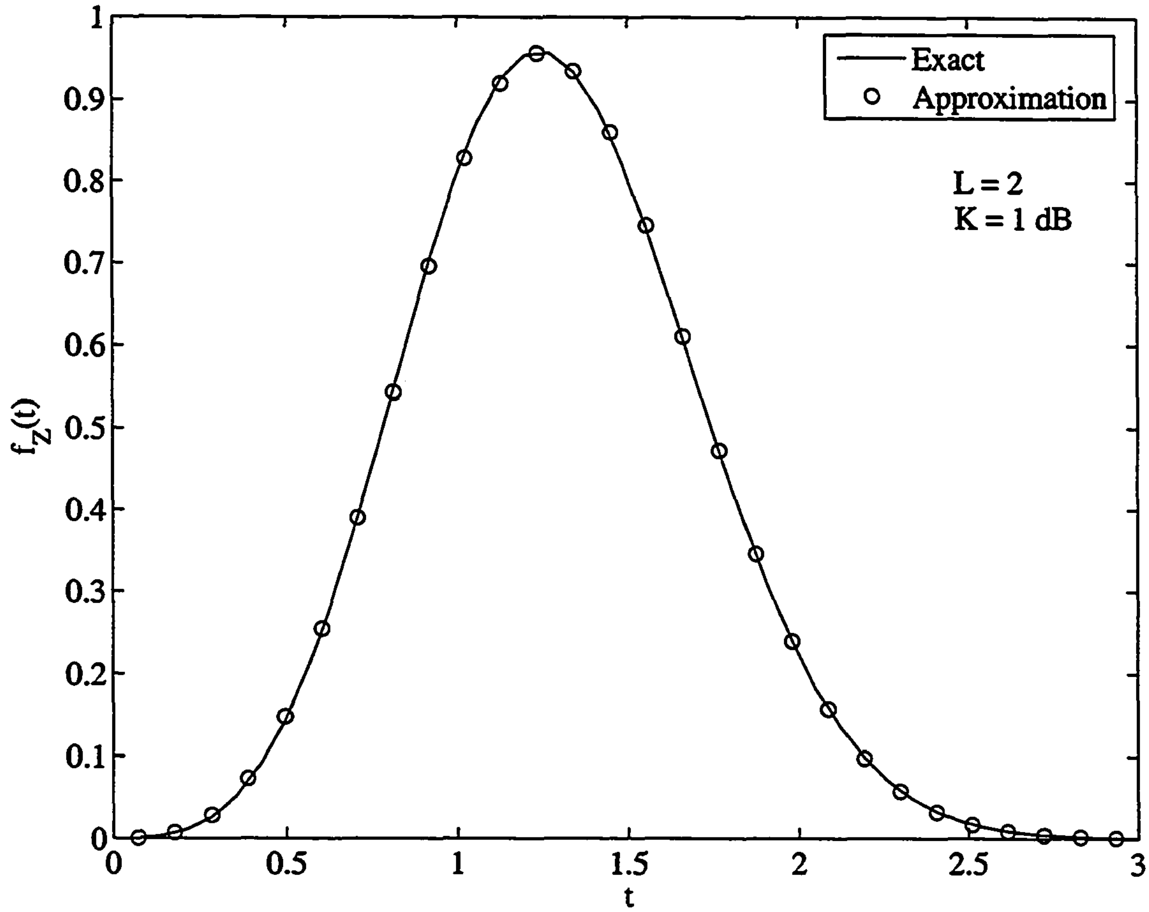

Fig. 3.5. The PDF of a sum of L Ricean RVs and the closed-form approximation for $L = 2$ with Rice factor $K = 1$ dB.

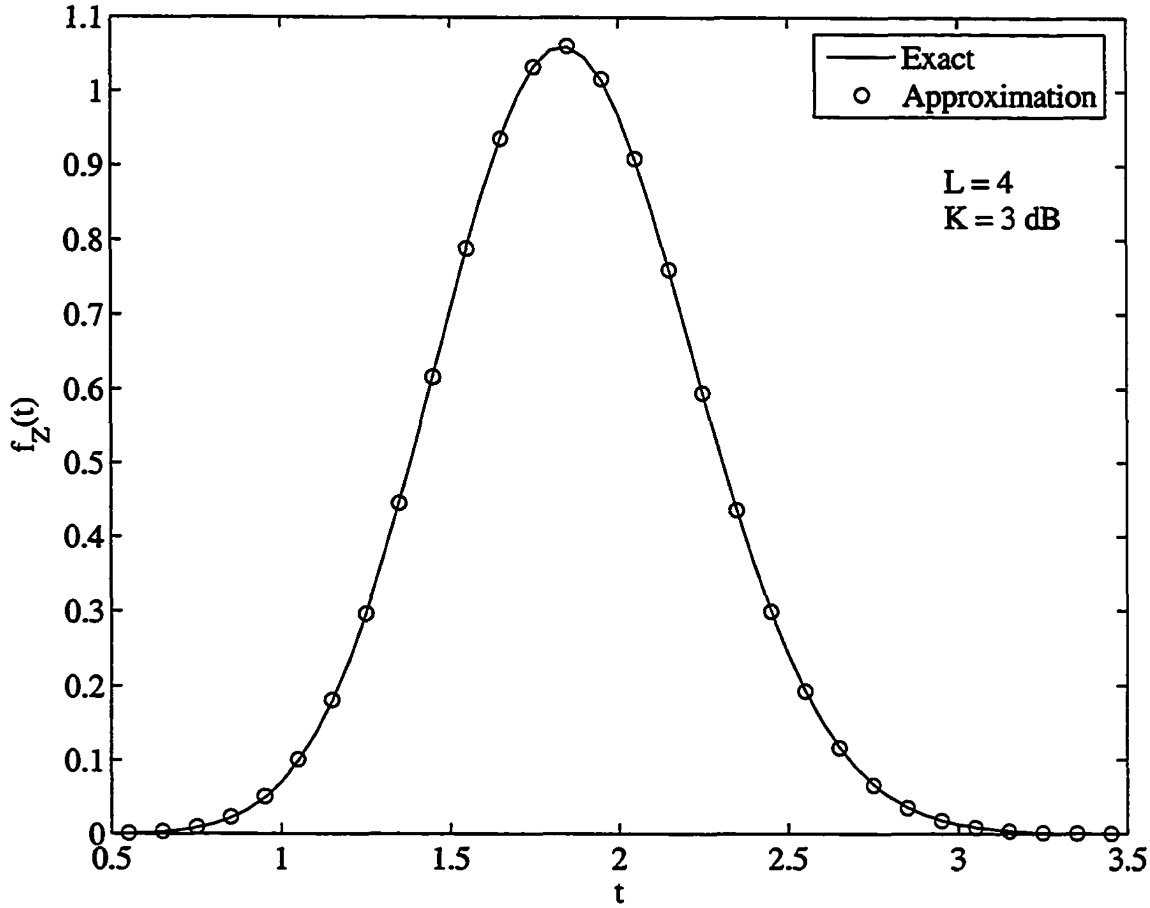

Fig. 3.6. The PDF of a sum of L Ricean RVs and the closed-form approximation for $L = 4$ with Rice factor $K = 3$ dB.

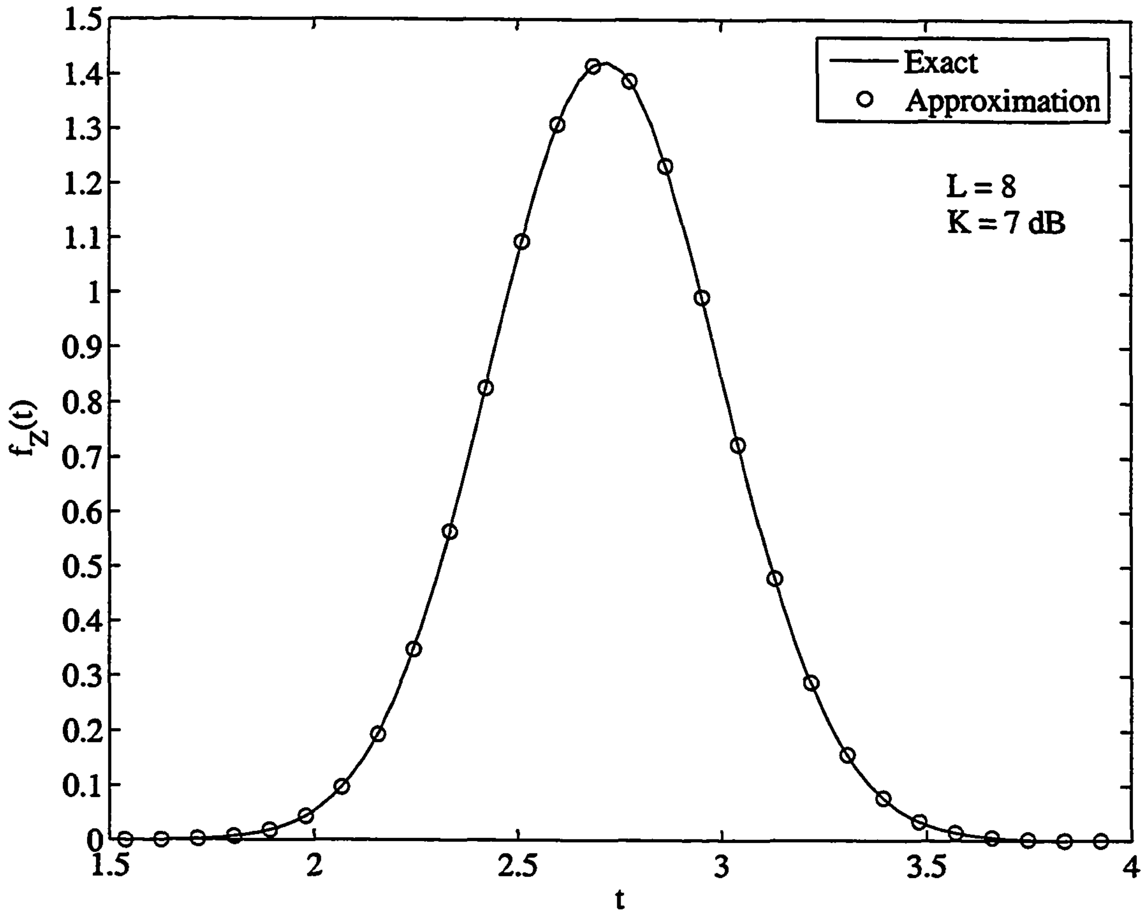

Fig. 3.7. The PDF of a sum of L Ricean RVs and the closed-form approximation for $L = 8$ with Rice factor $K = 7$ dB.

TABLE 3.1

Coefficients for the Ricean sum CDF and PDF approximations.

$$F_L(t) = 1 - Q_L\left(\frac{v}{d_1}, \frac{t}{d_2}\right)$$

$$f_L(t) = \frac{t^L}{d_2^2}\left(\frac{d_1}{d_2 v}\right)^{L-1} \exp\left(-\frac{t^2}{2d_2^2} - \frac{v^2}{2d_1^2}\right) I_{L-1}\left(\frac{tv}{d_1 d_2}\right)$$

$$v = \sqrt{\frac{LK\Omega}{K+1}}, \quad \Omega = 1$$

	$K=1$ dB		$K=2$ dB		$K=3$ dB		$K=4$ dB	
L	d_1	d_2	d_1	d_2	d_1	d_2	d_1	d_2
2	0.5194	0.4746	0.4782	0.4438	0.4395	0.4131	0.4019	0.3819
3	0.5411	0.4770	0.4958	0.4468	0.4518	0.4150	0.4113	0.3837
4	0.5507	0.4772	0.5032	0.4471	0.4580	0.4157	0.4157	0.3843
5	0.5589	0.4783	0.5086	0.4478	0.4621	0.4165	0.4187	0.3849
6	0.5634	0.4786	0.5122	0.4482	0.4646	0.4168	0.4205	0.3851
7	0.5675	0.4791	0.5149	0.4485	0.4668	0.4172	0.4221	0.3854
8	0.5699	0.4793	0.5163	0.4485	0.4680	0.4173	0.4232	0.3857
	$K=5$ dB		$K=6$ dB		$K=7$ dB		$K=8$ dB	
L	d_1	d_2	d_1	d_2	d_1	d_2	d_1	d_2
2	0.3657	0.3509	0.3313	0.3205	0.2992	0.2914	0.2694	0.2638
3	0.3726	0.3524	0.3363	0.3217	0.3027	0.2922	0.2721	0.2646
4	0.3761	0.3530	0.3389	0.3223	0.3048	0.2928	0.2734	0.2650
5	0.3782	0.3534	0.3406	0.3227	0.3058	0.2931	0.2743	0.2652
6	0.3796	0.3537	0.3416	0.3229	0.3066	0.2933	0.2749	0.2654
7	0.3806	0.3539	0.3424	0.3231	0.3073	0.2935	0.2752	0.2654
8	0.3815	0.3541	0.3430	0.3233	0.3076	0.2936	0.2753	0.2654

Chapter 4

Accurate Closed-Form Approximations to Nakagami Sum Distributions and Densities

4.1 Sum of Nakagami RVs

Many different statistical models have been used to describe the multipath fading effects in wireless communication channels. The Nakagami distribution (m-distribution) [10] is a generalized distribution which can accurately model different fading environments. Moreover, the versatility of the Nakagami distribution allows it to fit some urban wireless channel data better than the commonly used Rayleigh, Ricean, or lognormal distributions [11], [12]. In the analysis of certain communication systems, there is a need for the accurate computation of the CDF and the PDF of a sum of L statistically independent Nakagami RVs. For example, such sums are required in determining the error probabilities of EGC diversity systems in Nakagami fading [19].

The lack of a closed-form solution for the distribution of a sum of Nakagami RVs has led to several computational approaches and approximations. One well known approach [16], [19] involves using an infinite series representation to obtain the CDF precisely. However, the use of an infinite series results in a tradeoff between computational complexity and truncation errors. Other approaches involve numerical integration which are often computationally complex.

Let $r_1, r_2, \ldots, r_L$ be the amplitudes of L statistically independent RVs, each of which follows the Nakagami density

$$f_{R_i}(r_i) = \frac{2m_i^{m_i} r_i^{2m_i-1}}{\Gamma(m_i)\Omega_i^{m_i}} \exp\left(-\frac{m_i}{\Omega_i} r_i^2\right), \quad r_i \geq 0 \tag{4.1}$$

where $m_i \geq 0.5$ and $\Omega_i = E[R_i^2]$ controls the spread of the distribution. The degree of fading and average power can be changed by varying the m_i and Ω_i respectively. The Rayleigh ($m = 1$) and one-sided Gaussian ($m = 0.5$) distributions are special cases of the Nakagami distribution, as is the nonfading case ($m = \infty$). The sum of L iid Nakagami RVs is then given by

$$Z = \sum_{i=1}^{L} R_i = R_1 + R_2 + \cdots + R_L. \tag{4.2}$$

Note that Z may be used to describe the envelope of the signal component at the combiner output of an EGC system in Nakagami fading.

Much insight into formulating an accurate approximation to the distribution of Z in (4.2) can be gained by once again considering the SAA to the PDF of a Rayleigh sum derived in [14]. This approximation is motivated by the near parallelism between the EGC and MRC statistics at small SNRs. Thus, for small values of the argument, the statistics of EGC should have a form very similar to the statistics of MRC with appropriately scaled arguments. From this observation, an approximation to the density of Rayleigh sums based on the density of sums of squared Rayleigh RVs was proposed.

In this chapter, an accurate closed-form approximation to the Nakagami sum distribution is presented. In addition, an accurate closed-form approximation to the Nakagami sum PDF is derived. These approximations are based on modifying the sum distribution of squared Nakagami RVs.

4.2 Nakagami Sum CDF Approximation

First consider the RV

$$H = \sum_{i=1}^{L} R_i^2 = R_1^2 + R_2^2 + \cdots + R_L^2 \tag{4.3}$$

where the R_i's are Nakagami RVs with PDFs given by (4.1). The R_i^2's are iid gamma RVs, thus, H is also a gamma distributed RV with PDF [29]

$$f_H(r) = \left(\frac{m}{\Omega}\right)^{mL} \frac{r^{mL-1}}{\Gamma(mL)} \exp\left(-\frac{m}{\Omega} r\right), \quad r \geq 0. \tag{4.4}$$

Integration of (4.4) yields the CDF of H given by

$$F_H(r) = 1 - \frac{\gamma\left(mL, \frac{m}{\Omega} r\right)}{\Gamma(mL)} \tag{4.5}$$

where $\gamma(\cdot,\cdot)$ is the incomplete gamma function. Just as the RV Z describes the envelope of the signal component at the combiner output of an EGC system in Nakagami fading, here, the RV H represents the envelope of the signal component at the combiner output of a MRC system in Nakagami fading.

Now using the same observation in [14], that is, that the EGC statistics follow appropriately scaled MRC statistics, it may be possible to align the distributions by using appropriate scaling factors. Thus, the proposed approximation for the CDF of Z is given as

$$F_L(t) = 1 - \frac{\gamma\left(c_1 mL, c_2 \frac{m}{\Omega} t^2\right)}{\Gamma(c_1 mL)} \tag{4.6}$$

where c_1 and c_2 are constants and $t = r/\sqrt{L}$ is the normalized argument.

A nonlinear least squares method based on the interior-reflective Newton method described in [25] is used to optimize the constants c_1 and c_2 in (4.6). These constants are given in Table 4.1 for practical values of m, L, and for normalized power, $\Omega = 1$. When $m = 1$, that is, Rayleigh fading, the approximation has a form similar to the SAA proposed in [14] but with different constants. Figures 4.1-4.5 compare the new closed-form CDF approximation represented by the symbols with the exact CDF represented by the solid lines. Observe that the approximation is very accurate for a very wide range of probabilities and for all values of fading severity parameters and L considered. It has been observed that high accuracy is obtained for values of $m > 1.0$. For values of $m < 1.0$, the approximation is still accurate over a slightly smaller range. Note that for $m = 1$, the Nakagami sum approximation reduces to a Rayleigh sum approximation. Comparing this approximation with the Rayleigh sum approximation derived in Chapter 2, it was found that the Nakagami sum approximation with $m = 1$ is slightly less accurate but benefits from not having an additional correction term.

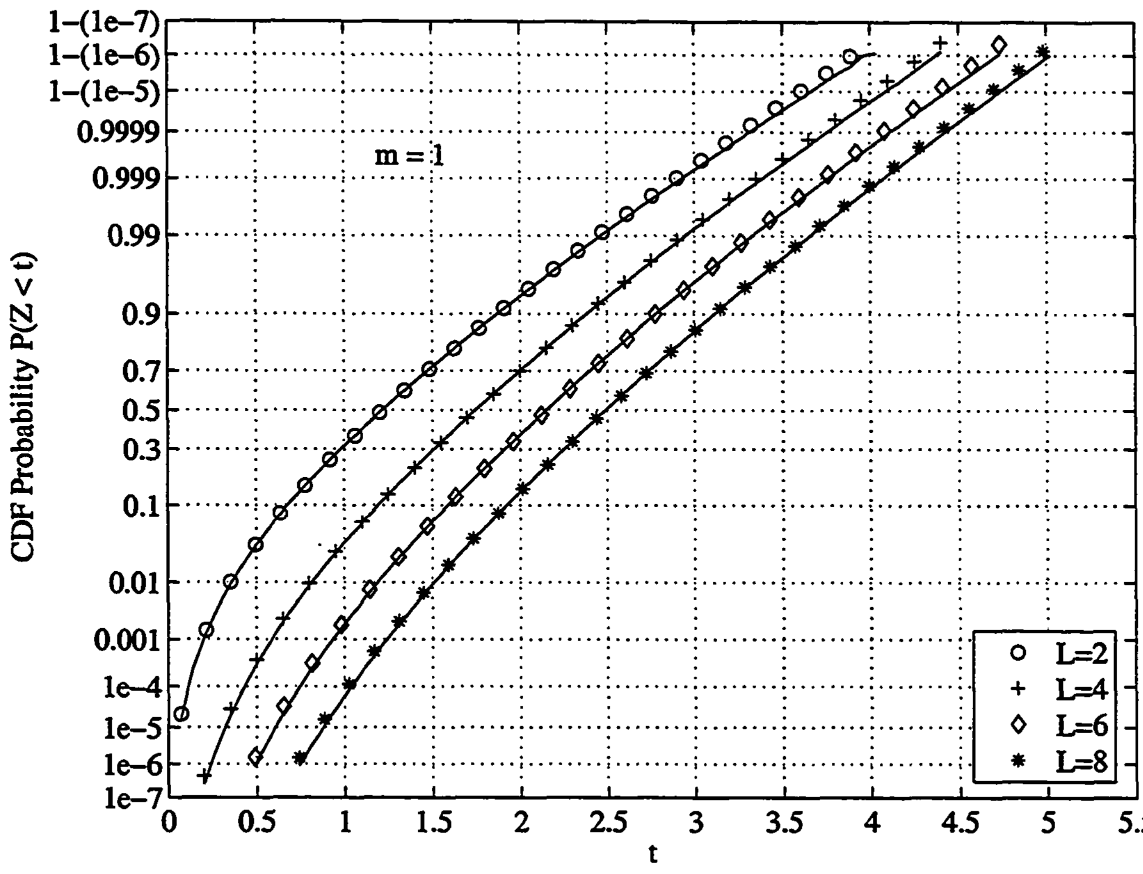

Fig. 4.1. The CDF of a sum of L Nakagami RVs and the closed-form approximation for L = 2, 4, 6, and 8 with fading severity parameter $m = 1$.

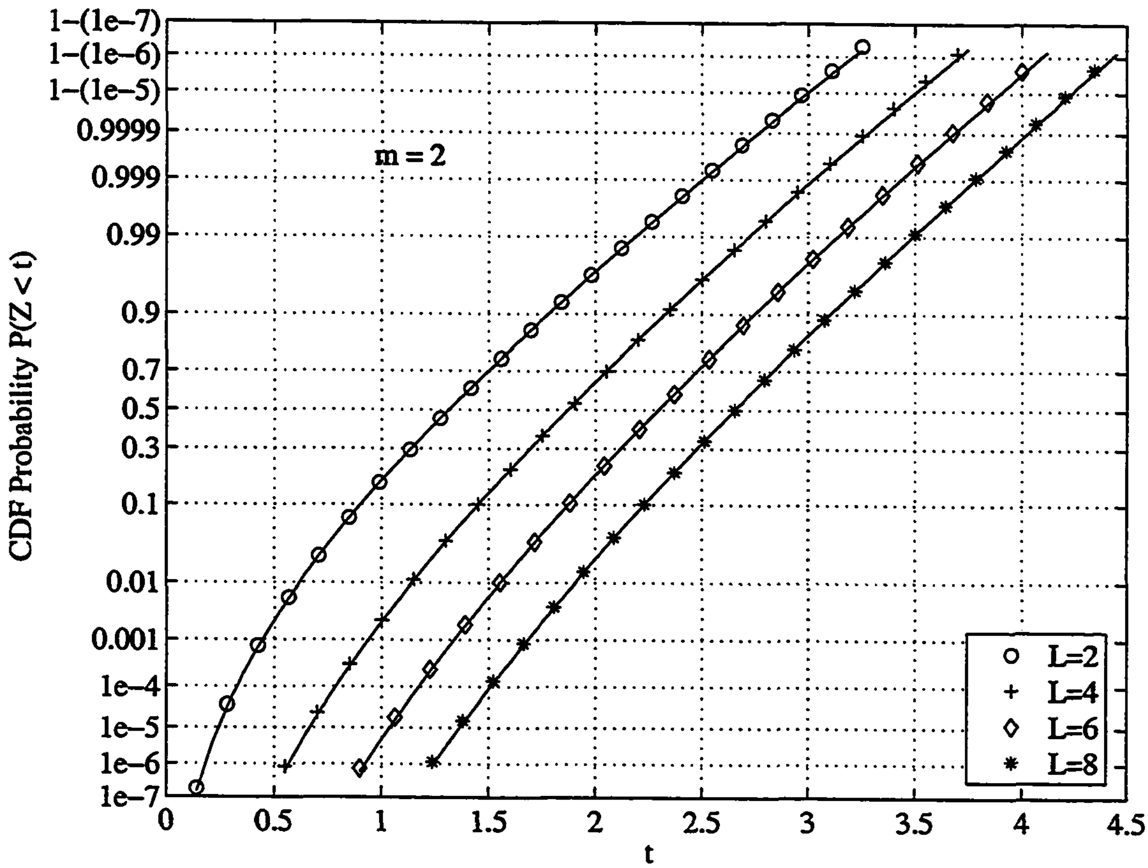

Fig. 4.2. The CDF of a sum of L Nakagami RVs and the closed-form approximation for L = 2, 4, 6, and 8 with fading severity parameter $m = 2$.

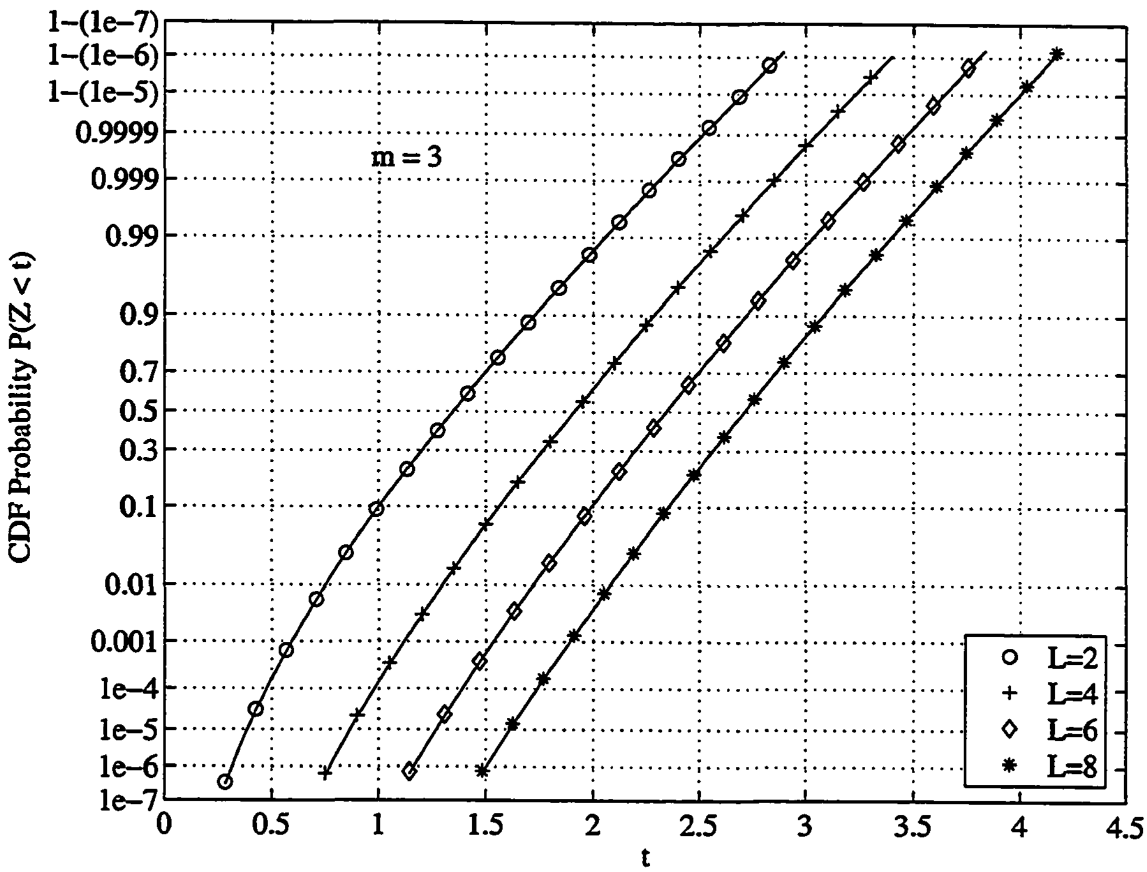

Fig. 4.3. The CDF of a sum of L Nakagami RVs and the closed-form approximation for L = 2, 4, 6, and 8 with fading severity parameter $m = 3$.

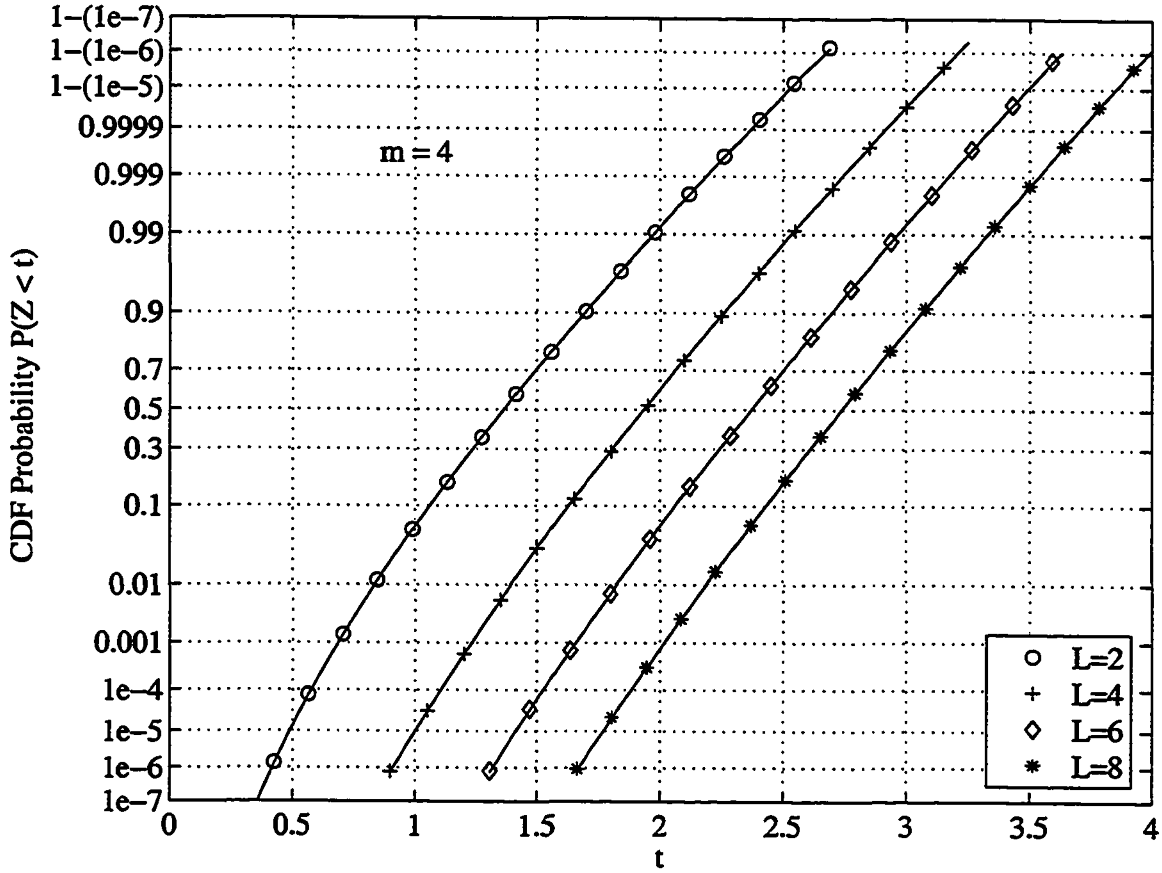

Fig. 4.4. The CDF of a sum of L Nakagami RVs and the closed-form approximation for L = 2, 4, 6, and 8 with fading severity parameter $m = 4$.

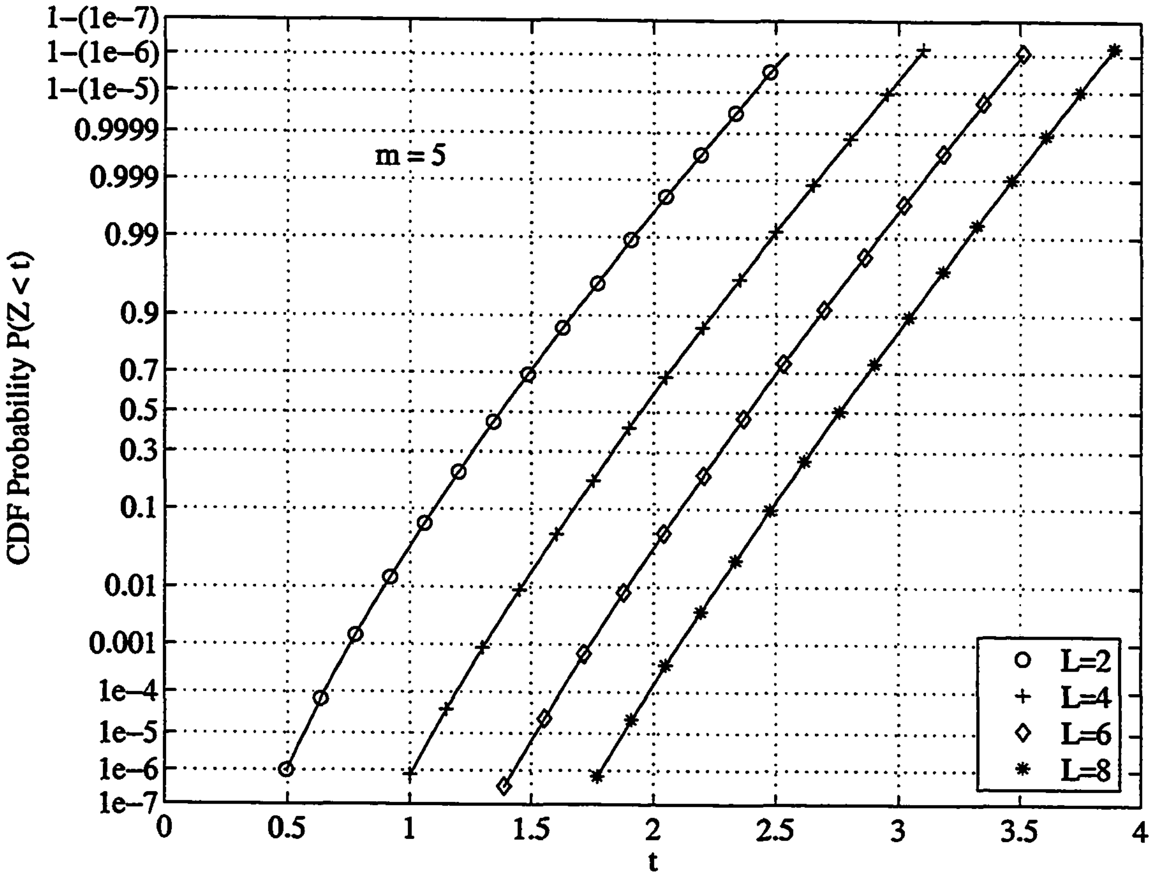

Fig. 4.5. The CDF of a sum of L Nakagami RVs and the closed-form approximation for $L = 2, 4, 6$, and 8 with fading severity parameter $m = 5$.

4.3 Nakagami Sum PDF Approximation

A new PDF approximation for Z can be formally derived from the CDF approximation as

$$f_L(t) \triangleq \frac{\mathrm{d}F_L(t)}{\mathrm{d}t}. \tag{4.7}$$

In this case, taking the derivative of the CDF approximation in (4.6) yields an accurate PDF approximation while using the same coefficients given in Table 4.1, as seen in Figures 4.6-4.8. The solid lines show the exact PDF and the circles represent the closed-form approximation. The proposed approximation to the PDF of a Nakagami sum is then

$$f_L(t) = 2\left(\frac{c_2 m}{\Omega}\right)^{c_1 mL} \frac{t^{2c_1 mL-1}}{\Gamma(c_1 mL)} \exp\left(-\frac{c_2 m}{\Omega}t^2\right). \tag{4.8}$$

4.4 Summary

An accurate closed-form approximation to the Nakagami sum distribution was introduced in this chapter. This approximation is based on modifying the sum distribution of squared Nakagami RVs. It was observed that the new approximation is accurate over a large range of argument values. In addition, the closed-form PDF approximation obtained by differentiating the CDF approximation is also accurate over the same large range.

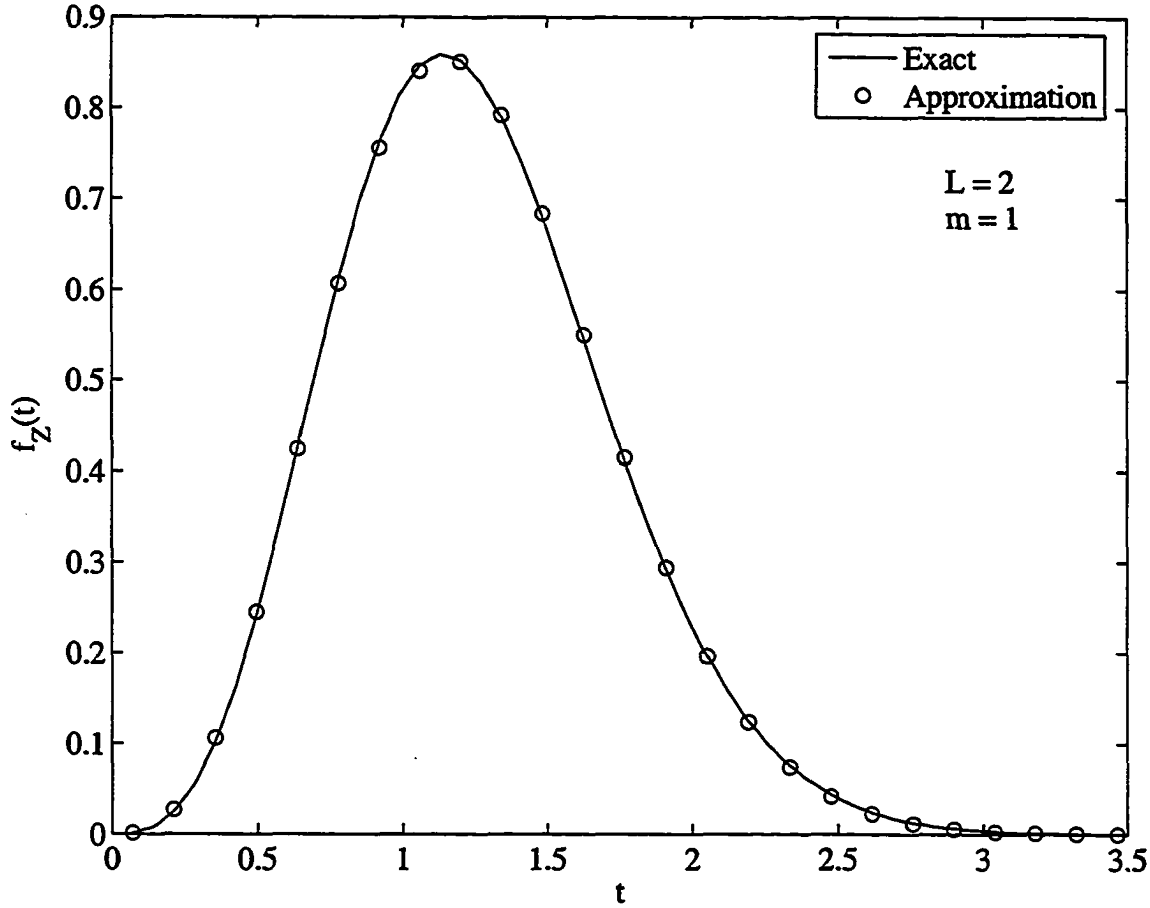

Fig. 4.6. The PDF of a sum of L Nakagami RVs and the closed-form approximation for $L = 2$ with fading severity parameter $m = 1$.

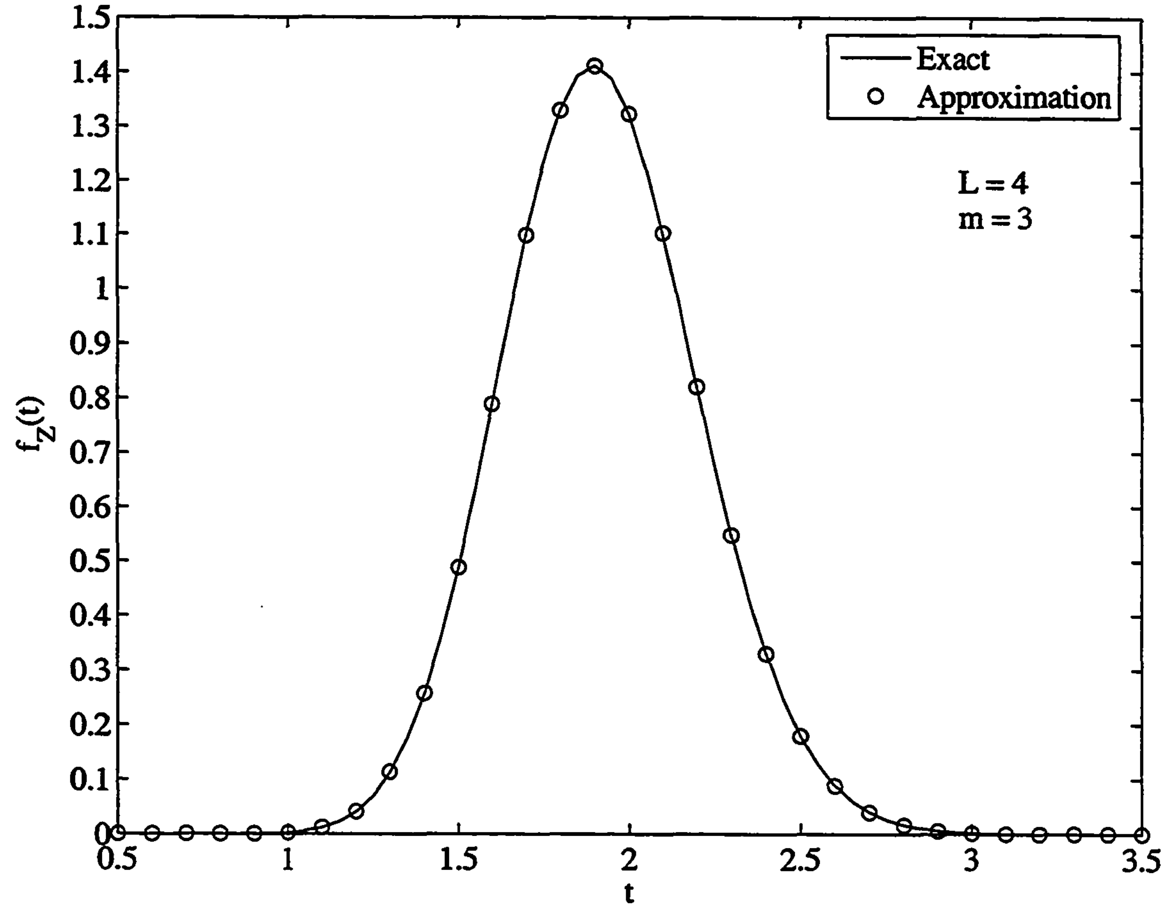

Fig. 4.7. The PDF of a sum of L Nakagami RVs and the closed-form approximation for $L = 4$ with fading severity parameter $m = 3$.

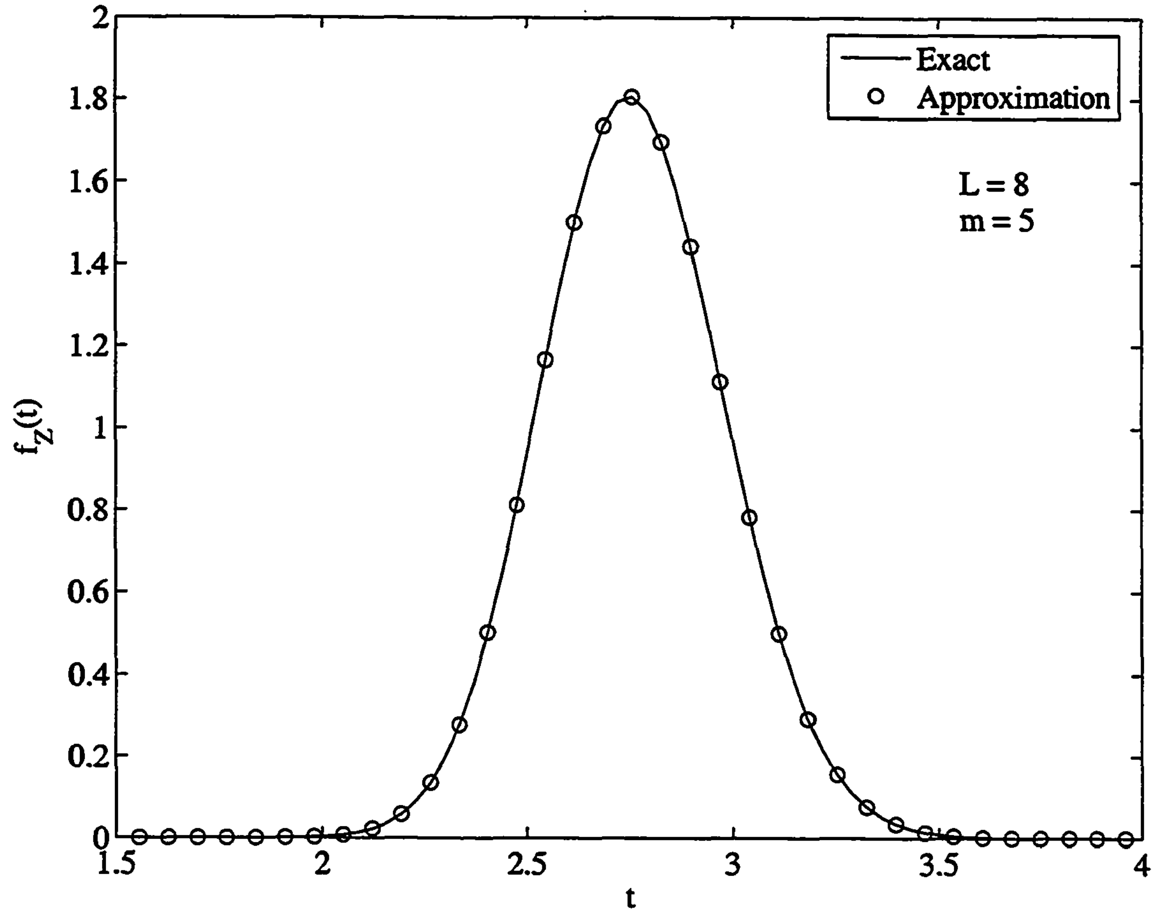

Fig. 4.8. The PDF of a sum of L Nakagami RVs and the closed-form approximation for $L = 8$ with fading severity parameter $m = 5$.

TABLE 4.1

Coefficients for the Nakagami sum CDF and PDF approximations.

$$F_L(t) = 1 - \frac{\gamma\left(c_1 mL, c_2 \frac{m}{\Omega} x^2\right)}{\Gamma(c_1 mL)}$$

$$f_L(t) = 2\left(\frac{c_2 m}{\Omega}\right)^{c_1 mL} \frac{t^{2c_1 mL - 1}}{\Gamma(c_1 mL)} \exp\left(-\frac{c_2 m}{\Omega} t^2\right)$$

$$\Omega = 1$$

	$m = 0.5$		$m = 1.0$		$m = 1.5$	
L	c_1	c_2	c_1	c_2	c_1	c_2
2	0.9691	1.1927	0.9688	1.0879	0.9734	1.0542
3	0.9477	1.2590	0.9538	1.1154	0.9621	1.0710
4	0.9338	1.2909	0.9464	1.1301	0.9560	1.0791
5	0.9243	1.3095	0.9396	1.1361	0.9521	1.0839
6	0.9174	1.3214	0.9356	1.1409	0.9495	1.0871
7	0.9119	1.3294	0.9329	1.1445	0.9477	1.0893
8	0.9079	1.3355	0.9312	1.1477	0.9462	1.0910

	$m = 2.0$		$m = 2.5$		$m = 3.0$	
L	c_1	c_2	c_1	c_2	c_1	c_2
2	0.9777	1.0388	0.9806	1.0297	0.9832	1.0242
3	0.9687	1.0508	0.9733	1.0392	0.9771	1.0321
4	0.9639	1.0566	0.9694	1.0438	0.9736	1.0356
5	0.9614	1.0605	0.9671	1.0465	0.9717	1.0380
6	0.9590	1.0624	0.9655	1.0483	0.9703	1.0394
7	0.9581	1.0647	0.9643	1.0496	0.9695	1.0407
8	0.9564	1.0652	0.9635	1.0506	0.9689	1.0415

L	$m = 3.5$		$m = 4.0$		$m = 4.5$	
	c_1	c_2	c_1	c_2	c_1	c_2
2	0.9850	1.0203	0.9874	1.0184	0.9879	1.0154
3	0.9796	1.0268	0.9818	1.0232	0.9835	1.0203
4	0.9768	1.0300	0.9794	1.0260	0.9813	1.0228
5	0.9751	1.0319	0.9778	1.0271	0.9800	1.0243
6	0.9739	1.0332	0.9768	1.0287	0.9791	1.0252
7	0.9731	1.0341	0.9761	1.0295	0.9784	1.0259
8	0.9725	1.0348	0.9755	1.0301	0.9780	1.0265

L	$m = 5.0$		$m = 5.5$		$m = 6.0$	
	c_1	c_2	c_1	c_2	c_1	c_2
2	0.9889	1.0137	0.9898	1.0124	0.9906	1.0113
3	0.9856	1.0182	0.9862	1.0164	0.9873	1.0149
4	0.9831	1.0204	0.9844	1.0184	0.9856	1.0167
5	0.9819	1.0217	0.9833	1.0196	0.9846	1.0178
6	0.9810	1.0225	0.9826	1.0203	0.9839	1.0185
7	0.9804	1.0232	0.9820	1.0209	0.9834	1.0191
8	0.9800	1.0237	0.9816	1.0213	0.9830	1.0194

Chapter 5

Performance Analysis of EGC Diversity Systems in Nakagami Fading Channels

5.1 System Model and Performance Measures

Diversity is a commonly used technique for combating signal fading in wireless communication systems. EGC diversity receivers are of considerable interest since they offer comparable performance to the optimum MRC scheme with reduced complexity [1]. EGC applies equal weights to the diversity branches and as a result, no knowledge of the branch SNR is required. This translates to a simpler receiver structure that is hardware feasible and cheaper to implement. Despite its practicality, few published results exist for the performance of EGC diversity systems in fading channels. This lack may be attributed to the difficulty in deriving the PDF of the SNR at the diversity combiner output which involves a sum of random fading amplitudes. Indeed, the performance evaluation of EGC is known to be a much more difficult task in comparison to other popular diversity combining schemes. In fact, in his classic diversity paper [3], Brennan acknowledges that the problem of computing the distribution of a sum of independent Rayleigh RVs is "frightful."

In [16], an infinite series technique for computing the PDF of a sum of independent RVs was derived. Applying this technique, the error rate performance of EGC diversity systems in Nakagami fading channels was analyzed in [19]. A moment-based approach to the performance analysis of EGC in Nakagami fading is presented in [30]. This method relies on numerically approximating the moment-generating function of the SNR at the combiner output. Other studies on EGC diversity systems in Nakagami fading are found in [20], [21], and [22]. Despite providing accurate analysis, these results are somewhat complex since they require the computation of an infinite series or numerical integration. Hence, closed-form approximate expressions for the performance of EGC diversity systems in Nakagami fading will be useful because they allow for rapid evaluation of system performance. In this chapter, the performance of EGC diversity systems in Nakagami fading channels is approximated with closed-form expressions. Since the Rayleigh distribution is a special case of the more general Nakagami distribution, the performance of EGC diversity systems in Rayleigh fading is also included. The closed-form approximations to the CDF and PDF of a sum of Nakagami RVs derived in Chapter 4 will be used to derive closed-form expressions for the error probabilities when coherent and noncoherent modulations are used. In addition, a closed-form expression for the outage probability of EGC systems in Nakagami fading will be derived. The approximate error rates and outage probabilities will be compared to the solutions found by numerical integration or simulation.

Consider the L-branch EGC diversity receiver shown in Figure 5.1. In this analysis, it is assumed that each of the diversity channels experience slow and flat Nakagami fading. In addition, the fading processes among the diversity channels are iid and each channel is corrupted by AWGN. The noise components are assumed to be independent of the signals, uncorrelated with each other, and have identical autocorrelation functions. Thus, if $s_m(t)$ is transmitted, the signal on the i-th diversity branch can be written as

$$z_i(t) = g_i(t)s_m(t) + n_i(t), \quad i = 1, \cdots, L \tag{5.1}$$

where

$$g_i(t) = R_i(t)e^{-j\phi_i(t)}, \quad i = 1, \cdots, L \tag{5.2}$$

are the complex fading gains and $n_i(t)$ is AWGN with power spectral density $N_0/2$. The

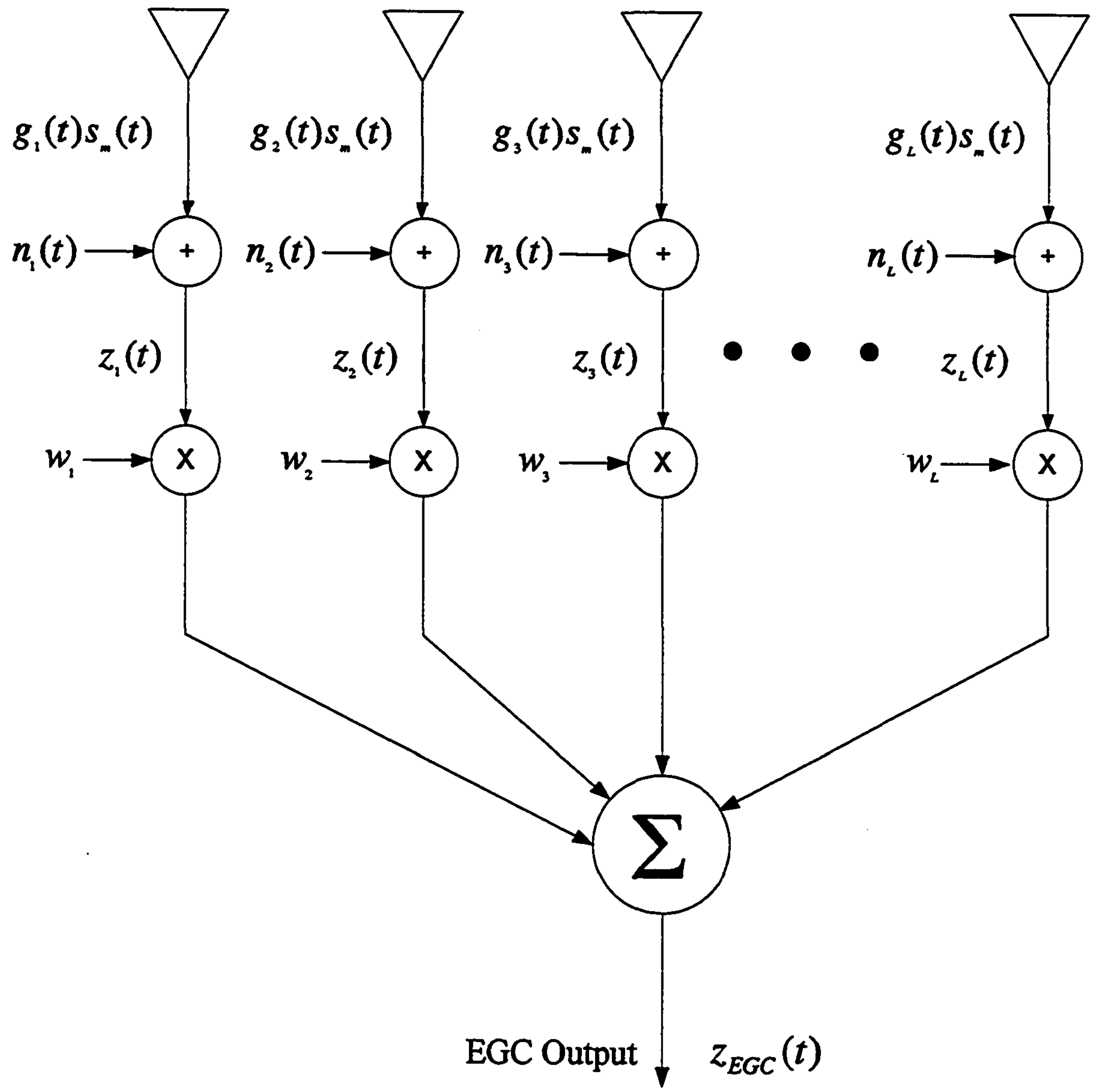

Fig. 5.1. The L-branch EGC diversity receiver.

resultant signal at the output of the combiner can be expressed as

$$z_{EGC}(t) = \sum_{i=1}^{L} w_i z_i(t) \tag{5.3}$$

where w_i is the combining weight used on the i-th diversity branch. In EGC, the received signals are co-phased by setting the weights equal to

$$w_i = e^{j\phi_i}, \quad i = 1, \cdots, L \tag{5.4}$$

and as a result,

$$z_{EGC}(t) = \sum_{i=1}^{L} e^{j\phi_i} z_i(t). \tag{5.5}$$

In this analysis, it is assumed that a perfect phase reference is available at the receiver for co-phasing. The envelope of the composite signal component after co-phasing and combining is

$$R_{EGC} = \sum_{i=1}^{L} R_i \tag{5.6}$$

and the weighted sum of the branch noise powers is

$$\sigma_{EGC}^2 = L\frac{N_0}{2}. \tag{5.7}$$

This results in a combiner output SNR of

$$\gamma_{EGC} = \frac{R_{EGC}^2}{2\sigma_{EGC}^2} = \frac{\left(\sum_{i=1}^{L} R_i\right)^2}{LN_0}. \tag{5.8}$$

Observe that since Nakagami fading is assumed, the R_i's are Nakagami distributed RVs and the PDF of a sum of Nakagami RVs is required to determine the SNR or envelope PDFs at the output of the combiner.

The performance of a communication system is often measured by its error probability, that is, the likelihood that the intended message at the transmitter is incorrectly detected at the receiver. For digital communications, the error performance is given by the average symbol error probability (SEP) or average bit error probability (BEP). If the channel fading is assumed to be slowly-varying and flat, then this measure can be obtained for any modulation scheme by averaging the error probability of the particular modulation in a time-invariant channel over the fading distribution. Hence, the average error probability for a diversity system can be expressed as [7]

$$P_e = \int_0^\infty P_s(\varepsilon|\gamma_O) f_{\gamma_O}(\gamma)\,\mathrm{d}\gamma \tag{5.9}$$

where $P_s(\varepsilon|\gamma_O)$ denotes the SEP for an arbitrary modulation scheme conditioned on a specific SNR at the combiner output and $f_{\gamma_O}(\gamma)$ is the PDF of the SNR at the output of the combiner. The SNR at the output of the combiner is given by

$$\gamma_O = \frac{R_O^2}{2\sigma_N^2} \tag{5.10}$$

where R_O and σ_N^2 are the faded signal envelope and noise power, respectively, after weighting and combining. In some cases, it may be more convenient if the conditional error probability is expressed in terms of the combined signal amplitude and is averaged over the faded signal amplitude. Thus, the average error probability for a diversity system can also be expressed as

$$P_e = \int_0^\infty P_s(\varepsilon|R_O) f_{R_O}(r)\,\mathrm{d}r \tag{5.11}$$

where $P_s(\varepsilon|R_O)$ denotes the SEP for an arbitrary modulation scheme conditioned on a specific signal amplitude value at the combiner output and $f_{R_O}(r)$ is the PDF of the combined output envelope. As shown in (5.6), if the fading is assumed to be Nakagami, then $f_{R_O}(r)$ is the PDF of a sum of Nakagami RVs. This particular approach is used in this analysis since the Nakagami sum PDF approximation derived in Chapter 4 can be readily utilized.

Another useful measure of performance for diversity systems operating in fading channels is the outage probability. This criterion is defined as the probability that the instantaneous SNR at the output of the linear combiner falls below a certain specified threshold, γ_{th}. If the PDF of the SNR at the output of the combiner is $f_{\gamma_O}(\gamma)$, then the outage probability is given by

$$P_{out} = \int_0^{\gamma_{th}} f_{\gamma_O}(\gamma)\,\mathrm{d}\gamma. \tag{5.12}$$

In the following sections, closed-form expressions for the error and outage probabilities of L-branch EGC diversity systems in Nakagami fading are derived. The main benefit of these results is that they allow for efficient evaluation of system performance by saving the time and effort required to perform complex numerical calculations and simulations.

5.2 Closed-Form Expressions for the Average Error Probability of EGC Diversity Systems in Nakagami Fading

5.2.1 Coherent Binary Signalling

Coherent demodulation requires that the carrier phase be recovered at the receiver. Here, coherent phase-shift keying (CPSK) and coherent frequency-shift keying (CFSK) are considered.

In CPSK, a binary signal $m(t)$ consisting of symbols 1 and 0 are represented by constant levels of +1 and -1, respectively, for a time duration of T seconds. This signaling is said to be antipodal and the average energy in a signal pulse is E_{avg}. To transmit the digital signal over a wireless channel, the information in $m(t)$ is multiplied by a sinusoidal carrier wave $\cos(2\pi f_c t)$, where f_c is the carrier frequency, and t is time. Assuming the two signals are equally likely, the received signal from the matched filter demodulator in an AWGN channel with no fading is

$$R = \begin{cases} \sqrt{E_{avg}} + n & \text{for symbol 1} \\ -\sqrt{E_{avg}} + n & \text{for symbol 0} \end{cases} \tag{5.13}$$

where n represents AWGN with zero-mean and variance $N_0/2$. The error probability for CPSK in a time-invariant channel is found to be [7]

$$P_s(\varepsilon|\gamma) = Q\left(\sqrt{\frac{2E_{avg}}{N_0}}\right) = Q\left(\sqrt{2\gamma}\right) \tag{5.14}$$

where $Q(\cdot)$ is the Q-function and $\gamma = E_{avg}/N_0$ is the SNR per symbol. For an EGC diversity system, using (5.8) and (5.14), the conditional error probability when CPSK is used can be written as

$$P_s(\varepsilon|R_O) = Q\left(\sqrt{\frac{2R_{EGC}^2}{LN_0}}\right). \tag{5.15}$$

Next, define the normalized signal envelope as

$$R_{Norm} = \frac{R_{EGC}}{\sqrt{L}}. \tag{5.16}$$

Thus, the average error probability for an EGC diversity system in Nakagami fading when CPSK is used can be expressed

$$P_e = \int_0^\infty Q\left(\sqrt{\frac{2r^2}{N_0}}\right) f_{R_{Norm}}(r)\,\mathrm{d}r \tag{5.17}$$

where $f_{R_{Norm}}(r)$ is the normalized approximation derived in (4.8), namely,

$$f_{R_{Norm}}(r) = 2\left(\frac{c_2 m}{\Omega}\right)^{c_1 mL} \frac{r^{2c_1 mL-1}}{\Gamma(c_1 mL)} \exp\left(-\frac{c_2 m}{\Omega} r^2\right). \tag{5.18}$$

Evaluating the integral in (5.17), the average BEP of a L-branch EGC diversity system in Nakagami fading with CPSK signalling can be approximated as

$$P_e = \frac{1}{2} - \sqrt{\frac{\gamma\Omega}{\pi c_2 m}} \frac{\Gamma\left(\frac{1}{2}+c_1 mL\right)}{\Gamma\left(c_1 mL\right)} {}_2\mathbf{F}_1\left(\frac{1}{2},\frac{1}{2}+c_1 mL;\frac{3}{2},-\frac{\gamma\Omega}{c_2 m}\right) \tag{5.19}$$

where ${}_2\mathbf{F}_1(\cdot,\cdot;\cdot;\cdot)$ denotes the Gauss hypergeometric function. Figures 5.2-5.4 show the BEP curves as a function of branch SNR for varying diversity orders and fading severities. The solid lines represent the exact BEP obtained by numerical integration and the symbols represent the approximate BEP obtained by the closed-form expression in (5.19). Observe that the approximate BEP is very close to the exact BEP for all values of L and m considered.

This analysis is now repeated for CFSK modulation. In CFSK, orthogonal signal waveforms that differ in frequency are used to represent the binary signals. For a given signal power, the effective distance-squared between orthogonal signals is a factor of two less than the distance-squared between antipodal signals. Thus, the error probability for CFSK in a time-invariant channel is found to be [7]

$$P_s(\varepsilon|\gamma) = Q\left(\sqrt{\frac{E_{avg}}{N_0}}\right) = Q(\sqrt{\gamma}). \tag{5.20}$$

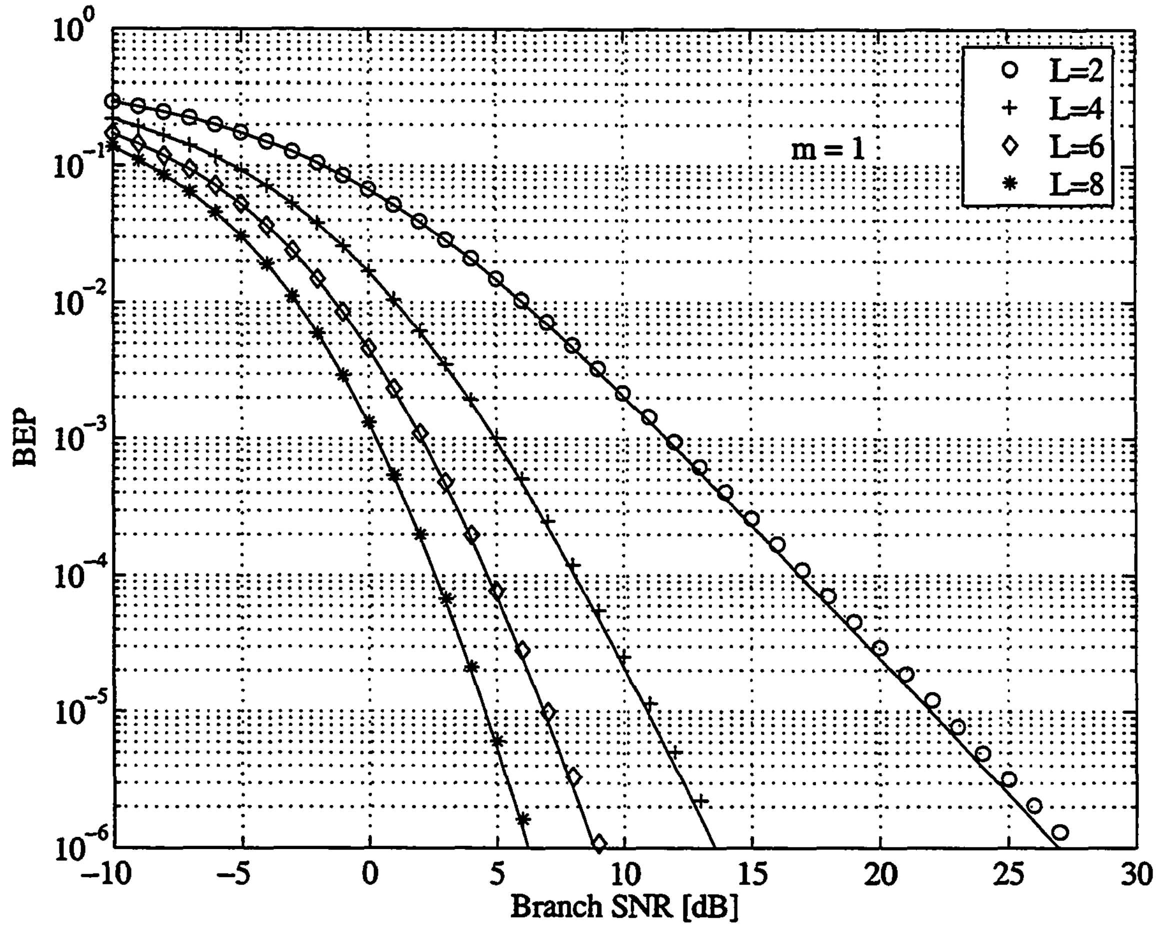

Fig. 5.2. The BEP estimated using the closed-form approximation of a L-branch EGC diversity system with CPSK signalling, for L = 2, 4, 6, and 8 with fading severity parameter $m = 1$ and normalized power $\Omega = 1$.

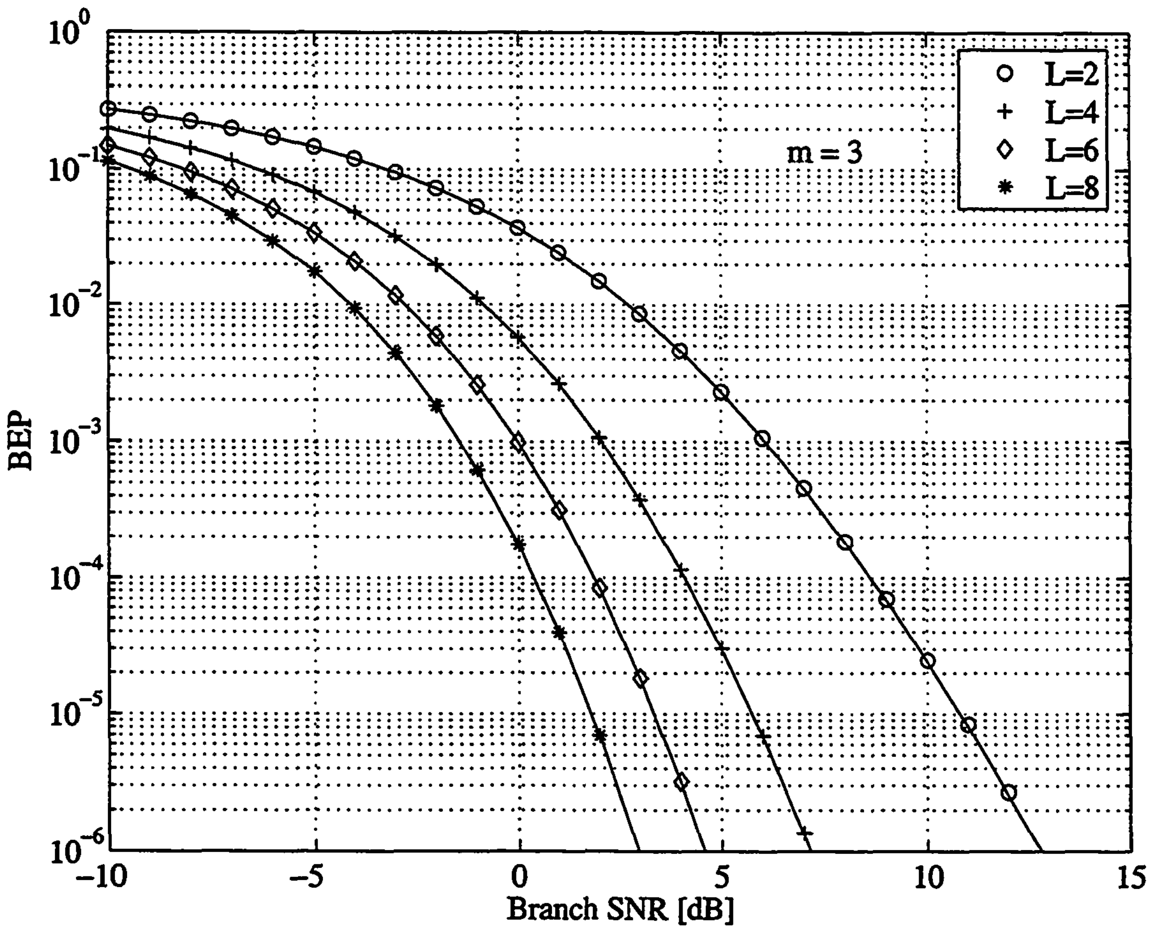

Fig. 5.3. The BEP estimated using the closed-form approximation of a L-branch EGC diversity system with CPSK signalling, for $L = 2, 4, 6$, and 8 with fading severity parameter $m = 3$ and normalized power $\Omega = 1$.

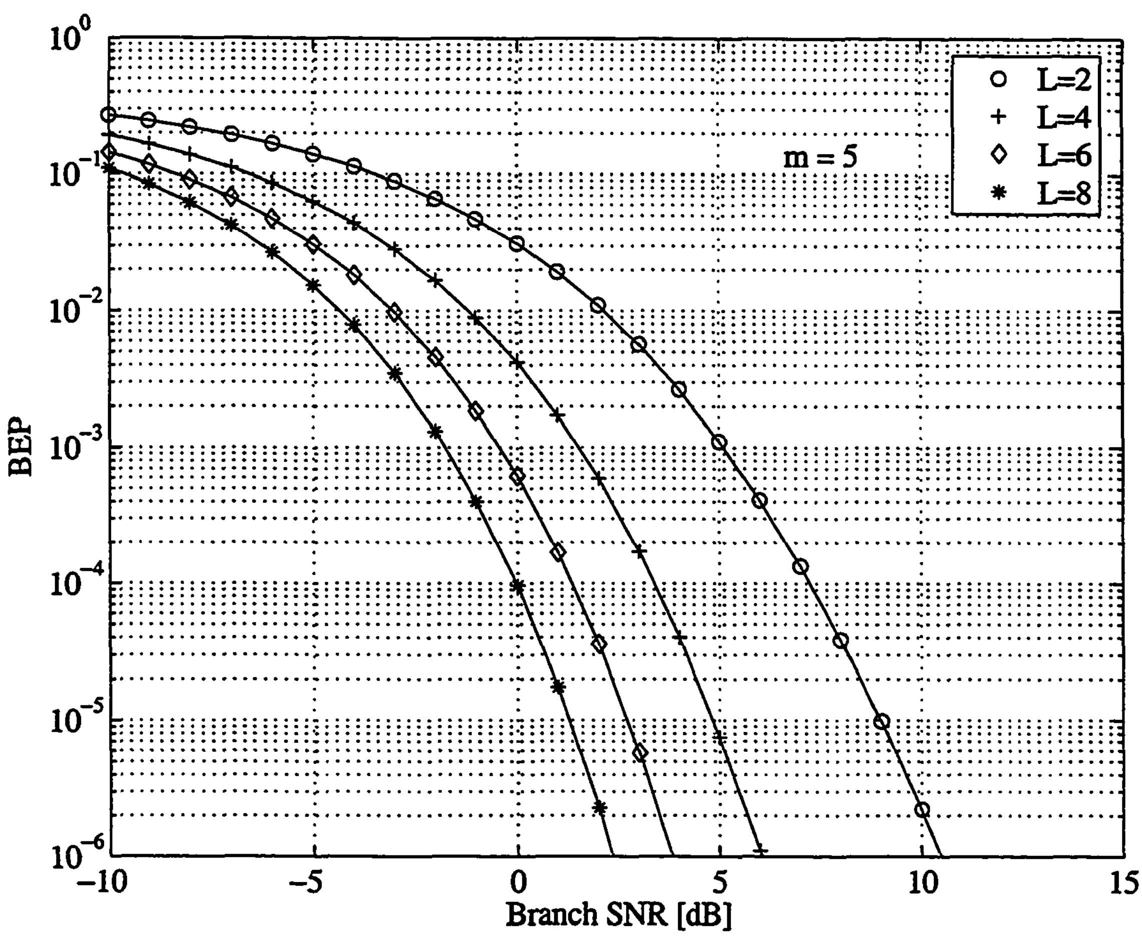

Fig. 5.4. The BEP estimated using the closed-form approximation of a L-branch EGC diversity system with CPSK signalling, for $L = 2, 4, 6$, and 8 with fading severity parameter $m = 5$ and normalized power $\Omega = 1$.

Again, using (5.8), (5.16), and (5.20), the conditional error probability for an EGC diversity system when CFSK is used can be written as

$$P_s(\varepsilon|R_O) = Q\left(\sqrt{\frac{R_{EGC}^2}{LN_0}}\right) = Q\left(\sqrt{\frac{R_{Norm}^2}{N_0}}\right). \tag{5.21}$$

Thus, the average error probability for an EGC diversity system in Nakagami fading when CFSK is used can be expressed as

$$P_e = \int_0^\infty Q\left(\sqrt{\frac{r^2}{N_0}}\right) f_{R_{Norm}}(r)\,\mathrm{d}r. \tag{5.22}$$

Using the same approximation for $f_{R_{Norm}}(r)$ as in (5.18) and evaluating the integral in (5.22), the average BEP of a L-branch EGC diversity system in Nakagami fading with CFSK signalling can be approximated as

$$P_e = \frac{1}{2} - \sqrt{\frac{\gamma\Omega}{2\pi c_2 m}}\frac{\Gamma\left(\frac{1}{2}+c_1 mL\right)}{\Gamma\left(c_1 mL\right)}\,{}_2\mathrm{F}_1\left(\frac{1}{2},\frac{1}{2}+c_1 mL,\frac{3}{2},-\frac{\gamma\Omega}{2c_2 m}\right). \tag{5.23}$$

Figures 5.5-5.7 show the BEP curves as a function of branch SNR for varying diversity orders and fading severities. The solid lines represent the exact BEP obtained by numerical integration and the symbols represent the approximate BEP obtained by the closed-form expression in (5.23). Observe that the approximate BEP is very close to the exact BEP for all values of L and m considered.

5.2.2 Noncoherent Binary Signalling

In time-varying fading channels, the carrier phase may be difficult to recover. Therefore, it is often more practical to use noncoherent modulations. Two common forms of noncoherent modulation are differential phase-shift keying (DPSK) and noncoherent FSK (NCFSK).

In DPSK, the phase of the previous bit is used as a reference for the detection of the current bit. The error probability for DPSK in a time-invariant channel is found to be [7]

$$P_s(\varepsilon|\gamma) = \frac{1}{2}e^{-\frac{E_{avg}}{N_0}} = \frac{1}{2}e^{-\gamma}. \tag{5.24}$$

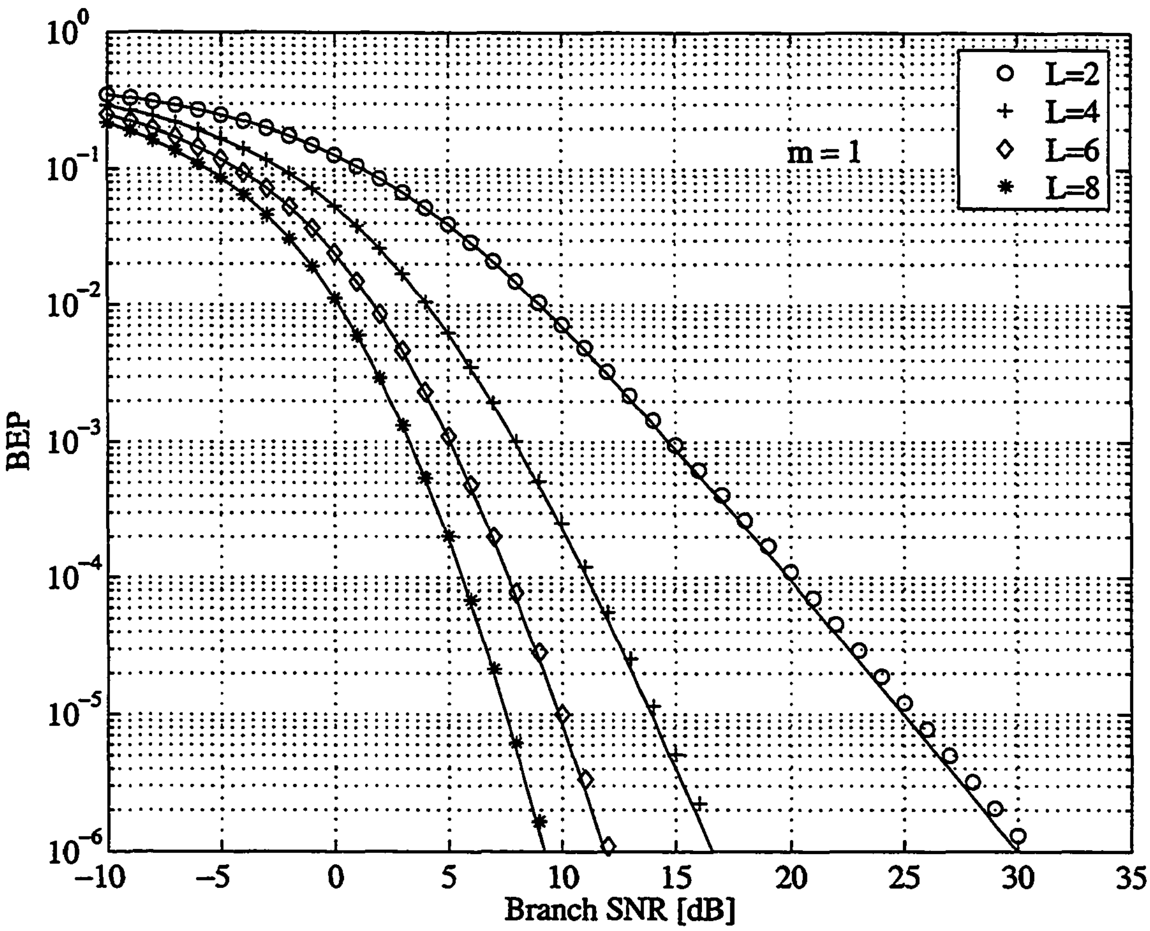

Fig. 5.5. The BEP estimated using the closed-form approximation of a L-branch EGC diversity system with CFSK signalling, for $L = 2, 4, 6,$ and 8 with fading severity parameter $m = 1$ and normalized power $\Omega = 1$.

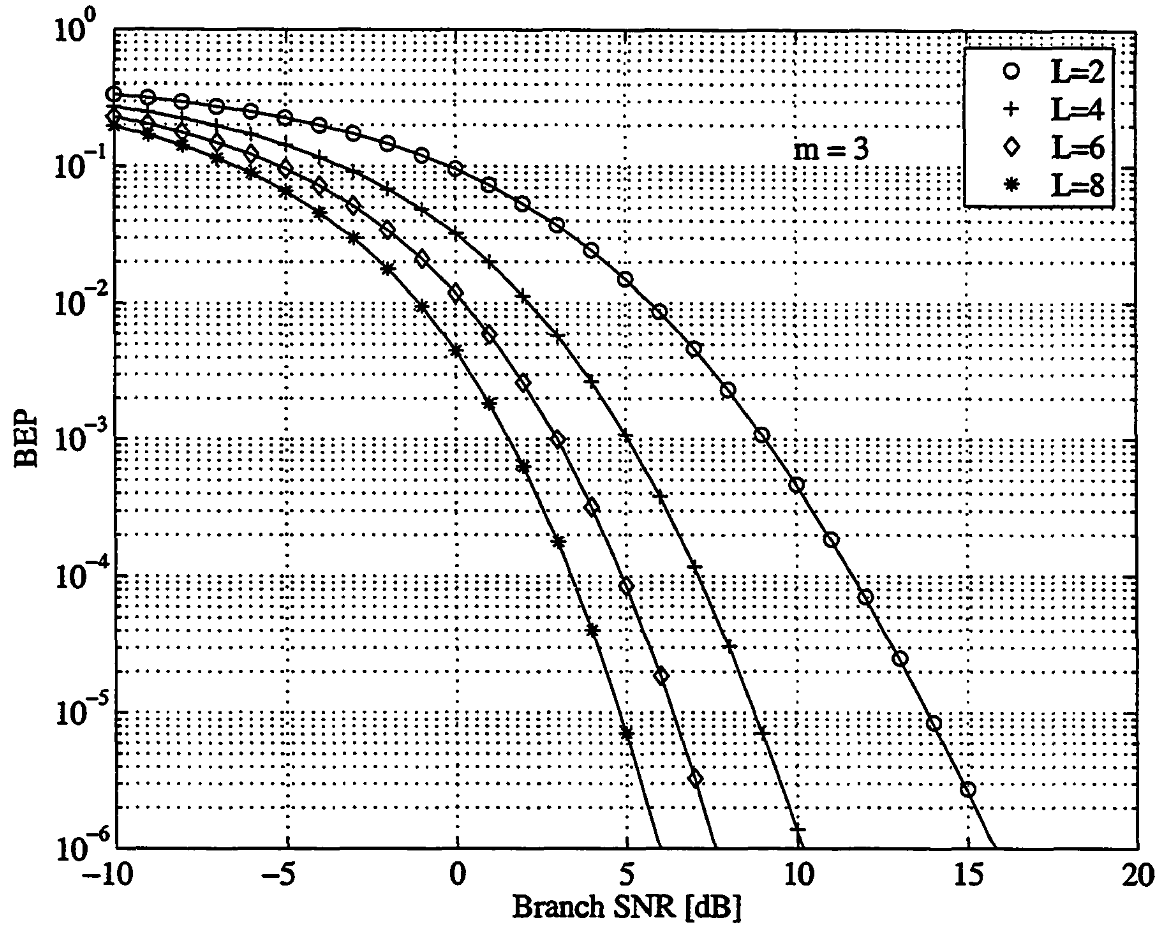

Fig. 5.6. The BEP estimated using the closed-form approximation of a L-branch EGC diversity system with CFSK signalling, for L = 2, 4, 6, and 8 with fading severity parameter $m = 3$ and normalized power $\Omega = 1$.

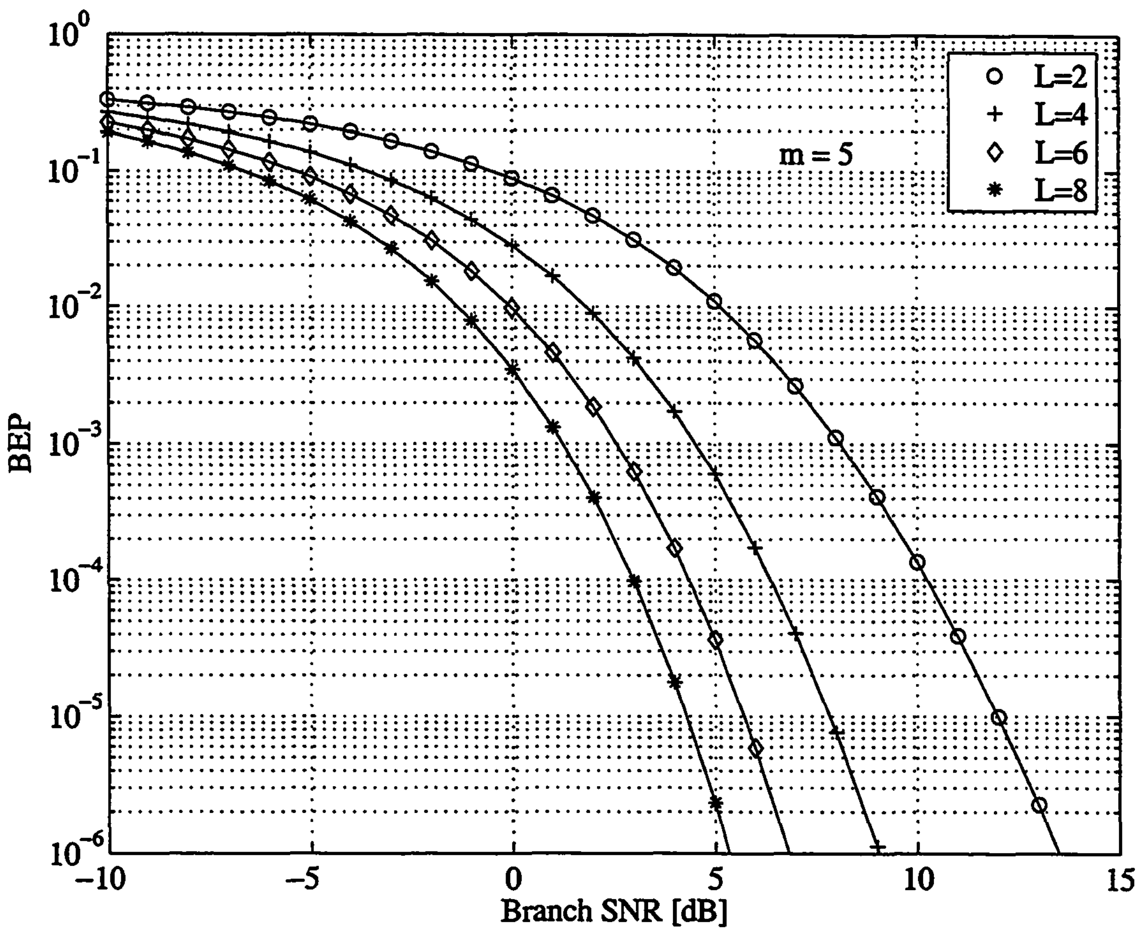

Fig. 5.7. The BEP estimated using the closed-form approximation of a L-branch EGC diversity system with CFSK signalling, for L = 2, 4, 6, and 8 with fading severity parameter $m = 5$ and normalized power $\Omega = 1$.

For an EGC diversity system, using (5.8), (5.16), and (5.24), the conditional error probability when DPSK is used can be written as

$$P_s(\varepsilon|R_O) = \frac{1}{2}e^{-\frac{R_{EGC}^2}{LN_0}} = \frac{1}{2}e^{-\frac{R_{Norm}^2}{N_0}}. \tag{5.25}$$

Thus, the average error probability for an EGC diversity system in Nakagami fading when DPSK is used can be expressed as

$$P_e = \int_0^\infty \frac{1}{2}e^{-\frac{r^2}{N_0}} f_{R_{Norm}}(r)\,\mathrm{d}r \tag{5.26}$$

where $f_{R_{Norm}}(r)$ is the normalized approximation given in (5.18). Evaluating the integral in (5.26), the average BEP of a L-branch EGC diversity system in Nakagami fading with DPSK signalling can be approximated as

$$P_e = \frac{1}{2}\left(\frac{c_2 m}{\gamma\Omega + c_2 m}\right)^{c_1 mL}. \tag{5.27}$$

Figures 5.8-5.10 show the BEP curves as a function of branch SNR for varying diversity orders and fading severities. The solid lines represent the exact BEP obtained by numerical integration and the symbols represent the approximate BEP obtained by the closed-form expression in (5.27). Observe that the approximate BEP is very close to the exact BEP for all values of L and m considered.

Lastly, this analysis is repeated for NCFSK modulation. In NCFSK, the transmitted signals are orthogonal with minimum frequency separation that is twice as large as that required for CFSK. The error probability for NCFSK in a time-invariant channel is found to be [7]

$$P_s(\varepsilon|\gamma) = \frac{1}{2}e^{-\frac{E_{avg}}{2N_0}} = \frac{1}{2}e^{-\frac{\gamma}{2}}. \tag{5.28}$$

Again, using (5.8), (5.16), and (5.28), the conditional error probability for an EGC diversity system when NCFSK is used can be written as

$$P_s(\varepsilon|R_O) = \frac{1}{2}e^{-\frac{R_{EGC}^2}{2LN_0}} = \frac{1}{2}e^{-\frac{R_{Norm}^2}{2N_0}}. \tag{5.29}$$

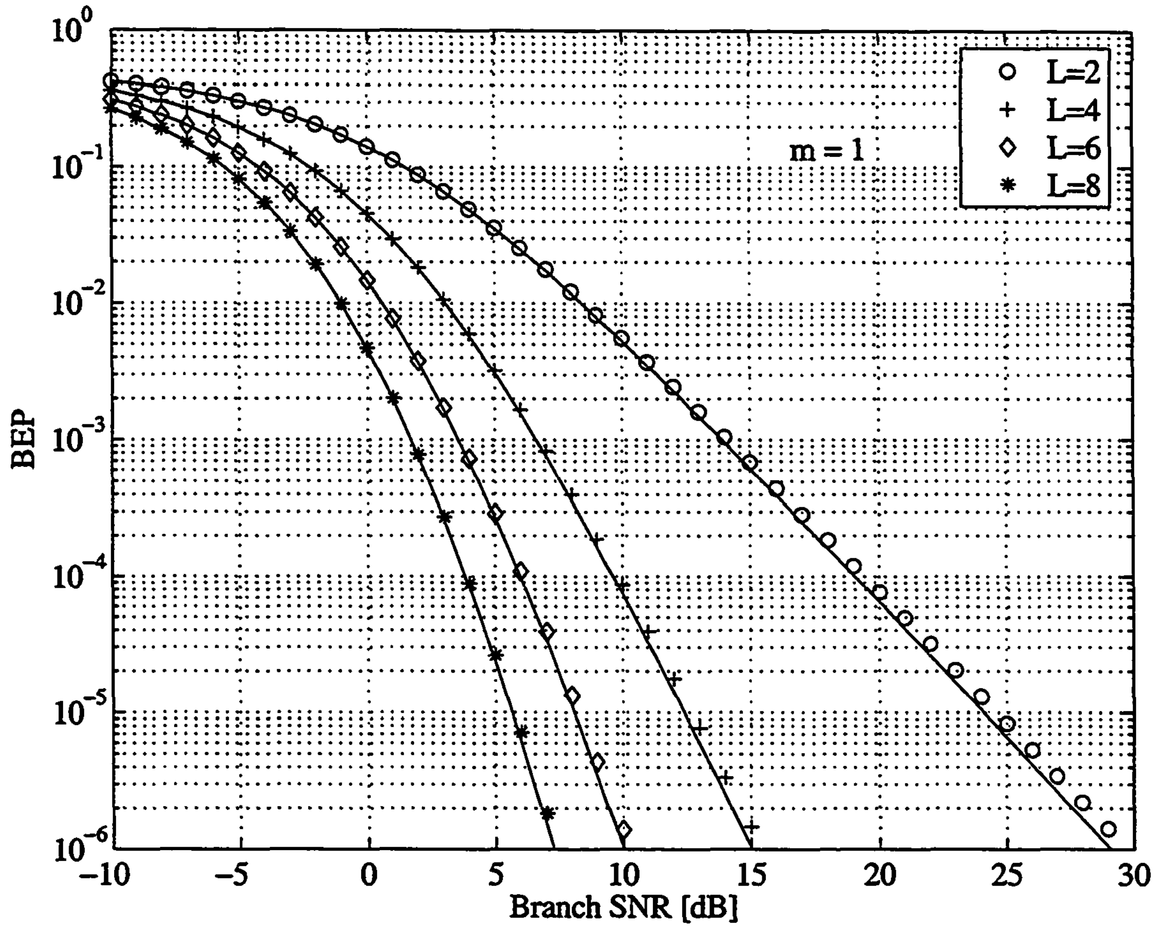

Fig. 5.8. The BEP estimated using the closed-form approximation of a L-branch EGC diversity system with DPSK signalling, for L = 2, 4, 6, and 8 with fading severity parameter $m = 1$ and normalized power $\Omega = 1$.

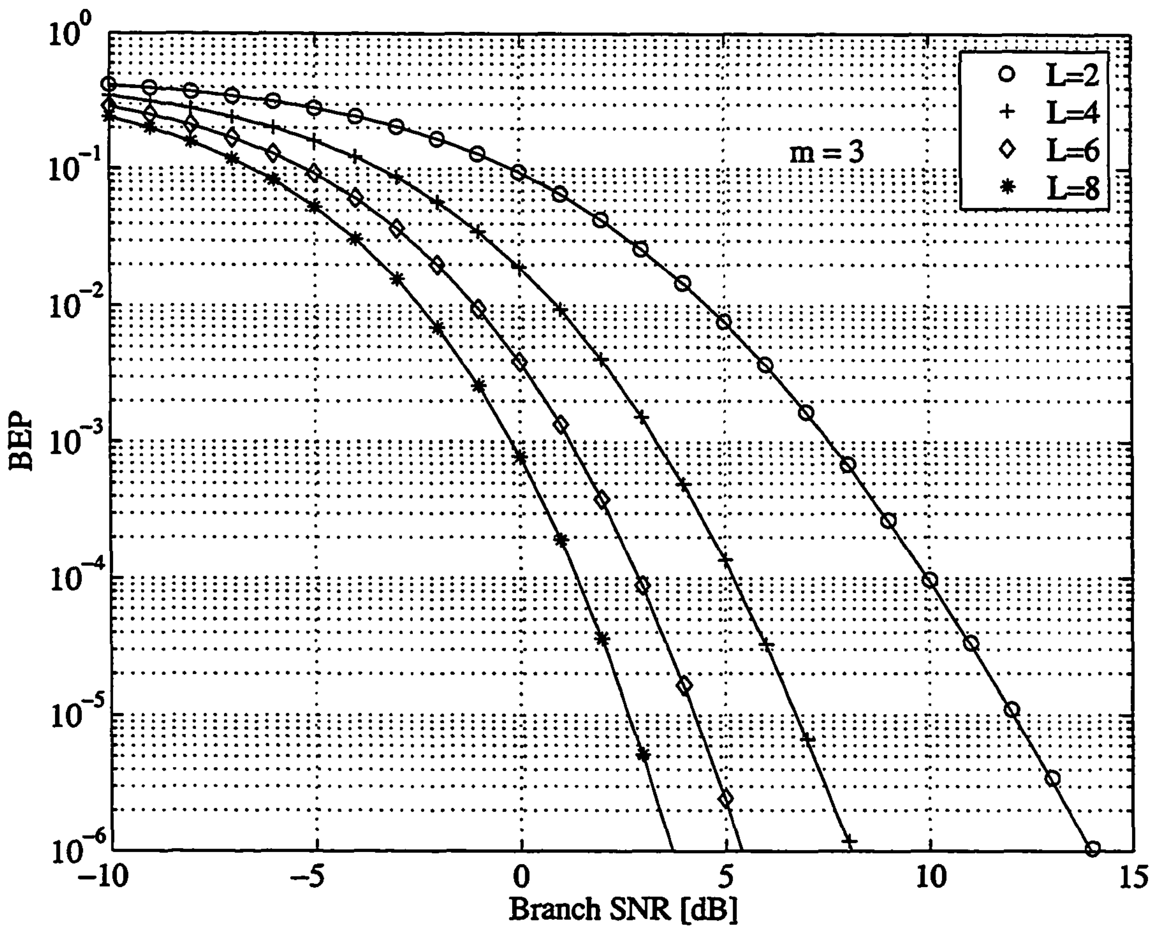

Fig. 5.9. The BEP estimated using the closed-form approximation of a L-branch EGC diversity system with DPSK signalling, for L = 2, 4, 6, and 8 with fading severity parameter $m = 3$ and normalized power $\Omega = 1$.

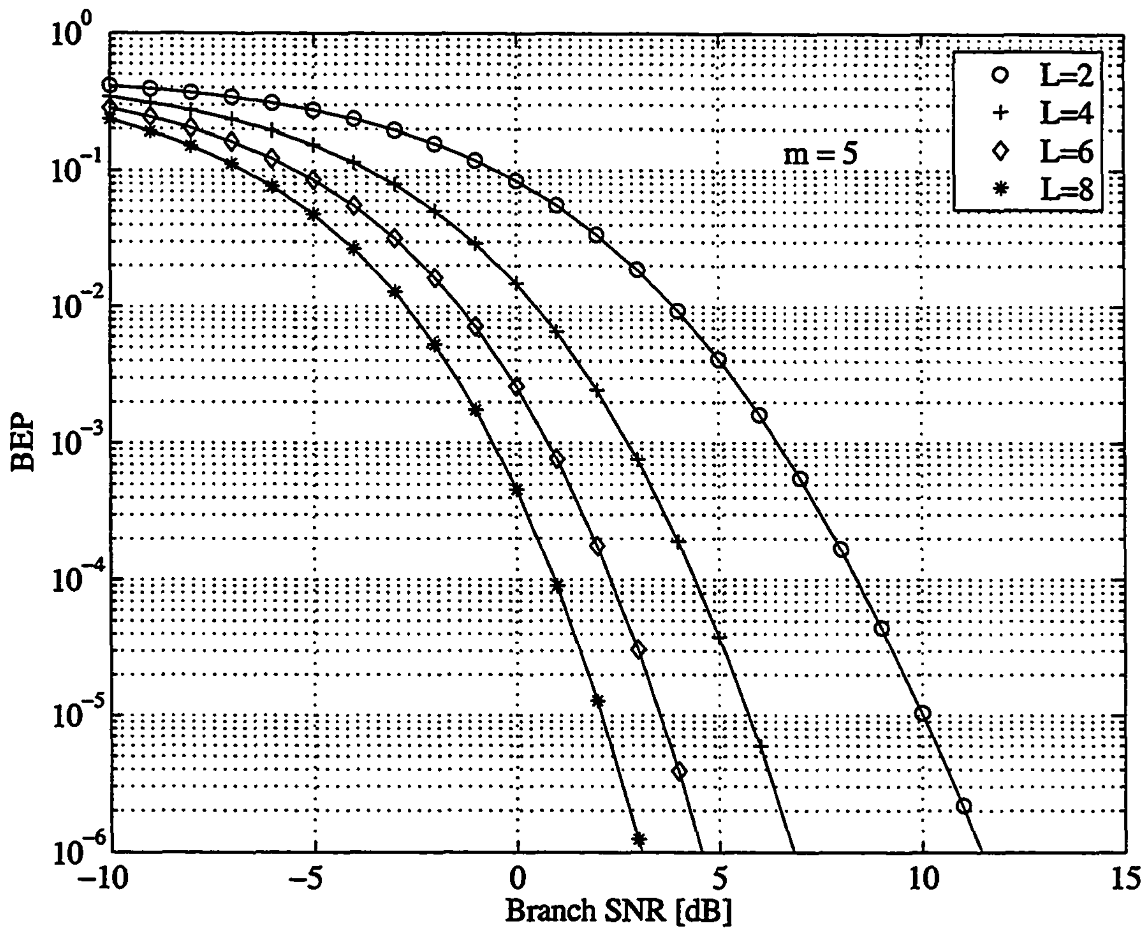

Fig. 5.10. The BEP estimated using the closed-form approximation of a L-branch EGC diversity system with DPSK signalling, for $L = 2, 4, 6$, and 8 with fading severity parameter $m = 5$ and normalized power $\Omega = 1$.

Thus, the average error probability for an EGC diversity system in Nakagami fading when NCFSK is used can be expressed as

$$P_e = \int_0^{\infty} \frac{1}{2} e^{-\frac{r^2}{2N_0}} f_{R_{Norm}}(r)\, \mathrm{d}r. \tag{5.30}$$

Using the same approximation for $f_{R_{Norm}}(r)$ as in (5.18) and evaluating the integral in (5.30), the average BEP of a L-branch EGC diversity system in Nakagami fading with NCFSK signalling can be approximated as

$$P_e = \frac{1}{2}\left(\frac{2c_2 m}{\gamma\Omega + 2c_2 m}\right)^{c_1 mL}. \tag{5.31}$$

Figures 5.11-5.13 show the BEP curves as a function of branch SNR for varying diversity orders and fading severities. The solid lines represent the exact BEP obtained by numerical integration and the symbols represent the approximate BEP obtained by the closed-form expression in (5.31). Observe that the approximate BEP is very close to the exact BEP for all values of L and m considered.

5.2.3 Coherent M-ary Signalling

In this section, the SEP for coherent M-ary phase-shift keying (MPSK) is considered. MPSK uses M different phases of the carrier to transmit M possible information symbols. The error probability for MPSK in a time-invariant channel is found to be [7]

$$P_s(\varepsilon|\gamma) = 1 - \int_{-\pi/M}^{\pi/M} f_{\theta_r}(\theta_r)\, \mathrm{d}\theta_r, \tag{5.32}$$

where $f_{\theta_r}(\theta_r)$ is the PDF of the phase fluctuation due to AWGN and is given by

$$f_{\theta_r}(\theta_r) = \sqrt{\frac{\gamma}{\pi}}\cos\theta e^{-\gamma\sin^2\theta} + \frac{e^{-\gamma}}{2\pi}\left[1 - \sqrt{\pi\gamma}\cos\theta e^{\gamma\cos^2\theta}\mathrm{erfc}(\sqrt{\gamma}\cos\theta)\right] \tag{5.33}$$

where $\mathrm{erfc}(\cdot)$ is the complementary error function. In general, (5.32) does not reduced to a closed-form expression except for the cases when $M = 2$ or $M = 4$. Consequently, upper

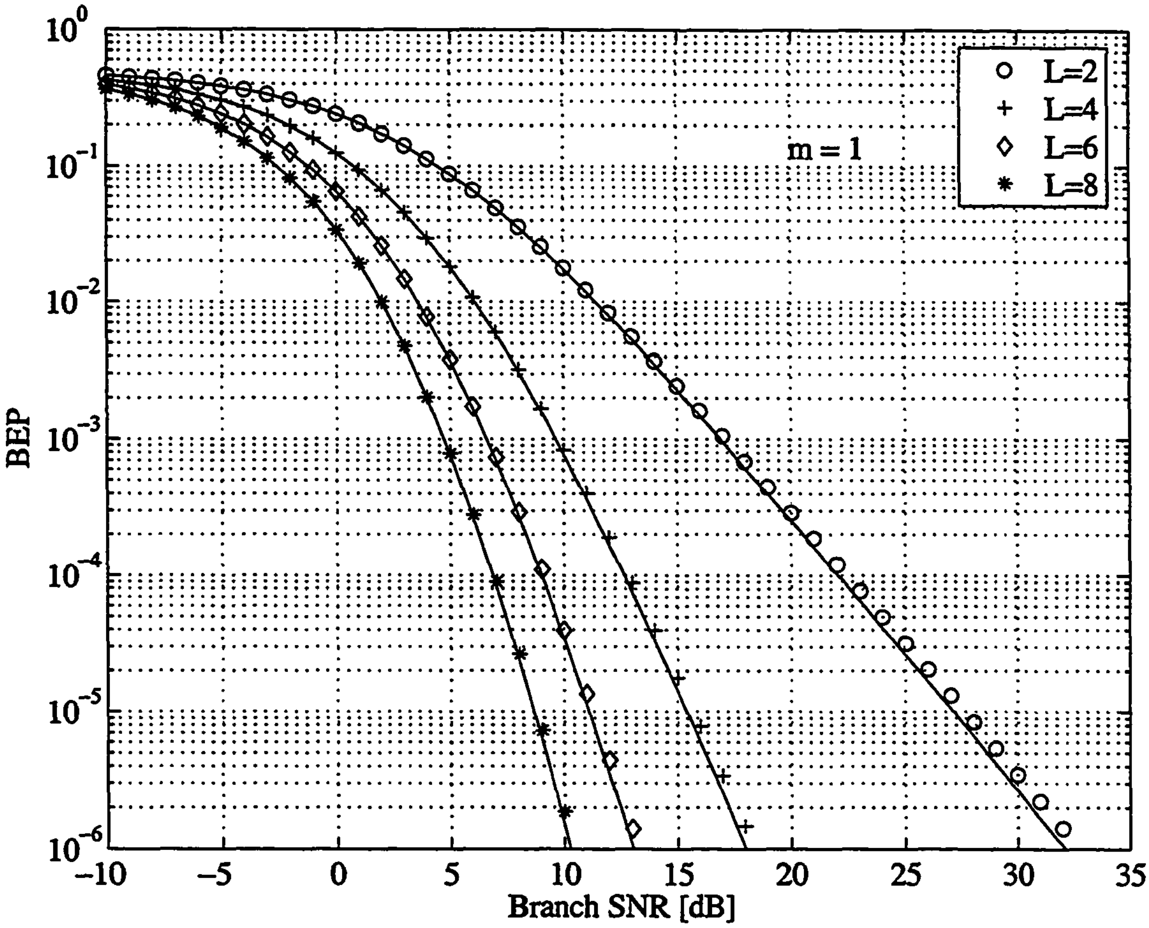

Fig. 5.11. The BEP estimated using the closed-form approximation of a L-branch EGC diversity system with NCFSK signalling, for $L = 2, 4, 6$, and 8 with fading severity parameter $m = 1$ and normalized power $\Omega = 1$.

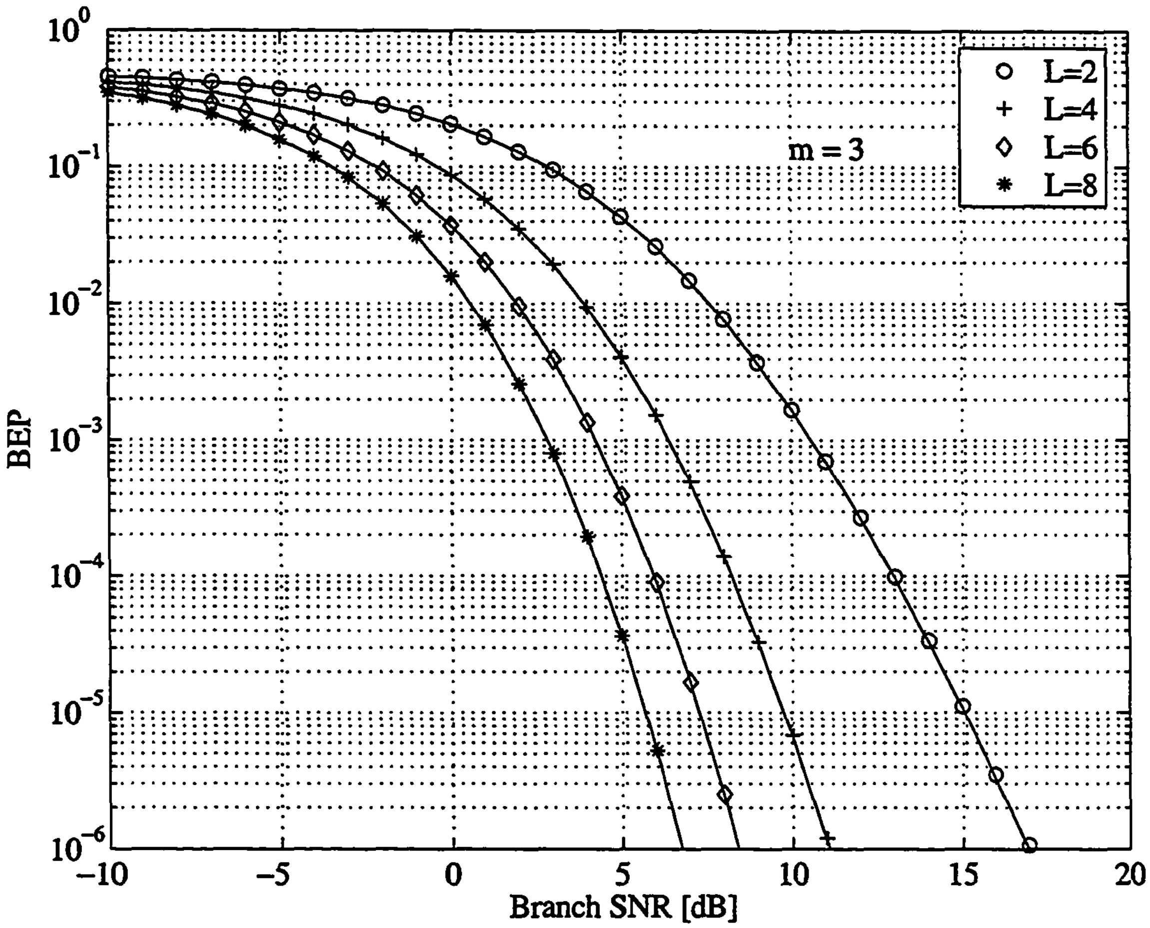

Fig. 5.12. The BEP estimated using the closed-form approximation of a L-branch EGC diversity system with NCFSK signalling, for $L = 2, 4, 6$, and 8 with fading severity parameter $m = 3$ and normalized power $\Omega = 1$.

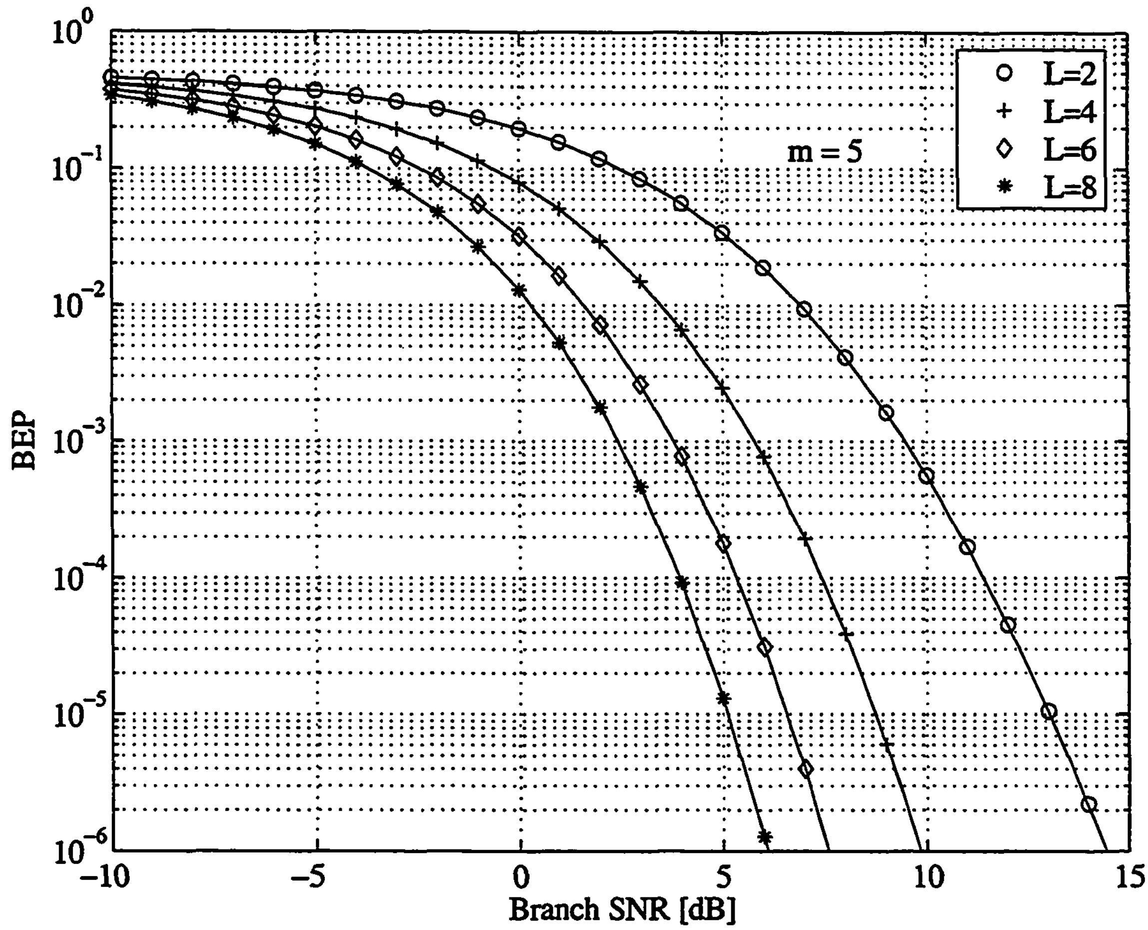

Fig. 5.13. The BEP estimated using the closed-form approximation of a L-branch EGC diversity system with NCFSK signalling, for $L = 2, 4, 6,$ and 8 with fading severity parameter $m = 5$ and normalized power $\Omega = 1$.

and lower bounds or approximations for the SEP have been used extensively. In [31], a tight approximation for the SEP of coherent MPSK is obtained as

$$P_s(\varepsilon|\gamma) \cong \operatorname{erfc}\left(\sqrt{\gamma}\sin\left(\frac{\pi}{M}\right)\right) - \frac{e^{-\gamma}}{\pi}\tan\left(\frac{\pi}{M}\right) + \sqrt{\frac{\gamma}{\pi}}\tan\left(\frac{\pi}{M}\right)\operatorname{erfc}(\sqrt{\gamma}). \tag{5.34}$$

For an EGC diversity system, using (5.8), (5.16), and (5.34), the conditional error probability when MPSK is used can be approximated as

$$\begin{aligned}
P_s(\varepsilon|R_O) &\cong \operatorname{erfc}\left(\sqrt{\frac{R_{EGC}^2}{LN_0}}\sin\left(\frac{\pi}{M}\right)\right) - \frac{e^{-\frac{R_{EGC}^2}{LN_0}}}{\pi}\tan\left(\frac{\pi}{M}\right) \\
&\quad + \sqrt{\frac{R_{EGC}^2}{LN_0\pi}}\tan\left(\frac{\pi}{M}\right)\operatorname{erfc}\left(\sqrt{\frac{R_{EGC}^2}{LN_0}}\right) \\
&\cong \operatorname{erfc}\left(\sqrt{\frac{R_{Norm}^2}{N_0}}\sin\left(\frac{\pi}{M}\right)\right) - \frac{e^{-\frac{R_{Norm}^2}{N_0}}}{\pi}\tan\left(\frac{\pi}{M}\right) \\
&\quad + \sqrt{\frac{R_{Norm}^2}{N_0\pi}}\tan\left(\frac{\pi}{M}\right)\operatorname{erfc}\left(\sqrt{\frac{R_{Norm}^2}{N_0}}\right).
\end{aligned} \tag{5.35}$$

Thus, the average error probability for an EGC diversity system in Nakagami fading when MPSK is used can be expressed as

$$\begin{aligned}
P_e &= \int_0^\infty \left[\operatorname{erfc}\left(\sqrt{\frac{r^2}{N_0}}\sin\left(\frac{\pi}{M}\right)\right) - \frac{e^{-\frac{r^2}{N_0}}}{\pi}\tan\left(\frac{\pi}{M}\right)\right. \\
&\quad \left. + \sqrt{\frac{r^2}{N_0\pi}}\tan\left(\frac{\pi}{M}\right)\operatorname{erfc}\left(\sqrt{\frac{r^2}{N_0}}\right)\right] f_{R_{Norm}}(r)\,dr
\end{aligned} \tag{5.36}$$

where $f_{R_{Norm}}(r)$ is the normalized approximation given in (5.18). Evaluating the integral in (5.36), the average SEP of a L-branch EGC diversity system in Nakagami fading with MPSK signalling can be approximated as

$$\begin{aligned}
P_e &= 1 - \frac{\tan\left(\frac{\pi}{M}\right)}{\pi}\left[\left(\frac{c_2 m}{\gamma\Omega + c_2 m}\right)^{c_1 mL} + \frac{2c_1 L\gamma\Omega}{c_2}\,{}_2\mathrm{F}_1\left(\frac{1}{2}, 1 + c_1 mL, \frac{3}{2}, -\frac{\gamma\Omega}{c_2 m}\right)\right] \\
&\quad - \left[{}_2\mathrm{F}_1\left(\frac{1}{2}, \frac{1}{2} + c_1 mL, \frac{3}{2}, -\frac{\gamma\Omega\sin^2\left(\frac{\pi}{M}\right)}{c_2 m}\right) 2\sin\left(\frac{\pi}{M}\right) - \tan\left(\frac{\pi}{M}\right)\right] \\
&\quad \times \sqrt{\frac{\gamma\Omega}{\pi c_2 m}}\frac{\Gamma\left(\frac{1}{2} + c_1 mL\right)}{\Gamma\left(c_1 mL\right)}.
\end{aligned} \tag{5.37}$$

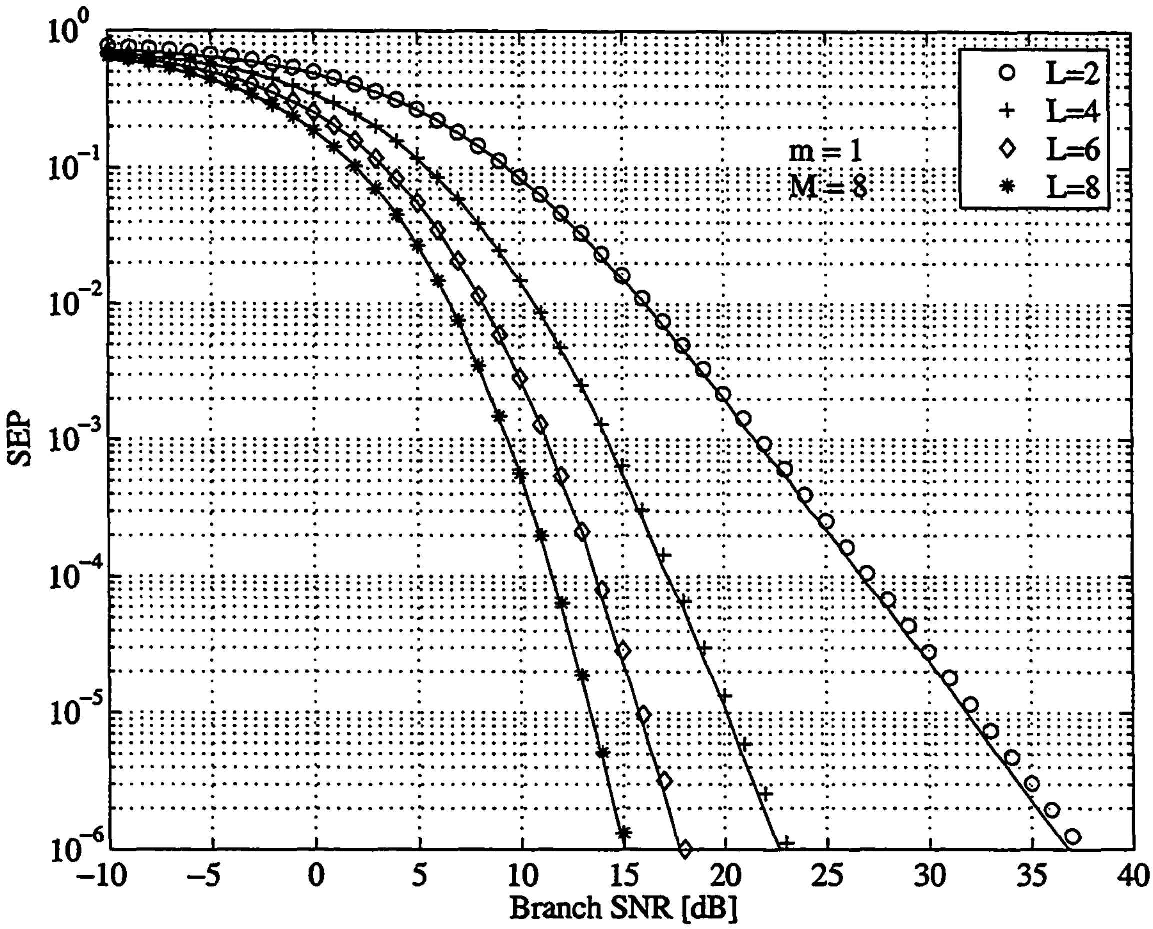

Fig. 5.14. The SEP estimated using the closed-form approximation of a L-branch EGC diversity system with MPSK signalling, for $L = 2, 4, 6$, and 8 with fading severity parameter $m = 1$, normalized power $\Omega = 1$, and $M = 8$.

Figures 5.14-5.19 show the SEP curves as a function of branch SNR for varying diversity orders, fading severities, and for a fixed number of modulation symbols. The solid lines represent the exact SEP obtained by simulation and the symbols represent the approximate SEP obtained by the closed-form expression in (5.37). Observe that the approximate SEP is very close to the simulated SEP for all values of L, m, and M considered.

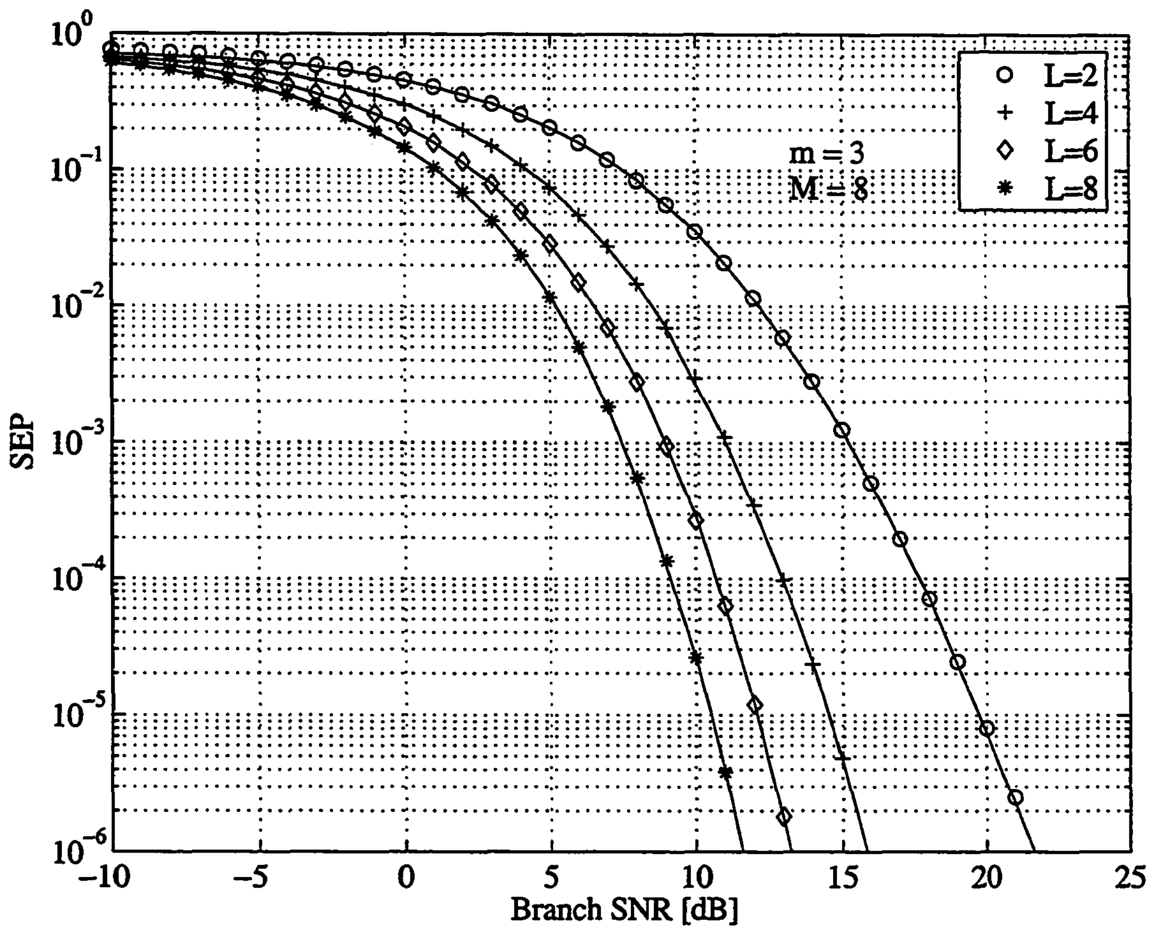

Fig. 5.15. The SEP estimated using the closed-form approximation of a L-branch EGC diversity system with MPSK signalling, for $L = 2, 4, 6,$ and 8 with fading severity parameter $m = 3$, normalized power $\Omega = 1$, and $M = 8$.

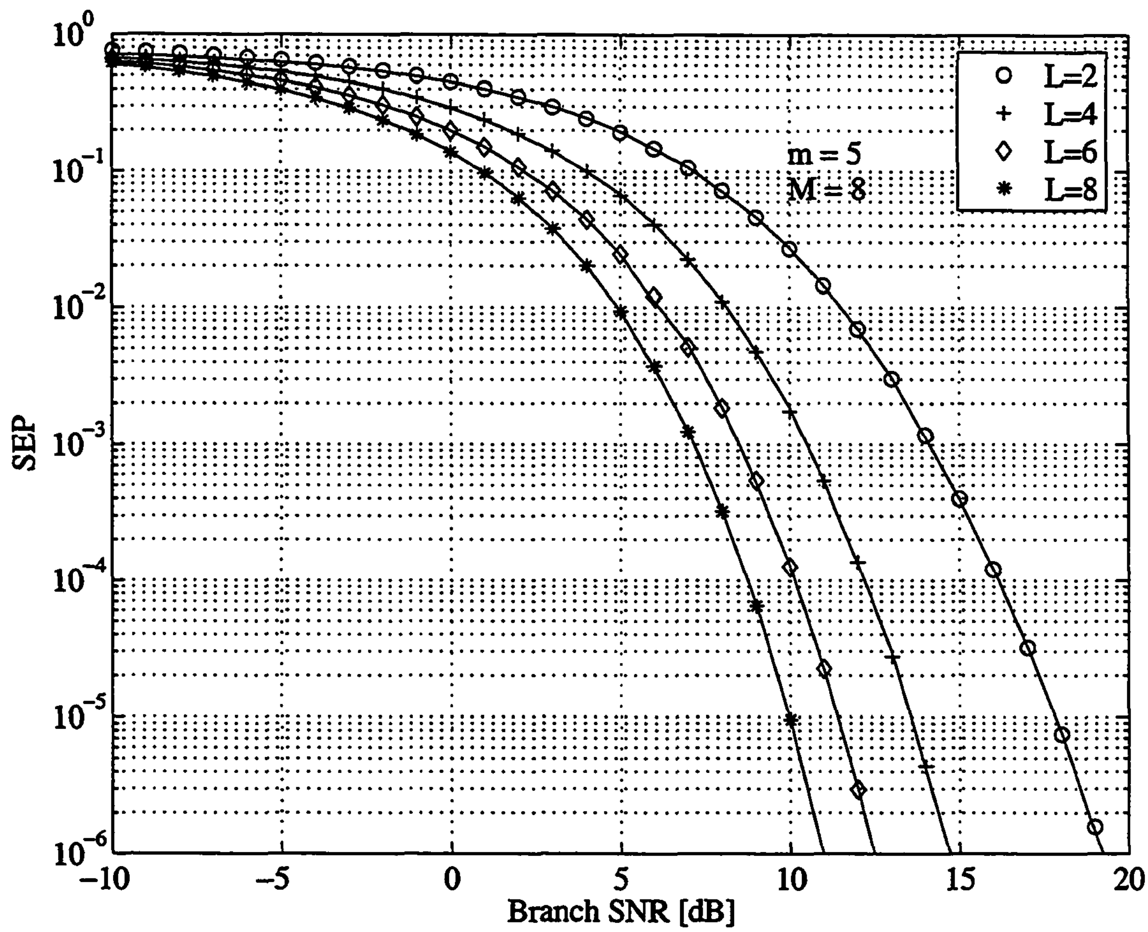

Fig. 5.16. The SEP estimated using the closed-form approximation of a L-branch EGC diversity system with MPSK signalling, for $L = 2, 4, 6$, and 8 with fading severity parameter $m = 5$, normalized power $\Omega = 1$, and $M = 8$.

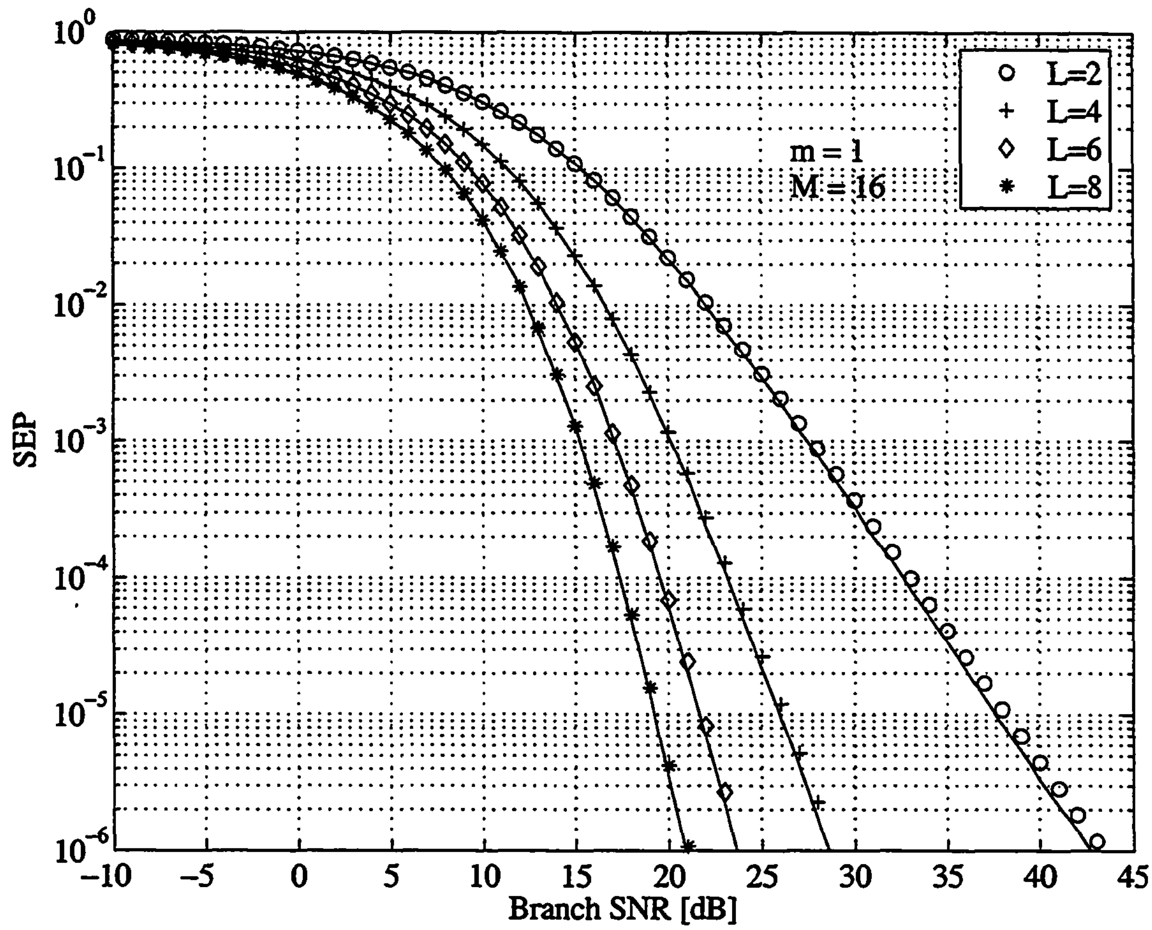

Fig. 5.17. The SEP estimated using the closed-form approximation of a L-branch EGC diversity system with MPSK signalling, for L = 2, 4, 6, and 8 with fading severity parameter m = 1, normalized power Ω = 1, and M = 16.

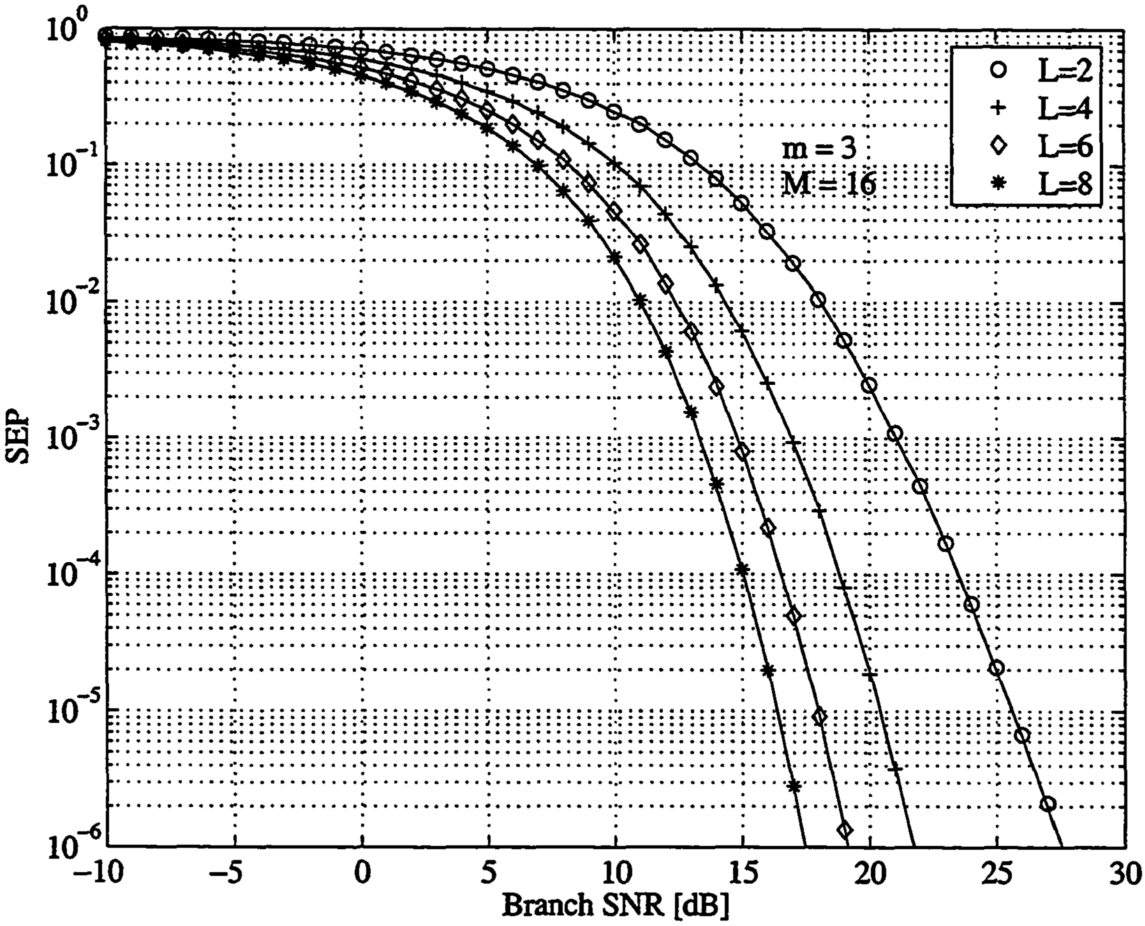

Fig. 5.18. The SEP estimated using the closed-form approximation of a L-branch EGC diversity system with MPSK signalling, for L = 2, 4, 6, and 8 with fading severity parameter $m = 3$, normalized power $\Omega = 1$, and $M = 16$.

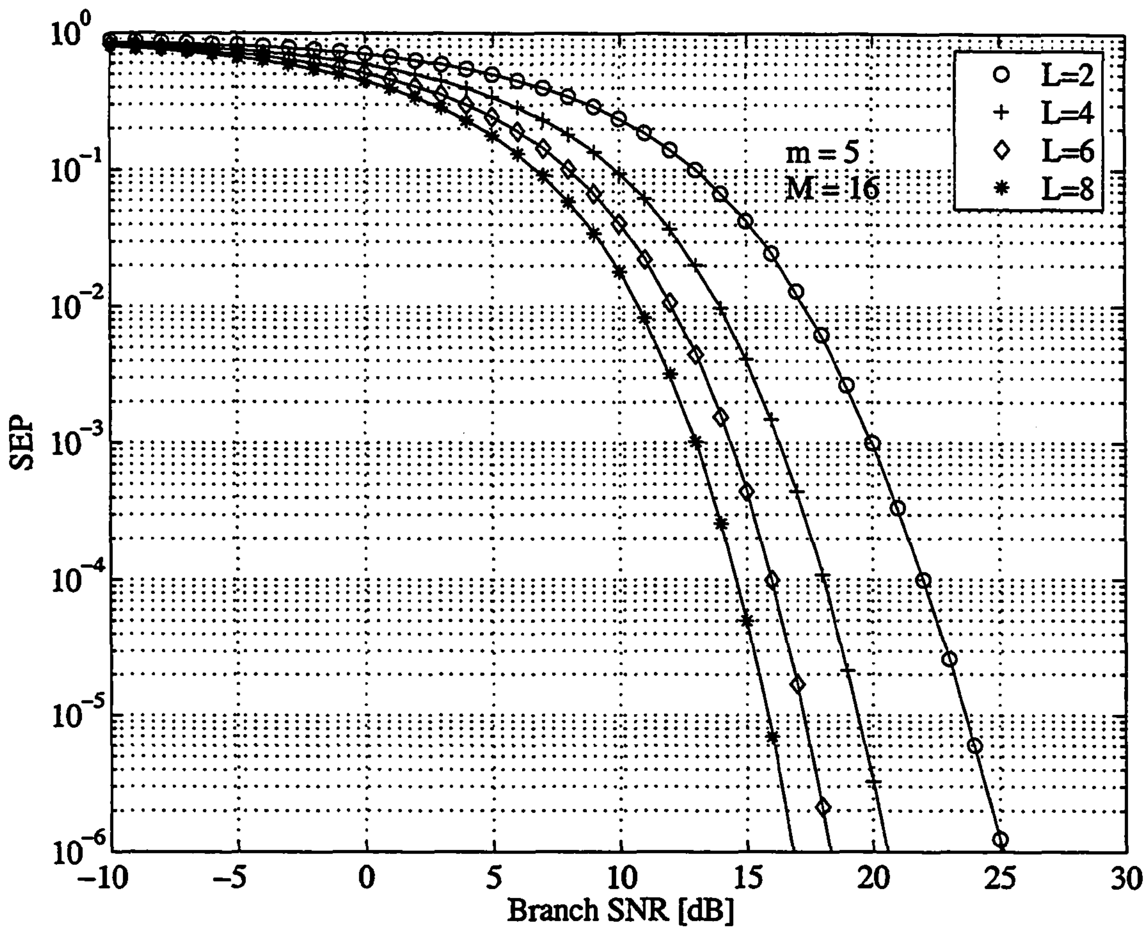

Fig. 5.19. The SEP estimated using the closed-form approximation of a L-branch EGC diversity system with MPSK signalling, for L = 2, 4, 6, and 8 with fading severity parameter m = 5, normalized power Ω = 1, and M = 16.

5.3 A Closed-Form Expression for the Outage Probability of EGC Diversity Systems in Nakagami Fading

As mentioned previously, outage probability is another criterion that is often used to evaluate the performance of diversity receivers. Recall that the SNR at the output of the combiner is given by (5.10), namely

$$\gamma_O = \frac{R_O^2}{2\sigma_N^2}. \tag{5.38}$$

Instead of using a threshold SNR, a combined signal envelope threshold can be defined as

$$R_{th} = \sqrt{2\gamma_{th}\sigma_N^2} = \sqrt{\gamma_{th}LN_0}. \tag{5.39}$$

Then the outage probability can be equivalently found as

$$P_{out} = \int_0^{R_{th}} f_{R_O}(r)\,\mathrm{d}r \tag{5.40}$$

where $f_{R_O}(r)$ is the PDF of the combined output envelope. Since the diversity branches are iid and using the normalized signal envelope in (5.16), the outage probability can be expressed as

$$P_{out} = \int_0^{R_{th_{Norm}}} f_{R_{Norm}}(r)\,\mathrm{d}r \tag{5.41}$$

where $f_{R_{Norm}}(r)$ is the normalized approximation given in (5.18) and $R_{th_{Norm}} = R_{th}/\sqrt{L}$ is the normalized signal envelope threshold. Observe that P_{out} in (5.41) is simply the CDF of R_{Norm}, evaluated at $R_{th_{Norm}}$. Thus, the outage probability of a L-branch EGC diversity systems in Nakagami fading can be approximated as

$$P_{out} = 1 - \frac{\gamma\left(c_1 mL, c_2 \frac{m}{\Omega} R_{th_{Norm}}^2\right)}{\Gamma(c_1 mL)} = 1 - \frac{\gamma\left(c_1 mL, c_2 \frac{m}{\Omega} \frac{\gamma_{th}}{\gamma}\right)}{\Gamma(c_1 mL)}. \tag{5.42}$$

As expected, the outage probability of an EGC system is solely a function of the threshold SNR and SNR per diversity branch. Figures 5.20-5.22 show the outage probability curves as a function of the threshold SNR for varying diversity orders, fading severities, and for a

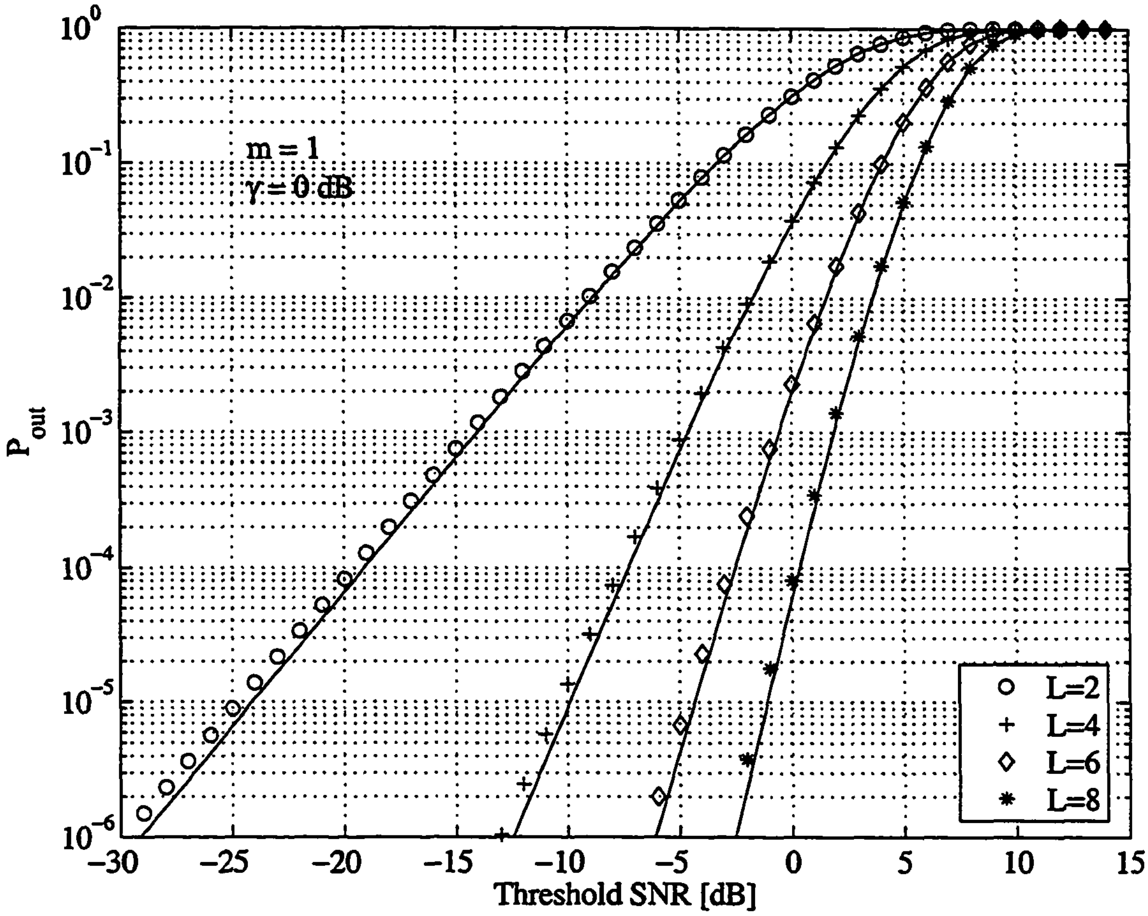

Fig. 5.20. The outage probability estimated using the closed-form approximation of a L-branch EGC diversity system, for $L = 2, 4, 6$, and 8 with fading severity parameter $m = 1$, normalized power $\Omega = 1$, and fixed SNR $\gamma = 0$ dB.

fixed SNR $\gamma = 0$ dB. The solid lines represent the exact outage probability obtained by numerical integration and the symbols represent the approximate outage probability obtained by the closed-form expression in (5.42). Observe that the approximate outage probability is very close to the exact outage probability for all values of L, m, and γ considered.

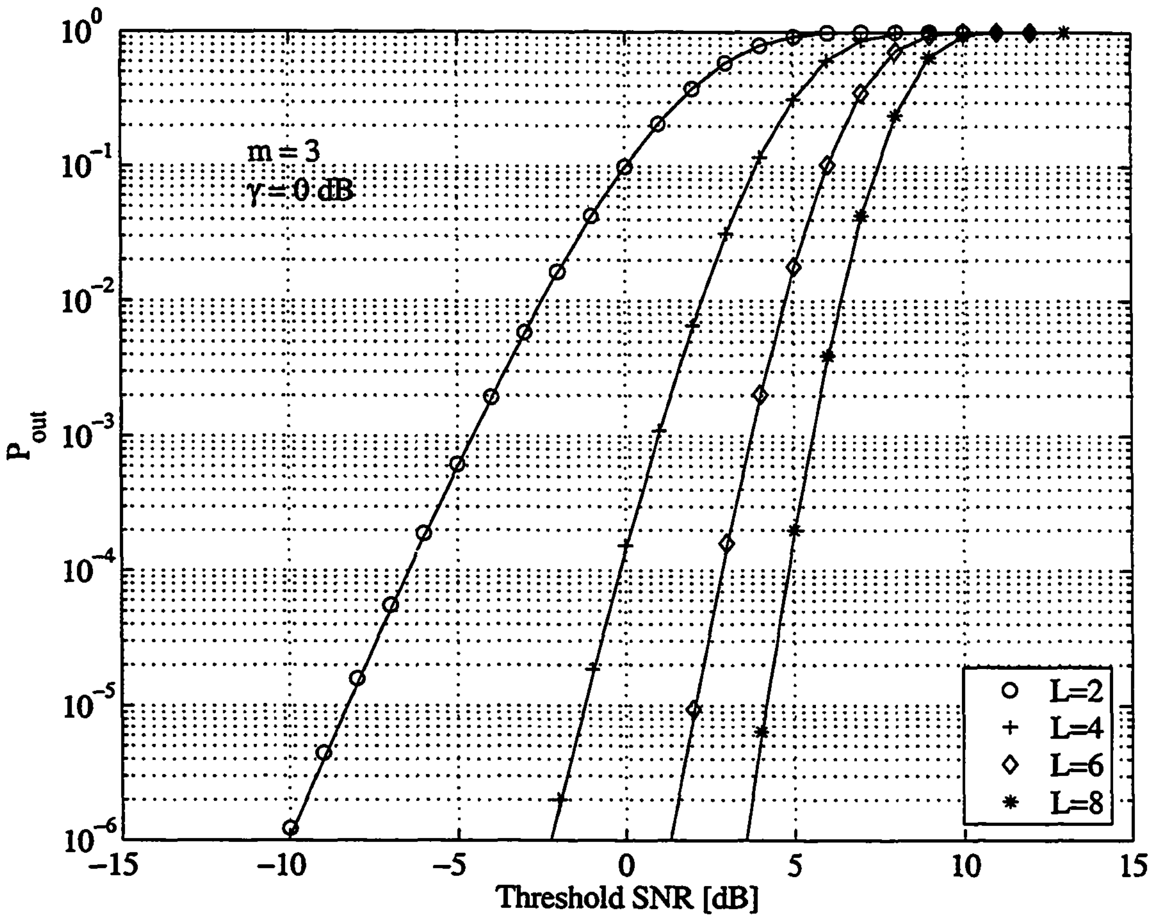

Fig. 5.21. The outage probability estimated using the closed-form approximation of a L-branch EGC diversity system, for $L = 2, 4, 6$, and 8 with fading severity parameter $m = 3$, normalized power $\Omega = 1$, and fixed SNR $\gamma = 0$ dB.

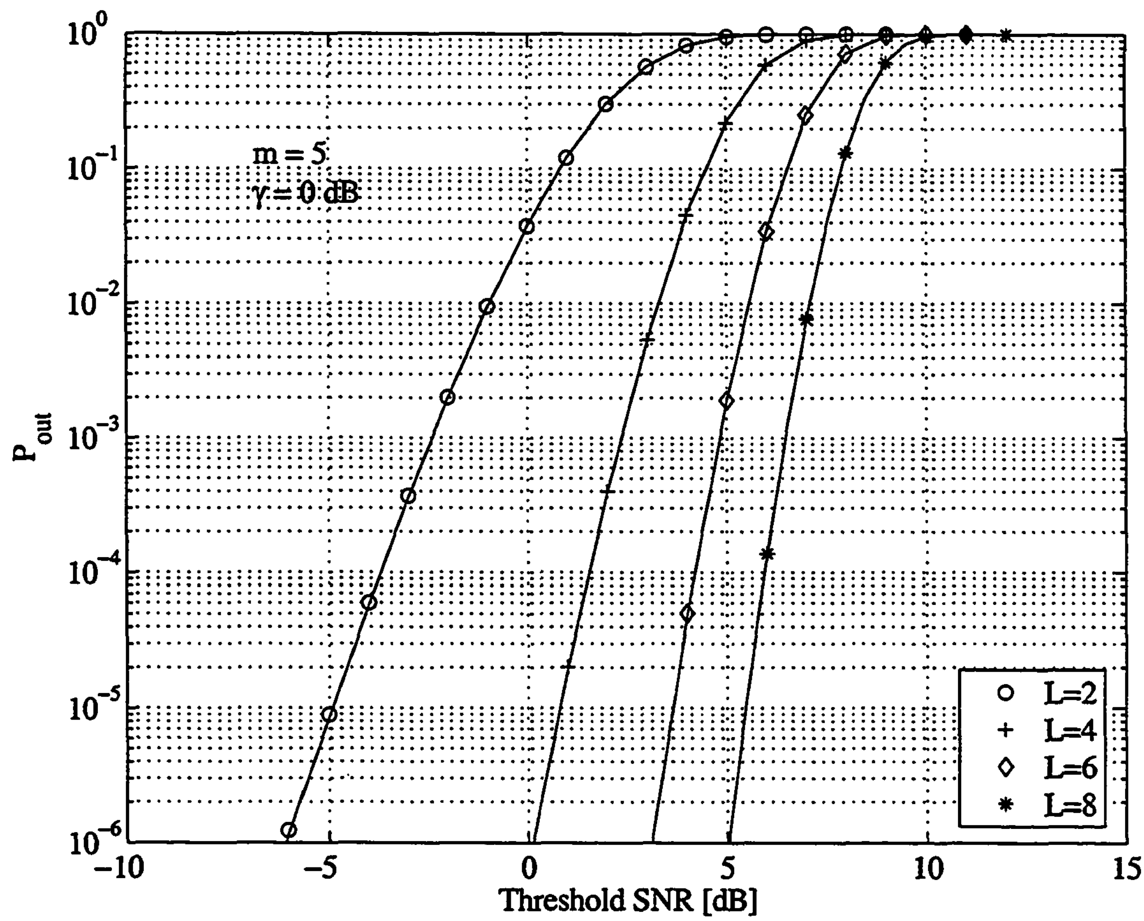

Fig. 5.22. The outage probability estimated using the closed-form approximation of a L-branch EGC diversity system, for $L = 2, 4, 6$, and 8 with fading severity parameter $m = 5$, normalized power $\Omega = 1$, and fixed SNR $\gamma = 0$ dB.

5.4 Summary

In this chapter, the performance of EGC diversity systems in Nakagami fading was analyzed. Closed-form expressions for the error probabilities were derived. Both coherent binary and M-ary, as well as noncoherent binary signalling were considered. In addition, a closed-form expression for the outage probability of EGC systems in Nakagami fading was also derived. These expressions are derived by using the closed-form approximations to the CDF and PDF of a sum of Nakagami RVs derived in Chapter 4. It was observed that the approximate error rates and outage probabilities are in excellent agreement with the solutions found by numerical integration or simulation. For example, at a SEP or outage probability of 10^{-6}, the worst case approximation error is 0.8 dB. This occurs when dual branch diversity in Rayleigh fading is considered. For most other cases, at a SEP or outage probability of 10^{-6}, the approximation error is less than 0.1 dB. It should also be noted that although this method of analysis may not provide closed-form solutions for the error probability of all modulation schemes, the PDF sum approximations generally eliminate several orders of integration while providing accurate approximations for the error rates of EGC diversity systems.

Chapter 6

Conclusion

Determining the sum distributions and densities of independent Rayleigh, Ricean, and Nakagami RVs is a longstanding problem in wireless communications. These sums have wide applicability in the modeling and performance analysis of wireless systems, in particular, EGC diversity systems. However, because closed-form expressions for the sum distributions and densities do not exist, there are relatively few published results in this area. The lack of closed-form expressions has resulted in several computational approaches which, despite providing accurate results, are often complex and time consuming. Thus, it is important to develop accurate and efficient methods for the computation of the sum distributions and densities.

In this thesis, new approximations for the sum distributions and densities of independent Rayleigh, Ricean, and Nakagami RVs were derived. It was demonstrated that the approximations are accurate for a wide range of probability values, statistical parameters, and number of summands. These results facilitate efficient performance analysis for a broad range of applications including wireless, satellite, and terrestrial communication systems. For example, analytical expressions for the performance of EGC diversity systems in Nakagami fading are derived in this thesis. Finally, it should be noted that although the approximations developed in this thesis were for iid RVs, the analysis can be extended to non-iid cases such as sums of correlated RVs or sums where each RV has arbitrary statistical parameters. The contributions of this thesis are summarized as follows:

1. For the Rayleigh sum distribution, a widely used SAA for the density is shown to be accurate if one considers only values in the lower tail of the density. If values near the mean or in the upper tail of the density are required, then this approximation lacks sufficient accuracy. In this thesis, a closed-form approximation to the Rayleigh sum distribution based on modifying the SAA to the PDF of a Rayleigh sum was derived. It was observed that the approximation is accurate over a wide range of probabilities. In addition, the closed-form PDF approximation derived from the CDF approximation is also accurate over the same large range.

2. The generic approach for determining a sum distribution of independent RVs via the CHF is somewhat difficult for Ricean RVs. This is because the Ricean RV does not have a closed-form CHF. Accurate closed-form approximations to the Ricean sum CDF and PDF are presented in this thesis. These approximations are based on modifying the sum distribution of squared Ricean RVs.

3. Next, accurate closed-form approximations to the Nakagami sum CDF and PDF are derived. These approximations are based on modifying the sum distribution of squared Nakagami RVs. The proposed approximations allow for efficient performance analysis for a broad range of applications.

4. Closed-form expressions for the average error and outage probabilities of EGC diversity systems in Nakagami fading channels were derived. These analytical expressions make use of the Nakagami sum CDF and PDF approximations proposed in this thesis. When compared to the solutions found by numerical integration and simulation, it is clear that the closed-form approximations are accurate. The benefit of these results is that they allow for rapid evaluation of the performance of EGC diversity communication systems. This will assist designers when making decisions on system parameters in order to achieve quality of service demands.

References

[1] W. C. Jakes, *Microwave Mobile Communications*. New York, NY: John Wiley & Sons, 1974.

[2] B. Sklar, *Digital Communications Fundamentals and Applications*, 2nd ed. Upper Saddle River, NJ: Prentice-Hall, 2001.

[3] D. G. Brennan, "Linear diversity combining techniques," *Proceedings of the IRE*, vol. 47, pp. 1075–1102, June 1959.

[4] G. L. Stüber, *Principles of Mobile Communication*, 2nd ed. Norwell, MA: Kluwer Academic Publishers, 2001.

[5] W. C. Y. Lee, *Mobile Communications Engineering: Theory and Applications*, 2nd ed. New York, NY: McGraw-Hill, 1998.

[6] T. S. Rappaport, *Wireless Communications Principles and Practice*, 2nd ed. Upper Saddle River, NJ: Prentice-Hall, 2002.

[7] J. G. Proakis, *Digital Communications*, 4th ed. New York, NY: McGraw-Hill, 2001.

[8] R. H. Clarke, "Statistical theory of mobile-radio reception," *Bell Systems Technical Journal*, vol. 47, pp. 957–1000, July 1968.

[9] A. Papoulis and S. U. Pillai, *Probability, Random Variables and Stochastic Processes*, 4th ed. New York, NY: McGraw-Hill, 2002.

[10] M. Nakagami, "The *m*-distribution - A general formula of intensity distribution of rapid fading," in *Statistical Methods in Radio Wave Propagation*, pp. 3–36. Pergamon Press, Oxford, U.K., 1960.

[11] H. Suzuki, "A statistical model for urban multipath propagation," *IEEE Transactions on Communications*, vol. 25, pp. 673–680, July 1977.

[12] W. R. Braun and U. Dersch, "A physical mobile radio channel model," *IEEE Transactions on Vehicular Technology*, vol. 40, pp. 472–482, May 1991.

[13] J. D. Parsons, M. Henze, P. A. Ratliff, and M. J. Withers, "Diversity techniques for mobile radio reception," *IEEE Transactions on Vehicular Technology*, vol. 25, pp. 75–85, Aug. 1976.

[14] M. Schwartz, W. R. Bennet, and S. Stein, *Communication Systems and Techniques*. New York, NY: McGraw-Hill, 1966.

[15] F. J. Altman and W. Sichak, "A simplified diversity communication system for beyond-the-horizon links," *IRE Transactions on Communications Systems*, vol. CS-4, pp. 50–55, Mar. 1956.

[16] N. C. Beaulieu, "An infinite series for the computation of the complementary probability distribution function of a sum of independent random variables and its application to the sum of Rayleigh random variables," *IEEE Transactions on Communications*, vol. 38, pp. 1463–1474, Sept. 1990.

[17] A. A. Abu-Dayya and N. C. Beaulieu, "Microdiversity on Ricean fading channels," *IEEE Transactions on Communications*, vol. 42, pp. 2258–2267, June 1994.

[18] N. C. Beaulieu and X. Dong, "Level crossing rate and average fade duration of MRC and EGC diversity in Ricean fading," *IEEE Transactions on Communications*, vol. 51, pp. 722–726, May 2003.

[19] N. C. Beaulieu and A. A. Abu-Dayya, "Analysis of equal gain diversity on Nakagami fading channels fading," *IEEE Transactions on Communications*, vol. 39, pp. 225–234, Feb. 1991.

[20] A. Annamalai, C. Tellambura, and V. K. Bhargava, "Equal-gain diversity receiver performance in wireless channels," *IEEE Transactions on Communications*, vol. 48, pp. 1732–1745, Oct. 2000.

[21] A. Annamalai and C. Tellambura, "Error rates for Nakagami-m fading multichannel reception of binary and M-ary signals," *IEEE Transactions on Communications*, vol. 49, pp. 58–68, Jan. 2001.

[22] M.-S. Alouini and M. K. Simon, "Performance analysis of coherent equal gain combining over Nakagami-m fading channels," *IEEE Transactions on Vehicular Technology*, vol. 50, pp. 1449–1463, Nov. 2001.

[23] W. C. Mason, M. Ginsburg, and D. G. Brennan, *Tables of the Distribution Function of Sums of Rayleigh Variables*, MIT Lincoln Laboratory, Lexington, MA, Mar. 1960.

[24] J. D. Parsons, *The Mobile Radio Propagation Channel*, 2nd ed. New York, NY: John Wiley & Sons, 2000.

[25] T. F. Coleman and Y. Li, "An interior trust region approach for nonlinear minimization subject to bounds," *SIAM Journal on Optimization*, vol. 6, pp. 418–445, May 1996.

[26] U. Charash, "Reception through Nakagami fading multipath channels with random delays," *IEEE Transactions on Communications*, vol. 27, pp. 657–670, Apr. 1979.

[27] S. W. Oh, K. L. Cheah, and K. H. Li, "Forward-link BER analysis of asynchronous cellular DS-CDMA over Nakagami-faded channels using combined PDF approach," *IEEE Transactions on Vehicular Technology*, vol. 49, pp. 173–180, Jan. 2000.

[28] R. J. C. Bultitude and G. K. Bedal, "Propagation characteristics on microcellular urban mobile radio channels at 910 Mhz," *IEEE Journal on Selected Areas in Communications*, vol. 7, pp. 31–39, Jan. 1989.

[29] W. Feller, *An Introduction to Probability Theory and Its Applications, Volume II*, 2nd ed. New York, NY: John Wiley & Sons, 1971.

[30] G. K. Karagiannidis, "Moment-based approach to the performance analysis of equal gain diversity in Nakagami-*m* fading," *IEEE Transactions on Communications*, vol. 52, pp. 685–690, May 2004.

[31] S. Park, D. Yoon, and K. Cho, "Tight approximation for coherent MPSK symbol error probability," *Electronics Letters*, vol. 39, pp. 1220–1222, Aug. 2003.